Rainfall Intensity Duration Frequency (RIDF) Relationships under the Changing climate

(Case study on Upper Blue Nile River Basin, Ethiopia)

Nigatu Merra keffale

September, 2011

ADDIS ABABA UNIVERSITY

SCHOOL OF POST GRADUATE STUDIES

Department of Hydraulic Engineering

Rainfall Intensity Duration Frequency (RIDF) Relationships under the Changing climate

(Case study on Upper Blue Nile River Basin, Ethiopia)

By

Nigatu Merra

September, 2011

Rainfall Intensity Duration Frequency (RIDF) Relationships under the Changing climate

(Case study on Upper Blue Nile River Basin, Ethiopia)

By

Nigatu Merra Keffale

A THESIS SUBMITTED
TO
THE UNVERSITY OF ADDIS ABABA

IN PARTIAL FULFILLMENT OF THE REQUIREMENTS OF THE DEGREE OF MASTER OF SCIENCE IN **HYDRAULIC ENGINEERING**

ADDIS ABABA UNIVERSITY

September, 2011

CERTIFICATION

The undersigned certify that he has read and here by recommend for acceptance by the University of Addis Ababa a thesis entitled: **Rainfall Intensity Duration Frequency (RIDF) Relationships for Upper Blue Nile River Basin under the changing climate** in partial fulfillment of the requirement of the degree of Masters of Science in Hydraulic Engineering.

____

Dr. Semu Ayalew Moges

Advisor

Date___________

Rainfall Intensity Duration Frequency (RIDF) Relationships under the Changing climate

(Case study on Upper Blue Nile River Basin, Ethiopia)

Thesis submitted to Addis Ababa University, Addis Ababa Institute of Technology, school of graduate studies for the partial fulfillment of the requirements for the Degree of Master of Science in Hydraulic Engineering.

Date defended--------------------------------

Members of Examining Board:

--- -----------------------------------

(Chairman) (Signature)

-- ----------------------------------

(Advisor) (Signature)

--- ----------------------------------

(Internal examiner) (Signature)

-- -----------------------------------

(External examiner) (Signature)

DECLARATION AND COPYRIGHT

I, Nigatu Merra, declare that this is my own original work and that it has not been presented and will not be presented to any other University for similar or any other degree award.

Signature_________________

DEDICATION

This work is dedicated to my lovely Brother, Mr. Addisu Merra who taught me the best skills to tackle life challenges.

Abstract

The main focus of this study is to see how intensity of rainfall changes in the Upper Blue Nile River Basin under the conditions of the changed climate. Predicted future climate change impacts indicate that there will be increases in rainfall, leading to an intensification of the hydrologic cycle. One of the expected consequences of change is an increase in the magnitude and frequency of extreme events (e.g. high intensity rainfall, flash flooding, severe droughts, etc.).

Water management infrastructure designs are typically based on the use of local rainfall Intensity Duration Frequency (IDF) curves which are with the assumptions stationary of the future extreme events. However; this assumption is not valid under changing climatic conditions that may bring shifts in the magnitude and frequency of extreme rainfall. Such shifts in extreme rainfall at the local level demand new regulations for water infrastructure management as well as changes in design practices.

IDF curves were constructed for observed as well as projected rainfall events after climate change and compared to see the changes.

The methodologies implemented to assess changes in rainfall magnitude resulting from climate change are at first the regional downscaled grid rainfall data was downscaled to point level and further projected under current and future climate scenarios using statistical downscaling method. Then, disaggregation of daily rainfall into hourly ones was done by rainfall ratio method. Lastly, the statistical analysis of rainfall of various durations was done to develop intensity duration frequency relationships under the different possible climate scenarios.

The results this research indicate that rainfall magnitude (as well as intensity) will be different than historically observed for a range of durations and return periods.

Keywords: SDSM, intensity duration frequency curves, Upper Blue Nile, Climate change, extreme rainfall events.

Acknowledgements

Above all I thank the almighty of GOD for his mercy and grace upon me during all my works and in all my life.

I would like to express my sincere gratitude to my employer Wollo University (WU) for providing me to learn my MSc. Program.

Very special thanks to my Advisor, Dr.Semu Ayalew Moges, for giving me valuable guidance and for his friendly approach throughout my research. Without him, this work wouldn't have been realized.

I would also like to express my appreciation to Addis Ababa Institute of Technology (AAIT) staff members and libraries for their provision of the necessary reference books and assistance for my study.

Last but the bests, I would like to thank my wonderful brother Addisu Merra, for his ultimate support throughout my life.

Nigatu Merra

rnigatu@gmail.com

TABLE OF CONTENTS

List of tables

Lists of figures

1.0 INTRODUCTION AND BACKGROUND

1.1 Introduction

Increased industrial activity and excessive deforestation during the last century and a half has increased concentration of carbon dioxide in Earth's atmosphere. This has in turn initiated large scale atmospheric processes resulting in change of global temperature and precipitation (among other variables). Changes in Earth's climate system can disrupt the delicate balance of hydrologic cycle and can eventually lead to increased occurrence of extreme events (such as flood droughts, heat waves, summer and ice storms, etc.).

One way of reducing vulnerability to adverse impacts of climate change is to anticipate their possible effects, and adapt; the other is to actually reduce the rate of carbon dioxide released into the atmosphere. Reducing climate change vulnerability means that decision makers and stakeholders need to understand its effects, and develop suitable measures to deal with them in the future. The report by Mehdi et al. (2006) outlines a number of important points regarding why decision makers need to consider climate change. The main point is that "**even small shifts in climate normals will have potentially large ramifications for existing infrastructure**." Further, the report states that climate change "will affect large and small, urban and rural, and have positive and negative consequences for the various type of infrastructure, e.g., roads and bridges; natural systems, e.g., watersheds and forests; and human system, e.g.,health and education" (Mehdi et al., 2006, p. 7).

Of all possible impacts resulting from changed climatic conditions at the country level, this research focuses on those resulting from changes in extreme rainfall. Any change in extreme rainfall could demand new regulations in the form of storm water management strategies, guidelines and design practices, as well as altered infrastructure design standards. In some cases changing hydro climatic conditions may also require upgrading, retrofitting, rebuilding, or even constructing additional water management infrastructure.

The current design standards are based on historic climate information and required level of protection from natural phenomena. For example, a dyke designed to resist a 100 yr flood event (meaning that each year the probability of occurrence of a flood exceeding the design value is 0.01) will, if rainfall magnitude increases, provide significantly lower level of protection.

With changing climate, it is necessary to thoroughly review and/or update the current design standards for water management infrastructure in order to prevent the possibility of future infrastructure performing below its designed guideline.

The objective of this research is to provide data and information necessary for design guidelines modification using Statistical Down**s**caling Model (SDSM 4.2) which is a decision support tool for assessing local climate change impacts using a robust statistical downscaling technique that facilitates the rapid development of multiple, low cost, single site scenarios of daily surface weather variables under present and future climate forcing. Additionally, the software performs ancillary tasks of data quality control and transformation, predictor variable prescreening, model calibration, generation of rainfall for various scenarios and basic diagnostic testing, statistical analyses and graphing of climate data.

In order to take into consideration the impact of changing climatic conditions, design standards for much of the region’s water management infrastructure depend on rainfall, information is therefore provided regarding how rainfall (and extreme rainfall events in particular) is expected to change as climate changes.

One of the first steps in many hydrologic design projects, such as in urban drainage design, is the determination of the rainfall event or events to be used.The most common approach is to use a design storm or event that involves a relationship between rainfall intensity (or depth), duration, and the frequency or return period appropriate for the facility and site location. In many cases, the hydrologist has standard intensity duration frequency (IDF) curves available for the site and does not have to perform this analysis. However, it is worthwhile to understand the procedure used to develop the relationships. Usually, the information is presented as a graph, with duration plotted on the horizontal axis, Intensity on the vertical axis, and a series of curves, one for each design return period (Chow, 1988).

Rainfall Intensity Duration Frequency curves (IDF curves) are graphical representations of the amount of water that falls within a given period of time. The Intensity of rainfall (I) is the rate at which it is falling, Duration(D) is the time for which it is falling with that given intensity and Frequency(F) is the average recurrence time of that magnitude of rainfall.

The development of intensity duration frequency IDF curves for precipitation remains a powerful tool in the risk analysis of natural hazards. Indeed the IDF curves allow for the estimation of the return period of an observed rainfall event or conversely of the rainfall amount corresponding to a given return period for different aggregation times (Gerbi, 2002).

Synthesis of this research is presented in the form of intensity duration frequency (IDF) Curves and equations which can show the impacts of climate change for a number of different future climate scenario and intended to develop IDF relationships for selected climatological stations in the region.

To develop IDF curves Annual maximum values of rainfall for different durations will be collected from selected meteorological stations. And from this data intensities can be driven directly. The minimum criteria proposed where each station should have a length of more than 10 years record (Asres , 2008).

1.2 Background

The IPCC finding indicates that developing countries, such as Ethiopia will be more vulnerable to climate change. Because of the less flexibility to adjust the economical structure and being largely dependent on agriculture, the impact of climate change has far reach implication in Ethiopia.

Blue Nile Basin is one of the largest basins in the country with high population pressure, degradation of land and highly dependent on agricultural economy (Tsegay, 2006). The increase in population growth, economical development and climate change have been proven by IPCC, (2007) to cause rise in water demand, necessity of improving flood protection system and drought (water scarcity).

1.3 Statement of the problem

Flooding due to rainfall is probably the most severe among hydro meteorological hazards that cause damages to roads, bridges, residential, and agricultural areas. Therefore, planning and protection of these basins, requires estimate of expected discharge from rainfall events of different magnitudes based on the current global problem of climate change. At the same time, the economic design of bridges, culverts, dams and other hydraulic structures demands good knowledge of the likely floods which the structure would have to withstand during its estimated economic life. However, reliable estimates of flood frequency in terms of peak flows and volumes remain a current challenge in hydrology. Besides this, the change in rainfall duration and frequency depending on the changing climate is one sort of challenge to hydrologists. In our country ,Ethiopia, many researchers like Asres ,(2008) and Eyoel ,(2010) and others have been involved in intensity duration frequency relationships of rainfall but they did not try to see the impact of climate change.

However; the focus of this paper is to see that gap which is the impact of climate change on IDF.

1.4 Research question

- ✓ What is the relationship between intensity, duration and frequency before and after climate change?
- ✓ How is spatial difference of rainfall change in the study area?
- ✓ How much accurate the mathematical relations between depth, time and frequency?
- ✓ Which type of probability distribution best fits the station under consideration in the changing climate?
- ✓ Are IDF curves affected by climate change?

1.5. Objectives of the study

1.5.1 General objective

The main objective of this study is to evaluate the impact of future climate change on intensity duration and frequency of rainfall.

1.5.2 Specific objectives

- ✓ To develop families of Intensity- Duration- Frequency curves for different stations for durations and return periods for different scenarios.
- ✓ To evaluate the IDF changes for possible climate change scenario.

In order to meet the above objectives, the key question addressed in the study is that, what are the general trends of the future climate compared to the present condition and how can this affect the infrastructural design and operation of management parameters.

1.6. Significance of the study

The result of this study will be useful to estimate the intensity and duration of an extreme rainfall event which is ultimately required for planning and design of water resource projects, flood control and flood plain mapping program, urban drainage works, highway and culvert design, etc. Therefore, establishment of IDF curves and equations for the area based on the changing climate is an important task in a way that institutions and engineers involved in design and evaluation of water resource projects, highways, urban drainage works, etc. in the region as a whole will think of about the global issue, climate change.

1.7. Scope of the study

These research works is limited to the development of IDF relationships, and to observe the magnitude and trend of change on IDF that comes from climate variability based on the available data and those stations that have good correlation coefficient of the predictor and predictand relationships and representative rainfall stations in study area under the different climate change scenarios using conventional approach of frequency analysis.

1.8 General description of the study area

This area is the upper Blue Nile River Basin which is located in the Ethiopian Highlands and has a drainage area of about 176,000 km2 measured at El Deim (Figure1). The Blue Nile River runs from its origin, Lake Tana, to the Sudanese border and eventually meets the White Nile River at Khartoum, Sudan.

The climate of the study area varies from humid to semiarid. Most precipitation occurs in the wet Kiremt season (June through September), and the remaining precipitation occurs in the dry Bega season (October through January or February) and in the mild Belg season (February or March through May). The annual precipitation increases from northeast to southwest over the basin. Annual precipitation has been found to range from 1200 to 1600 mm, depending on the method and the period used (e.g., Gamachu, 1977; Conway, 1997, 2000; Tafesse, 2001; UNESCO, 2004; Kim and Kaluarachchi, 2007). The mean annual temperature from 1961 to 1990 was estimated to be 18.3 °C with a seasonal variation of less than 2°C, and the annual potential evapotranspiration was found to be about 1100 mm (Kim et al., 2007).

More than 80% of annual flow in the Blue Nile results from the summer monsoon and is concentrated between July and October. This runoff flows directly to downstream countries due to the absence of storage capacity in Ethiopia. Small tributaries in the mountainous region experience large fluctuations of streamflow due to the high seasonal variation of precipitation

(UNESCO, 2004). Using monthly discharge data at the Roseires/El Deim station just over the border in Sudan(national center for Atmospheric Research(NCAR), http://dss.ucar.edu/datasets/, March 2006), the mean annual discharge was 49 km3 for the period 1921-1990, ranging from a minimum of 31 km3 (1972 and 1984) to a maximum 70 km3 (1929). Based on the same data set, the 30-year mean annual discharge ranged from 38 km3 (1978 and 1985) to 56 km3 (1955 and 1964). Previous Nile studies have estimated the mean annual discharge from the Blue Nile to be 46-54 km3 (Kim and Kaluarachchi, 2008).

Figure 1: Map of study area with sample rainfall stations.

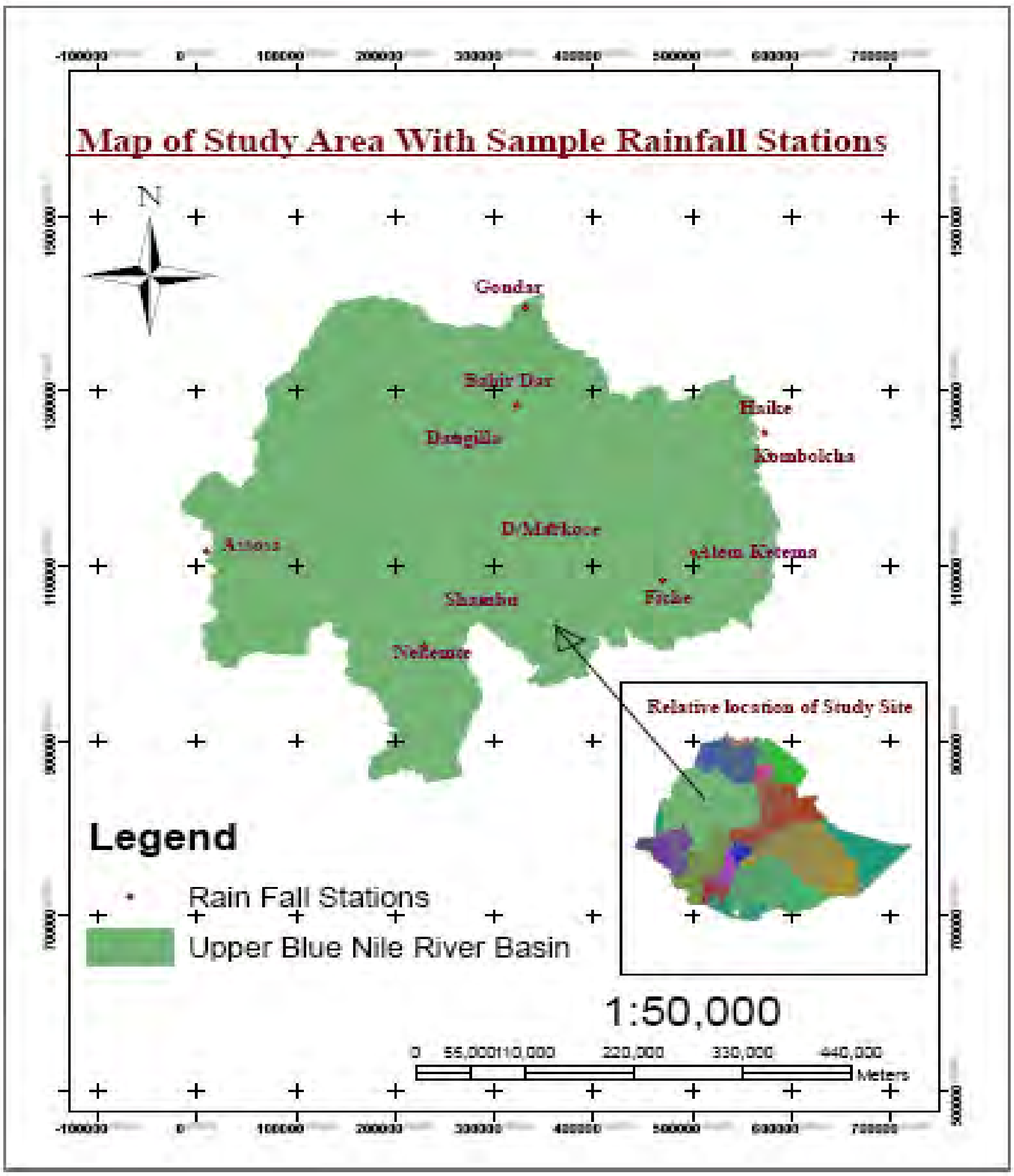

1.9 Thesis outline

This thesis contains five chapters organized as follows. Chapter one gives a general introduction to the study with its background, study area, objective, relevance, research questions and scope of the study. Chapter two gives a brief description of the reviewed literature related to the study. Chapter three deals with the procedures and methodology adopted for the study. Chapter four is concerned with data analysis, results and discussion. Chapter five lastly ends with the conclusions and recommendations by the study.

2.0 LITERATURE REVIEW

2.1 Over view of climate change

Climate change can simply defined as the change in the climatic elements or variables through time (USAID, 2007).

Climate change is the sever problem that the whole world facing today. It is now widely accepted that climate change is already happening and further change is inevitable; over the last century (between 1906 and 2005), the average global temperature rose by about 0.74 ^{o}C. This has occurred in two phases, from 1910s to 1940s and more strongly from the 1970s to the present (IPCC, 2007a).

Many studies into the detection and attribution of climate change have found that most of the increase in average global surface temperature over the last 50 years is attributable to human activities (IPCC, 2001a).

It is estimated that, for the 20th Century, the total global mean sea level has risen 12-22 cm, this rise has been caused by the melting of snow cover and mountain glaciers (both of which have decline on average in both hemispheres)(IPCC, 2007a). The IPCC also notes that observations over the past century shows, changes are occurring in the amount, intensity, frequency and types of precipitation globally (IPCC, 2007a).

At this point it is worth mentioning the role and remit of the Intergovernmental Panel on Climate Change (IPCC). The IPCC was established in 1988 by the World Meteorological Organization and the United Nations Environment Programme, and its role is to “assess on a comprehensive, objective, open and transparent basis the scientific, technical and socio economic information relevant to understanding the scientific basis of risk of human induced climate change, its potential impacts and options for adaptation and mitigation”. Among the different assessment that are carried out by the IPCC, the most recent which published in 2007, states the projected global surface warming lies within the range 0.6 to 4.0^{o}C, whilst the projected see level rise lies within the range 0.18 to 0.59 m at the end of next century (IPCC, 2007a).

2.2 Climate change in Ethiopia

According to the Ethiopian National Meteorological Services Agency (NMSA, 2001) study for 42 meteorological stations, the country has experienced both dry and wet years over the last 50 years. Trend analysis of the annual rainfall show that there was a declining trend in the northern half of the country and southern Ethiopia while there is **an increasing trend in the central part of** the country. However, the overall trend in the entire country is more or less constant.

2.3 Global circulation models

Currently, one of the best ways to study the effects of climate change is to use global circulation models. These models are the current state of the art in climate science. Their aim is to describe the functioning of the climate system through the use of physics, fluid mechanics, chemistry, as well as other sciences. More specifically, all global circulation models discretise the planet and its atmosphere into a large number of three dimensional cells.These can be thought of as a large number of checker boards stacked on top of each other (Kolbert, 2006, p. 100) to which relevant equations are applied.

In general, there are two different types of equations that are used in all global circulation models those describing fundamental governing physical laws, and those that are termed empirical (based on observed phenomena that are only partially understood). The former are representations of fundamental equations of motion, laws of thermodynamics, conservation of mass and energy, etc, and are well known; the latter, however, are those phenomena that are observed, but for which sound theory does not yet exist (i.e., small scale processes such as land use that can influence large scale processes such as the global circulation). For most studies that are concerned with the response of a smaller area (such as a city) to a changed climatic signal, the global models are inappropriate because they have special and temporal scales that are incompatible with those of a city. One way around this is to still use the global input, but scale it appropriately for the area under consideration.

Traditional way of studying the impacts of climatic change for small areas involves scaling down the outputs from global circulation models (temporally and spatially) from which user and location specific impacts are derived. A number of studies have implemented such methodologies, and thus estimated local impacts of climatic change (Coulibaly and Dibike, 2004; Palmer et al., 2004; Southam et al., 1999).

However, a number of uncertainties are inherent to this approach. First, the global models have temporal scales that are sometimes incompatible with temporal scales of interest at the local level. The global models are only able to produce monthly outputs with a higher degree of accuracy This is insufficient since at the local level we are often interested in changes in frequency of occurrence of short duration high intensity events, especially when studying the problem of flooding. Temporal downscaling of monthly global output must therefore be employed, and shorter duration events be estimated, thus compounding uncertainty. Second, spatial scales of global models are also incompatible with spatial scales at the local level. The global models typically have grid cells of 50 km by 50km, and are thus significantly larger than most watersheds.

2.4 Climate scenario models

The General/Regional Circulation Models (GCM/RCM) are used for the estimation of the future global/regional climate changes, based on the different global scenarios for technological change. The GCM/RCM predictions are employed to derive recommendations for policy makers.

Statistical Downscaling: **Statistical** downscaling assumes stationary of the projected climate system and cannot capture higher moments. Statistical downscaling is computationally inexpensive and many representations can be generated quickly.

Dynamic Downscaling:Dynamic downscaling is weather or climate (average of weather) simulation with complete meteorological equations resulting in weather variables and fluxes (Temperature, Precipitation, Relative Humidity, Wind, Radiation, Latent and Sensible Heat, Soil Moisture, Runoff...).

Dynamic downscaling requires a large amount of computational and data storage resources. It takes a long time to complete the simulations. Statistical downscaling is based on coarse resolution predictors that lead to high resolution predictands for temperature and precipitation.
The dynamical downscaling approach uses physically based regional climate models (RCMs) driven by conditions provided by a GCM to produce finer scale output (typically about 0.5^0). day, studies examining the impacts of changes in climate on water systems have adopted relatively simple statistical downscaling methods and have tended to use a small ensemble of climate models. In spite of RCMs are with limitation of computationally expensive, dependent on the deriving GCM, can be affected by any systematic errors on the deriving fields, and limited number of scenarios.For this study, the run model output of rainfall on monthly and daily basis is available in IWMI (international water management institute ,Ethiopia) and I used this output for my study .

2.5 An IPCC Scenarios

The following is taken from IPCC (2001) and represent four main families of climate change scenarios.

- The A1 storyline and scenario family describes a future world of very rapid economic growth, global population that peaks in mid-century and declines thereafter, and the rapid introduction of new and more efficient technologies. Major underlying themes are convergence among regions, capacity building, and increased cultural and social interactions, with a substantial reduction in regional differences in per capita income.

- The A2 storyline and scenario family describes a very heterogeneous world. The underlying theme is self-reliance and preservation of local identities. Fertility patterns across regions converge very slowly, which results in continuously increasing global population. Economic development is primarily regionally oriented and per capita economic growth and technological change are more fragmented and slower than in other story lines.

- The B1 storyline and scenario family descries a convergent world with the same global population that peaks in mid century and declines thereafter, as in the A1 storyline, but with rapid changes in economic structures toward a service and information economy, with reductions in material intensity, and the introduction of clean and resource efficient technologies. The emphasis is on global solutions to economic, social, and environmental sustainability, including improved equity, but without additional climate initiatives.

- The B2 storyline and scenario family describes a world in which the emphasis is on local solutions to economic, social, and environmental sustainability. It is a world with continuously increasing global population at a rate lower than A2, intermediate levels of economic development, and less rapid and more diverse technological change than in the B1 and A1 story lines. While the scenario is also oriented toward environmental protection and social equity, it focuses on local and regional levels.

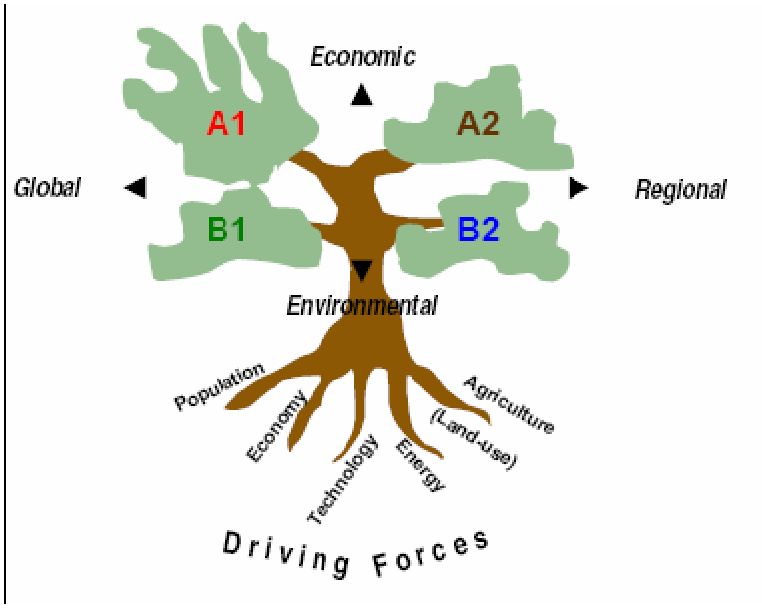

Figure 2.1 *The four IPCC scenario storylines (IPCC-TGICA, 2007)*

2.6. Impact of climate change on IDF curve

The reality of climate change is almost undisputed now, and the findings in the Fourth Assessment Report (AR4) of the Intergovernmental Panel on Climate Change (IPCC, 2007a, bare stronger and more definite than ever before. The planet is warming, largely as a consequence of anthropogenic emissions of greenhouse gases. Rainfall and evapotranspiration rates are changing too.

Hydrological changes and the impact of those changes constitute a fundamental global warming related concern (Vo¨ro¨smarty et al. 2000).Faced with threats to human life and natural ecosystems, such as droughts, floods, and soil erosion. So, water resources planners must, increasingly, make future risk assessments (Schnur2002).Historically, stable climatic conditions have been assumed for water resources management, planning, and civil engineering designs. However, global climate Change may lead to changes in rainfall events (Palmer and Ra¨lsa¨nen 2002). We must learn, therefore, to adapt to climate changes and cope with climate variability (Zwiers2002).

2.7 Rainfall Pattern in Ethiopia

2.7.1 Rainfall Distribution in Ethiopia

In Ethiopia rainfall is highly variable both in amount and distribution across regions and seasons (Tesfaye, 2003, Tilahun, 1999; Mersha, 1999). The seasonal and annual rainfall variations are results of the macro scale pressure systems and monsoon flows which are related to the changes in the pressure systems (Haile, 1986; Beltrando and Camberlin, 1993; NMSA, 1996). The most important weather systems that cause rain over Ethiopia include Sub Tropical Jet (STJ), Inter Tropical Convergence Zone (ITCZ), Read Sea Convergence Zone (RSCZ), Tropical Easterly Jet (TEJ) and Somalia Jet (NMSA, 1996). The spatial variation of the rainfall is, thus, influenced by the changes in the intensity, position, and direction of movement of these rain producing systems over the country (Taddesse, 2000). Moreover, the spatial distribution of rainfall in Ethiopia is significantly influenced by topography (NMSA, 1996; Camberlin, 1997; Taddesse, 2000), which also has many abrupt changes in the Rift Valley. However, the detail spatial and temporal variability of rainfall over the horn of Africa in general and Ethiopia in particular is highly complex and not well known yet. In general, the highest mean annual rainfall, over 2,400 mm, is in the southwestern highlands in Illubabor Zone of Oromia Region. The amount of rainfall gradually decrease about 600 mm in the north in areas bordering Eritrea, drops to less than 100 mm in the northeast in Afar, and to around 200 mm in the southeast in the Ogaden. Two moist wind systems, one blowing from the Atlantic Ocean, the other from the Indian Ocean, mainly influence the variation in the pattern and character of annual rainfall distribution in different parts of Ethiopia.

The seasonal (or intra annual) variability of precipitation is an important aspect of hydro climatology because it largely determines the seasonality of other hydrologic quantities, such as stream flow and ground water recharge. The seasonal pattern of relative heating of the continents and the migration of large scale circulation features largely control the seasonality of precipitation on a global scale. Monsoon regions in particular have pronounced seasonal variability of precipitation. One way of quantitatively describing seasonality is by means of circular statistics which is useful for quantifying the time of occurrence of events when time is measured on a circle like a clock. The quantification involves calculating average time of occurrence and the degree to which the events tend to be concentrated in time called the seasonality index (Dingman,2002).

2.7.2 Rainfall Regimes in Ethiopia

There are some regions, which experience three seasons (tri-modal type) with two rainfall peaks (where one peak is more prominent than the other), while some regions have four seasons with two distinct rainfall peaks (bi-modal type). There are still some regions, which have two seasons with single rainfall peak (mono-modal type). Based on this rainfall distribution pattern, three rainfall regimes can be delineated for Ethiopia as shown in the Fig. 2.2

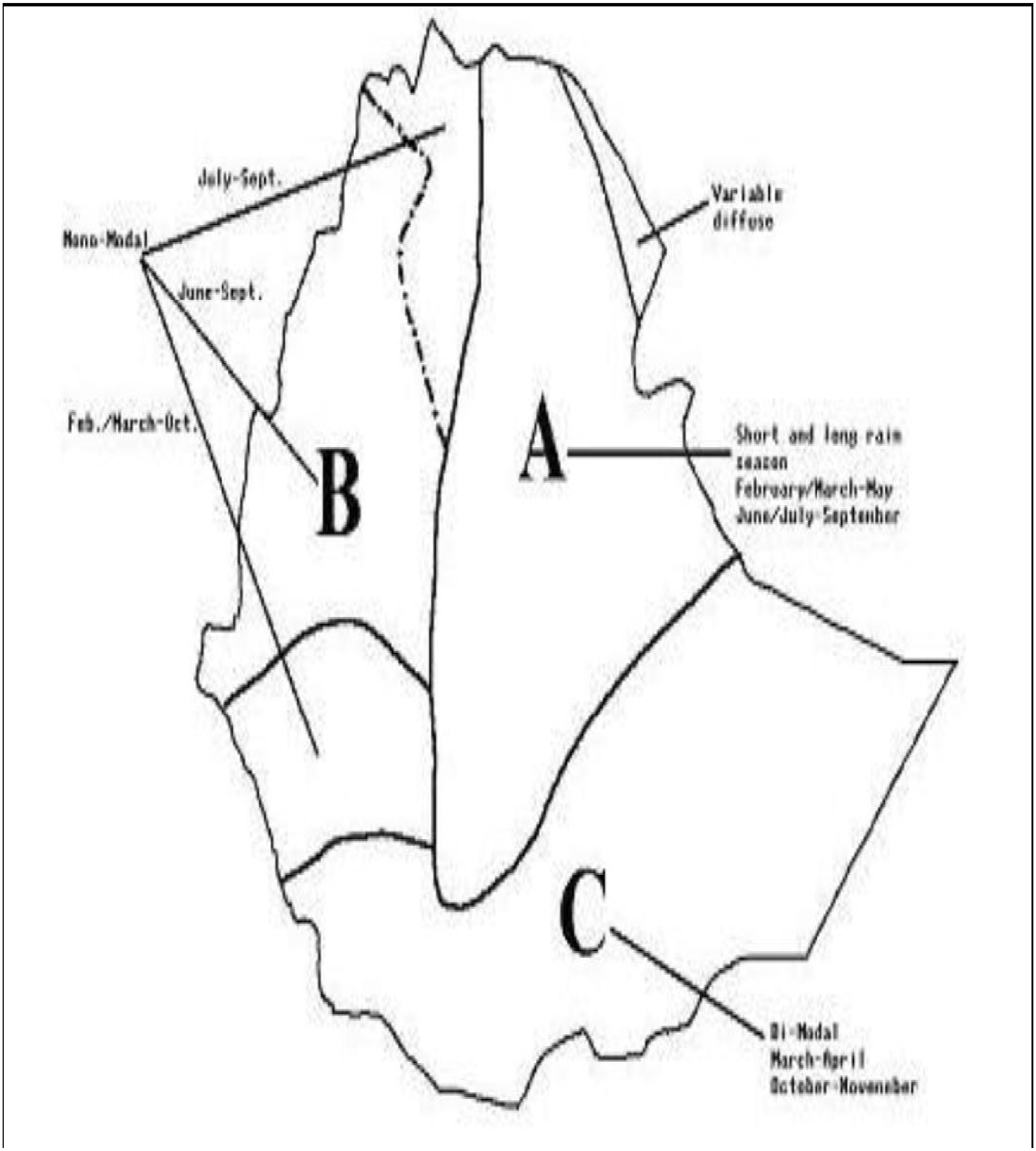

Figure 2. 2 Rainfall Regimes of Ethiopia (after Haile, 1996)

Areas under region A over the central, eastern and northern parts of the country experience three distinct seasons, which receives the majority of their rainfall from the Atlantic, while some derive from the Indian Ocean. The big rains from June to September come mainly from the Atlantic, while the small spring rains between February and May come from the Indian Ocean. A third rainy season exists that is brought by moist winds from Asia which crosses the Arabian Peninsula and cool as they rise over the Ethiopian escarpment. These bring mist and rain anytime between October and January. In each case, the amount of rainfall and the length of rainfall season decrease the further north one goes.

Areas under region C over the southern and southeastern parts of the country are characterized by a bimodal rainfall pattern brought about by the wind system coming from the Indian Ocean from September to November and from March to May. The most reliable rainy months are April and May.

Areas demarcated by region B are characterized by single rainfall peak during a year, where two distinct seasons, one being wet and the other dry are encountered. Mean monthly rainfall pattern shows that the southwestern, western and northwestern parts of the country are under their wet season during February/March to October/November, April/May to October/ November and June to September, respectively. The amount of rainfall and length of the rainy season decreases from south to north.

And also according to the study conducted by the minister of agriculture the mean annual rainfall distribution pattern of the country, six rainfall regimes can be delineated for Ethiopia as shown in the Fig. 2.3.

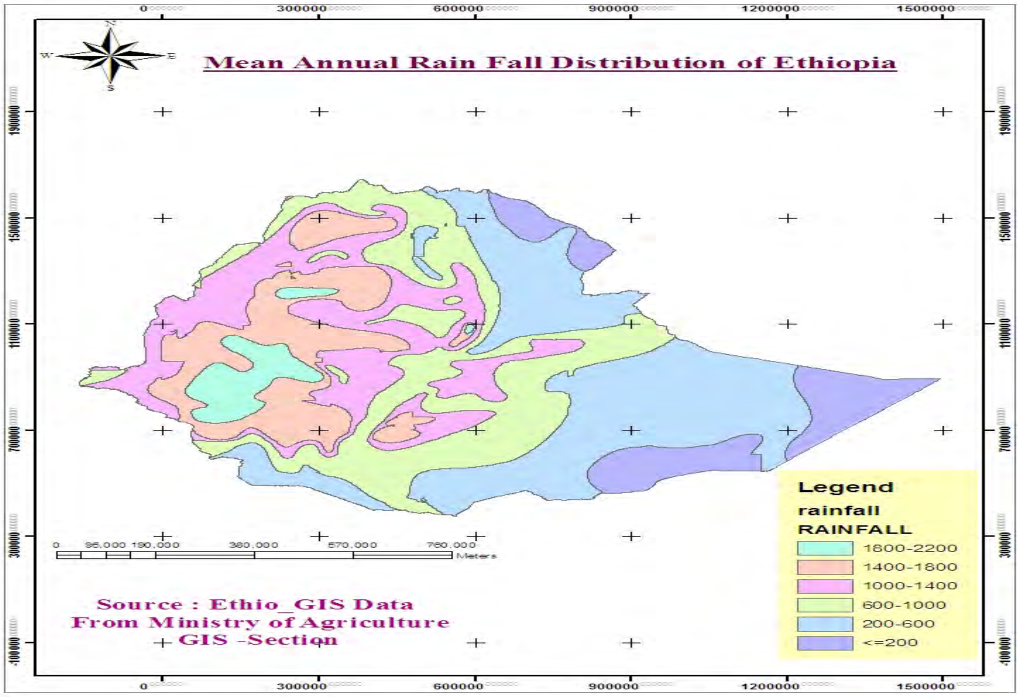

Figure 2.3 Mean annual rainfall distribution of Ethiopia

The National Meteorological Services Agency, considering the dominant regional atmospheric circulations and the rainfall patterns across the three major rainfall regimes over the country uses the following seasonal classification for operational monitoring and forecasting of the weather over the country.

I. October to January (Bega):- Predominantly called Bega(dry season)over areas in Region A, also part of the long dry season over northwestern parts of the country of region B, whereas over the western and southwestern parts of the country of region B, denotes the time when the long rainfall season comes to an end to be followed by a medium to short dry season during the same period. During the first half of this season, south and southeastern parts of the country of region C get their short rain season due to the southward retreating Inter Tropical Convergence Zone. Year to year variability of the weather during this season are largely related to intensities of the occurrences of west-ward moving depressions over the Arabian Sea, intensities of the Siberian High pressure system and its extension and the Saharan high pressure system which may affect the variability in the cloudiness and minimum temperature values over the central, eastern, western, southwestern and northwestern parts of the country (NMSA, 1996).

II. February to May (Belg):- Predominantly called Belg or Small rainy season over areas in region A, whereas over the southwestern parts of the country of region B it denotes the start of the long rainy season. Over the western parts of the country of region B also the rainy season starts during March/April. However over the northwestern parts of the country of region B, this season is predominantly dry except for the month of May. Southern and southeastern parts of the country of region C are expected to get their long rainy season during this time starting in March and peaking in April (NMSA, 1996).

III. June to September (Kiremt):- Predominantly called Kiremt season which is considered as the main rainy season in which about 85% to 95% of the food crops of the country are produced. The magnitude of rainfall is higher as compared to the other seasons for many parts of the country. It is to be noted that this rainfall season is not experienced over the southern and the southeastern lowlands of the country due to divergence field of the wind originating from the Indian Ocean over these areas. Thus, we have to note that there are variations in the timing of rainfall seasons and rainfall peaks over different parts of the country (NMSA, 1996).

2.8 Design Rainfall

Rainfall, in terms of its depth (intensity), duration and temporal patterns, known as design rainfall, is the basic input to many hydrological models as it affects the resulting runoff peak and volume. Although the design storm must reflect required levels of protection, the local climate, and catchments conditions, need not be scientifically rigorous. It is more important to define the storm and the range of applicability fairly precisely to ensure safe, economical and standardized design considering the climate change. Although estimation of design rainfall is based on frequency analysis of historical rainfall data, it is also important to consider the variability of rainfall with its magnitude and frequency depending on the changing climate. During estimation of design rainfall design storm duration is an important parameter that defines the rainfall depth or intensity for a given frequency. Correct practice is to select the design storm duration as equal as or longer than the time of concentration for the catchments (or some minimum value). Intensive rainfalls of short duration usually occur within longer duration storms rather than as isolated events. It is common practice (Packman and Kidd, 1980) to compute discharge for several design storms with different durations, and then base the design on the critical storm which produces the maximum discharge.

Different characteristics of rainfall are important to specialists involved in various fields, and therefore the number of ways of analyzing rainfall data is virtually unlimited. The method chosen depends up on the nature of the available data and the purpose of the investigation. A relatively small number of rainfalls measuring stations are equipped with continuously recording gauges, which yield data on the characteristics of individual storms such as timing and intensity as well as total amount.

A design rainfall can be defined by a value of precipitation depth at a point, by a design hyetograph specifying the time distribution of precipitation during a storm, or by an isohyetal map specifying the special pattern of precipitation.

Rainfall could be classified according to the amount of rain that is falling in a specified time. And thus it could be classified as Very light (< 0.25 mm/hr), Light (0.25 mm/hr - 1.0mm/hr), Moderate (1.0 mm/hr - 4.0 mm/hr), Heavy (4.0 mm/hr -16.0 mm/hr), Very heavy (16.0 mm/hr – 50 mm/hr), and Extreme (> 50.0 mm/hr) (www.najah.edu)

2.8.1 Point Rainfall

Point precipitation is precipitation occurring at a single point in space as opposed to a real precipitation which is precipitation over a region. For point precipitation frequency analysis, the annual maximum precipitation for a given duration is selected by applying statistical analysis to historical records. For each durations, frequency analysis is performed on the data, to derive the design precipitation depths for various return periods (Chow *et al*., 1988).

But in this thesis the different scenario data generated from the downscaled areal and regional climate model of 50km grid and downscaled once again to point precipitation by statistical downscaling model (SDSM 4.2) are used in the daily statistical and frequency analysis.

2.8.2 Areal Rainfall Depth

Frequency analysis of precipitation over an area has not been as well developed as analysis of point precipitation. In the absence of information on the true probability distribution of areal precipitation, point precipitation estimates are usually expected to develop an average precipitation depth over an area. The areal estimate may be either storm centered or location-fixed (Chow *et al*., 1988).

2.9 Frequency analysis of extreme events

2.9.1 Introduction

Extreme rainfall events and the resulting floods usually could cause significant damage to agriculture, ecology and infrastructure, disruption to human activities, injuries and loss of lives. Determination of frequencies and magnitudes of these events would enhance the management of water resources applications as well as the effective utilization of water resources. Such information can also be used for flood plain management and applied to the planning and designing of water resources related engineering, such as reservoir design, flood control work, drainage design, and soil and water conservation planning, etc (Smithers, 1998). All these works require the rainfall data as a design basis. Though the nature of rainfall is erratic and varies with time and space specially during global warming, yet it is possible to predict the pattern of rainfall fairly accurately for certain return periods using various probability distributions. Frequency analysis of rainfall data has been carried out at different places in Ethiopia without giving attention to the current word wide problem of climate variability.

2.9.2 Frequency Analysis

One of the important problems in hydrology deals with interpreting past records of hydrologic events in terms of a future probabilities of occurrence. The procedure for estimating frequency of occurrence of a hydrological event is known as frequency analysis. Frequency analysis is an information problem: if one had a sufficiently long record of flood flows, rainfall, low flows, or pollutant loadings, then frequency distribution for a site could be precisely determined, so long as change over time due to urbanization or natural processes did not alter the relationships of concern. In most situations, available data are insufficient to precisely define the risk or large floods, rainfall, pollutant loadings, or low flows. This forces hydrologists to use practical knowledge of the processes involved, and efficient and robust statistical techniques, to develop the best estimates of risk that they can. In hydrology the most frequent use of statistics has been that of frequency analysis (Haan, 1994). It uses a statistical technique that applies probability theory of extreme values with the primary objective of relating the magnitude of extreme events to their frequency of occurrence through the use of probability distributions (Chow *et al*., 1988). Rainfall frequency analysis derives functions that relate quantiles of rainfall depth with its recurrence intervals (return period) from the maximum rainfall depth series at particular duration.

2.9.3 Frequency Analysis of Rainfall

The frequency of rainfall of various intensities and durations is used in the hydrologic design of structures that control storm runoff and floods, such as storm sewers, high way culverts and dams. Rainfall frequency analysis typically provides rainfall accumulation values at a point for a specified exceedance probability and various durations (Maidment, 1993). Rainfall frequency analysis is used extensively for design of engineering works that control storm runoff. These include municipal storm sewer systems, high way and railway culverts, and agricultural drainage systems. Precipitation frequency analysis also plays an important role in a diverse range of non-structural problems involving natural hazards associated with extreme rainfall events (Maidment, 1993). The analysis of rainfall occurrence depends fundamentally on the length of the rainfall duration for which the information is required (Shaw, 1983). Though the nature of rainfall is erratic and varies with time and space, yet it is possible to predict the pattern of rainfall fairly accurately for certain return periods using various probability distributions. Frequency analysis of rainfall data has been carried out at different places in Ethiopia.

A random sample of rainfall data is required prior to the implementation of frequency analysis. The random sample often is an annual maximum series of total rainfall depth with respect to a pre specified duration t_r. The annual maximum series is obtained by continuously moving a window of size t_r along the time axis and selecting the maximum total values within the window in each year. The pr specified durations, also known as the design durations, are artificially designated durations which are used to determine the corresponding annual maximum depths. In contrast, event durations are actual raining periods of time of real storm events. Therefore, annual maximum rainfalls of specific design durations are considered random variables with duration specific parameters. Comparison of the two is shown in figure 2.2. below.

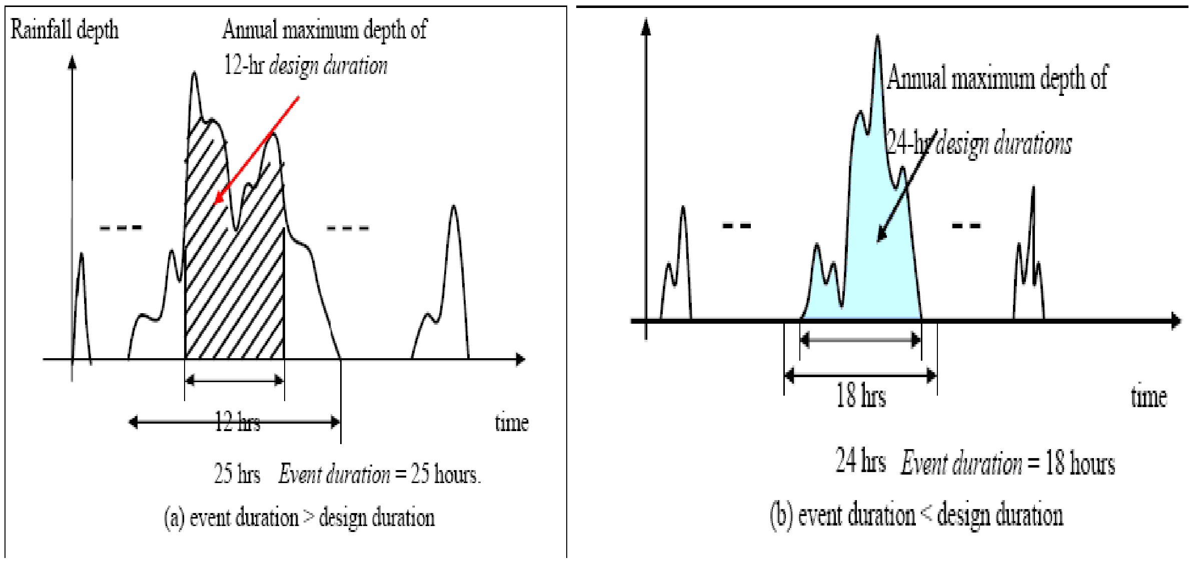

Figure 2. 4 Event duration vs Design duration Rainfall

Let t_r represent a specific (design) duration and its corresponding annual maximum series of total rainfall depth be represented by D (t_r, i), i=1, 2….N (N = record length). A goodness of fit test is conducted to determine the type of probability distribution for the annual maximum total depth of that duration. The amount of total depth $D_T(t_r)$ corresponding to return period T is then calculated using the frequency factor equation with the sample mean and sample standard deviation. Such duration-specific total depths are referred to as the design storm depths. The amount of $D_T(t_r)$ varies with the return period T and duration t_r and results from frequency analysis are usually presented in form of depth-duration frequency (DDF) curves or the intensity duration frequency (IDF) curves. The intensity in the IDF curves represents the average rainfall intensity and is calculated by:

$$i_T(t_r)=D_T(t_r)/t_r \text{-------------------------------} 2.1$$

Where $D_T(t_r)$ is the rainfall depth (mm or in) and tr is the duration, usually in hours.

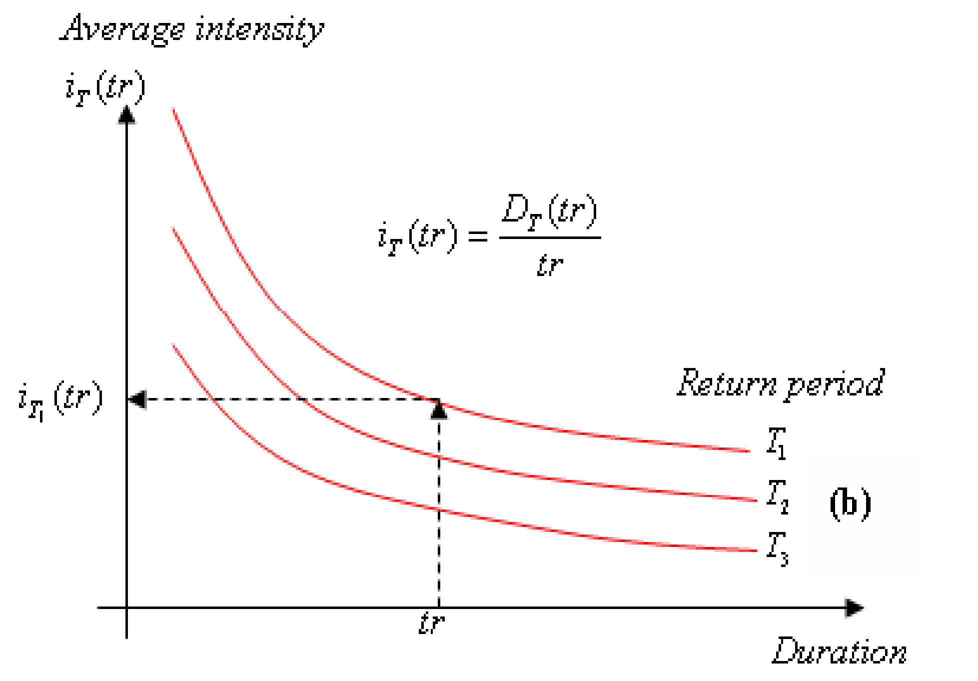

Figure 2. 5 Schematic diagrams of Intensity Duration Frequency relationship.

All forms of the generalized IDF relationships assume that rainfall depth or intensity is inversely related to the duration of a storm raised to a power, or scale factor. The Intensity duration frequency (IDF) relation is typically expressed in the form of the following Horner's equation:

$$\boldsymbol{i_T(t_r) = \frac{aT^m}{(t_r+b)^c}} \text{------------------------------------} 2.2$$

Where units for $i_T(t_r)$, T, and t_r are respectively mm/hr, year and minutes, the coefficients a, b, c, and m are site specific values.

Wenzel, (1982) has also proposed a relationship between intensity Duration

Frequency which is applicable in most locations by the equation of the form:

$$\boldsymbol{I = \frac{A}{(B+D)^C}} \quad \textbf{OR } \boldsymbol{I = \frac{A}{D^C+B}} \text{ --------------------------- } \quad 2.3$$

Where: I is intensity, D is duration, A is a constant for a given return period and B and C are constants that do not depend on return period. These equations have no theoretical basis; they are purely empirical devices that are sometimes useful for expressing relations such as depth exceedence probability and return period. The constants in the above equation have a strong geographic variation and must be determined by analysis of data for the location of interest.

The probability distributions in the preceding figure do not represent relations such as depth exceedence probability and return period. The constants in the above equation have a strong geographic variation and must be determined by analysis of data for the location of interest. distributions of total depth of real storm events since the total depth in the depth-duration-frequency relationship only represents the total amount of rainfall of the design duration (not the real storm duration) and, more specifically, it does not represent the bivariate distribution of duration and total depth of real storm events. Therefore, the usage of annual maximum series for rainfall frequency analysis is more of an intelligent and convenient engineering practice and the annual maximum data do not provide much information about the characteristics of the duration and total depth of real storm events.

2.10. Selection of parent distributions

2.10.1 Conventional moments

Several techniques have been used in the past for evaluating the suitability of different distributions for AM series. Moment about the origin or about the mean are used to characterize probability distributions. For a distribution with a probability density function *f(x)*, the *rth* moment about the origin is given by

$\mu'_{r}=\int_{-\infty}^{\infty} x^r f(x)dx,\quad \mu'_{1}=\mu$=mean -------------- (2.4)

The Central moments μ_r are computed by

$\mu_r=\int_{-\infty}^{\infty}(x-\mu'1)^r\, f(x)dx$------= $\mu_1=0$---------------- (2.5)

Sample moments m_r' and m_r , on the other hand, are calculated as

$m_r'=\frac{1}{n}\sum_i^n x^r i$, $m_1 1$=X= Sample mean -------------------------- (2.6)

$m_r= 1/n\sum_i^n (xi-X)^r$, $m_1=0$

These moments are often biased and may be corrected by (Cunnane, 1989)

$$m_2=\frac{1}{(N-1)}\sum(xi-X)^2$$

$$m_3=\frac{N}{(N-1)(N-2)}\sum(xi-X)^3 \qquad (2.7)$$

$m_4=\frac{N^2}{(N-1)(N-2)(N-3)}\sum(xi-X)^4$

The conventional moment ratios are defined as;

The coefficient of kurtosis $C_k=\frac{m_4}{m_2^2}$

--- *(2.8)*

The coefficient of skewness $C_s=\frac{m_3}{m_2^{3/2}}$

The coefficient of variation $C_v= m_2^{1/2}/m_1$

2.10.2 Probability weighted moments

Probability weighted moments (PWM) are defined by Green wood et al. (1979)
as stated in Rao and Hamed (2000).

$M\ p,r,s=\sum(x^p F^r (1-F)^S)=\int_0^1 (X(F))^P\ F^r (1-F)^S dF$-------------------------------(2.9)

In particular, the following two moments M1,0,s and M1,r,0 are often considered

$M\ 1,0,s=\alpha_s=x(F)(1-F)^S dF$ (2.10)

$M\ 1,r,o=\beta_r=x(F)(F)^r dF$

Where: p, r, and s are real numbers

The plotting position estimates for sample PWMS are given by

$\alpha_s= M\ 1,0,s=\frac{1}{N}\sum_{i=1}^{N}(1-F)^S X_i$ (2.11)

$b_r=\beta_r = M\ 1,r,o=\frac{1}{N}\sum_{i=1}^{N} F_i^r\ x_i$

L-moments are an alternative system of describing the shapes of probability distributions. Historically they arose as modifications of the probability weighted
moments.On the other hand, L – moments are defined by Hosking in terms of the PWMs α and β as

$\lambda_{r+1}=(-1)^r \sum_{k=0}^{r} p^*_{r,k\alpha_k} = \sum_{k=0}^{r} p_{r,k\beta_k}$--(2.12)

L- Moment ratios, which are analogous to conventional moment ratios, are
defined by Hosking (1990) as

$\tau= \lambda_2/\lambda$

$\tau_r= \lambda_r/\lambda_2\ \ r\geq 3$---(2.13)

Where: $\lambda 1$is a measure of location,τ is a measure of scale and dispersion
(L-Cv), $\tau_3$is a measure of skewness (L-Cs) and τ_4 is a measure of kurtosis
(Lck). Sample L moment rations (t and tr) are calculated by replacing λr by their sample estimates L_r.

The first few L-moments are

$L_1=M_{1,0,0}$

$L_2= M_{1,0,0}-2 M_{1,0,1}$ --(2.14)

$L_3 = M_{1,0,0}-6 M_{1,0,1}+ M_{1,0,2}$

$L_4= M_{1,0,0}-12 M_{1,0,1}+ 30M_{1,0,2}-20 M_{1,0,3}$

2.11. Parameter and quantile estimation

However, the rainfall frequency relationships are indispensable tools for statistical estimation of design rainfall depth at duration of interest for known return period or vice versa. The return period of design rainfall depth is determined from the design life of the intended project and from the economically permissible level of risk. The duration tr of the rainfall depth series is often regarded as the time of concentration of the catchment under consideration; which is the time surface flow takes to travel from the farthest point to the outlet of the catchment.

The frequency analysis of extreme events involves three fundamental procedures; which are selection of (i) model type, (ii) appropriate distribution function and (iii) unbiased parameter estimation method (Cunnane, 1989) .

I. Model Types

Two types of models are commonly applied for frequency analysis of rainfall data: the annual maximum (AM) model and partial duration (PD) model. The AM approach is easy to apply and, in general, guarantees that the chosen rainfall peak events are independent because only the peak event in each year of record is considered. Moreover, AM series are directly related to the commonly used concept of return periods for design rainfall. However, the use of an AM series may involve some loss of information. For example, the second or third peak within a year may be greater than the maximum rainfall depth in other years, and yet they are ignored. This situation is avoided in the partial duration (PD) or peak over a threshold (POT) model where all peaks above a certain base value are considered. The base is usually selected low enough to include at least one event in each year (Roa & Hamed, 2000). This usually produces much longer series than the AM, as more than one event per year could be chosen. The PD or POT model, however, is limited by the fact that observations may not be independent which violets the assumption of independence for statistical analysis. Therefore, to avoid the problem of dependency data, annual maximum (AM) series model was selected as relevant model for frequency analysis of extreme rainfall depth series at different duration in this study. In addition to this, AM series is widely and commonly used model by different researchers for the purpose of extreme rainfall and flood analysis. This is mainly due to the need to check for the independence of the PD series, and the question mark in relation to the choice of the threshold or the number of events to be chosen. In addition, the exceedance probability of the PDF, and in turn the corresponding return period, will not conform to the commonly recognized ones derived from the AM series.

II. Distribution Selection

Many hydrological random variables such as precipitation are statistically described by a probability distribution. In practice the true probability distributions of the phenomena in question are not known. Even if they were, their functional representation would likely have too many parameters to be of much practical use and the practical issue is how to select a reasonable and simple distribution to describe the phenomenon of interest, to estimate that distribution's parameters, and thus to obtain risk estimates of satisfactory accuracy for the problem at hand. The probability of an event is the chance that it will occur based on an observation of the random variable. The larger the samples size of random variables the better the estimate of the probability of the event. To determine the probability of events occurring, probability distribution functions are fit to the data to determine the appropriate function to use for estimation of the events.

The choice of distribution is influenced by many factors, such as methods of discrimination between distributions, methods of estimation parameters, the availability of data, etc. Generally, there is no general global agreement as to a preferable technique of model choice and no single one distribution accepted universally. The distribution functions most often used when estimating hydrologic events were: Normal, 2 Parameter Log Normal, Pearson Type III, Generalized Extreme-Value, and Gumbel Type I. Annual precipitation events tend to follow the normal distribution, and distribution varies over a continuous range and is symmetric about the mean but allows negative values. However, hydrologic variables tend to be skewed and all are non-negative. The log normal distribution eliminates the problem of non-negative variables as the data are greater than zero, permits the skewness of the data, and does require the data to be symmetric about the logarithm of the mean. This distribution has been broadly applied in the frequency analysis of annual maximum rainfall depth series (Burlando and Rosso, 1996).

The Pearson Type III methods transform the mean, standard deviation, and the coefficient of skewness into the three parameters of the distribution function. When the data are greatly skewed, the log transformation of the Pearson Type III is used to reduce the skewness. In the early 1980s, a comparison of the various distribution functions available for analysis of rainfall frequencies showed that the Log Pearson Type III distribution became method of choice for USA. As a result, in 1981 the U.S. Water Resources Council recommended the Log Pearson Type III distribution be used in an effort to promote consistency for flood flow analysis. The Generalized Extreme-Value distribution is recommended by the Natural Environmental Research council (NERC, 1975) for U.K. and Ireland and it is versatile enough to represent three different types of extreme-value distribution and they are preferable for the annual maximum series. Gumbel Type I distribution, also known as the Extreme Value Type I distribution, is a two-parameter distribution. One parameter is the most probable value of the distribution and the second is a measure of dispersion. Extreme value distributions have been widely used in hydrology (Chow *et al*., 1988). Analyzing data for the largest or smallest observations from sets of data became the basis for using the Gumbel (Extreme Value) Type I distribution. The Gumbel is also readily solved by hand calculations. In general, the selected distribution should be widely accepted; simple and convenient to apply; consistent, flexible or robust (low sensibility to outliers) and theoretically well based or established (Cunnane, 1989).

III. Estimation of parameters and quantiles:

After a distribution or a number of distributions are selected to fit the data series, their parameters must be estimated. There are a variety of methods to estimate the parameters of a statistical model. Among these approaches are the method of moments, the maximum likelihood method, least squares, the probability weighted moments method (PWM), maximum entropy, mixed moments (MIX), the generalized method of moments, and incomplete means method .

The most efficient approach for parameter estimation for a specified model should be applied. Three of the more commonly used methods of parameter estimation are discussed below:

a. Method of Moments (MOM)

In MOM estimation of parameters of a probability distribution function is straightforward and the parameters are obtained by equating the moments of the sample with the moments of the probability distribution function. For a distribution with k parameters the first k sample moments are set equal to the corresponding population moments that are given in terms of unknown parameters. These k equations are then solved simultaneously for the unknown parameters (Rao & Hamed, 2000).

b.Method of Maximum Likelihood (MLM)

Estimation by the ML method involves the choice of parameter estimates that produce a maximum probability of occurrence of the observations. The parameter estimates that maximize the likelihood function are computed by partial differentiation with respect to each parameters and setting these partial derivatives equal to zero and finally solve the resulting set of equations simultaneously. The equations are usually complex and can only be solved by numerical techniques. As a result of this difficulty, the solution set may not be properly found (Rao & Hamed, 2000).

c .Probability Weighted Method (PWM)

Parameter estimates are obtained in this method, as in the case of MOM, by equating moments of the distributions with the corresponding sample moments. For a distribution with k parameters, which are to be estimated, the first k sample moments are set equal to the corresponding population moments. The resulting equations are then solved simultaneously for the unknown parameters. Parameter estimation by PWM, which is relatively new, is as easy to apply as ordinary moments (MOM). It is usually unbiased and is almost as efficient as ML (Rao & Hamed, 2000).

2.12 Previous Extreme Rainfall Studies in Ethiopia

In the past different researchers have done analysis on rainfall intensity duration frequency analysis for different parts of the country; some of these research works include: IDF relationships which have been developed for SNNPR (Feleke Gerbi, 2006), Oromiya (Chali Edessa, 2007) and Tigray and Amhara (Asres G. 2008) regional states respectively. These relationships were developed based on the traditional approach which follows sequential steps and involves rigorous equation where the annual maximum rainfall data were analyzed using the method of frequency analysis and mathematical relationships were developed. In these models a large number of parameters are estimated and provided for only some specific return periods. In contrast to the above method Megersa T. (2009) and Eyoel L.(2010) developed depth duration frequency model for Oromia and Amhara and Tigray regions respectively based on scaling analysis.

The above studies were conducted using frequency analysis and scaling analysis but they did not say anything about the change and consequences of climate variability.

2.12.1 Previous Studies on the Impact of Climate Change on IDF of Upper Blue Nile River Basin

Development of IDF relationships and construction of IDF curves covering Amhara and Tigray regional states to estimate the intensity and duration of extreme rainfall event were developed by Asres Geda (2008) using conventional approaches by fitting probability distributions for several pre selected rainfall durations. For the same region mentioned above, Depth Duration and Frequency (DDF) relationships were developed using scale invariance approach. And also some research works were done about IDF in SNNPR, Oromia region, Northern Ethiopia. As it is clearly observed that, these researches about IDF or DDF had not covered the impact of climate change in Ethiopia as a whole and there was no chance to get standard IDF relationships considering climate change. This study will try to show the impacts of climate change and indicate how procedures and methods should be applied to cope up the problem.

2.12.2 Research on Climate Change Impact on Hydrology and Water Resources of the Upper Blue Nile River Basin, Ethiopia (IWMI RR-126)

The study divides the basin in to six sub basins and develops six different climate scenarios from global circulation models (GCMs). The research uses two simple hydrological models to simulate the runoff. The main findings of the study can be summarized as follows;

- ✓ The climate in most of the Upper Blue Nile River Basin is likely to become wetter and warmer in the 2050s.

- ✓ Low flow may become higher and sever mid to long term drought are likely to become less frequent throughout the basin; and
- ✓ The potential future dam operation are unlikely to significantly affect the water availability to Sudan and Egypt based on predicted outflow from six GCMs and many dam operational policies

This study indicates that the intensity duration and frequency relationships of the region will change depending on the activities of humans throughout the world.

3.0 METHODES AND PROCEDURES

3.1 Procedures

3.1.1 Data Description and Processing

The data used in this study are recorded rainfall (predictand) which are obtained by first setting selection criteria of stations to obtain a relatively better representation of the region and believed to be representing the region's different climatic characteristics and the regionally downscaled rainfall data of having A_1B scenario around the selected stations. Therefore, first class automatic recording stations in the region and those stations having good correlation coefficient relationship with the globally downscaled grid data (predictor) are considered to retrieve the required data for IDF development.

3.1.2 Rainfall Data

As per station selection criteria, nine different stations of the upper Blue Nile region and two neighboring stations were selected, by considering their regional representation and representation of the different climatic regions and those stations which can be correlated to the grid data (predictor) downscaled globally. This is done using statistical downscaling model (SDSM 4.2) which has a screening capability.

Rainfall data, which is rainfall depth used for this study, was collected from daily recorded rainfall available in NMSA and the scenario data were obtained from the international water management institute, Ethiopia. Then the annual maximum time series for each year of data for a specific station obtained in this way was used for the analysis. Figure 3.1 shows the location of these stations which are located in such a way that they represent the region's different geographical coverage. Concerning the length of years of record regardless of the record length of each station, 10 years of data were taken for each station since the grid scenario data given from international water management institute (IWMI), Ethiopia has 10 years of length.

The Intensity duration frequency (IDF) analysis starts by gathering time series records of different durations. After time series data is gathered, annual extremes are extracted from the record of each durations. The annual extreme data is then fit to a probability distribution which is necessary to standardize the character of rainfall across stations with widely varying lengths of record.

Table 3.1 Location and description of Sample Rainfall Stations in the Study area

No.	Station Name	Length (years)	Location			Period of Record given	Areal Scenario data given	Areal Scenario data Given
			Lat. (degrees)	Long. (deg)	Elevan (masl)	1991-2000	2031-2040	2091-2100
1	Bahirdar	10	11.60	37.40	1770	1991-2000	2031-2040	2091-2100
2	Gonder	10	12.55	37.42	1967	1991-2000	2031-2040	2091-2100
3	Dangilla	10	11.12	36.42	1290	1991-2000	2031-2040	2091-2100
4	D/Markose	10	10.33	37.67	2515	1991-2000	2031-2040	2091-2100
5	Kombolcha	10	11.32	39.07	1900	1991-2000	2031-2040	2091-2100
6	Haike	10	11.07	39.44	1903	1991-2000	2031-2040	2091-2100
7	Nekmte	10	9.11	37.45	2010	1991-2000	2031-2040	2091-2100
8	Alem ketema	10	10.03	39.03	2264	1991-2000	2031-2040	2091-2100
9	Fiche	10	9.81	38.3	2796	1991-2000	2031-2040	2091-2100
10	Assosa	10	10.07	36.4	1514	1991-2000	2031-2040	2091-2100
11	Shambu	10	9.57	37.10	2556	1991-2000	2031-2040	2091-2100

3.2 Software Used

In this study, different softwares are used, depending on the need. The softwares used are : Arc GIS to locate the station and delineate the study area. MS Excel 2007 was also used for data analysis and graphical distribution fitting. Statistical down scaling model (SDSM 4.2) is used to bring the areal grid data to station data and also a decision support tool for assessing local climate change impacts using a robust statistical downscaling technique that facilitates the rapid development of multiple, low cost, single site scenarios of daily surface weather variables under present and future climate forcing. Additionally, the software performs ancillary tasks of data quality control and transformation, predictor variable pre screening, model calibration, generation of rainfall for various scenarios and basic diagnostic testing, statistical analyses and graphing of climate data ,easy fit soft ware for evaluating parent distribution and IDF curve fitting tool (miduss software version 2.25) for IDF curve and parameter estimation .

3.3 Methodology

The Intensity duration frequency (IDF) analysis was started by downscaling the 50km by 50km grid data in to station data using statistical down scaling model (SDSM 4.2) followed by generating different scenario data at the station for different ranges of scenario and gathering time series records of different scenarios. After time series data is gathered, annual extremes are extracted from the record of each range. The annual extreme data is then fit to a probability distribution which is necessary to standardize the character of rainfall across stations with the same lengths of record.

Based on the estimated quantiles intensity of rainfall is determined. With the help of IDF curve fit tool (Miduss software) and calculated intensity values, IDF parameters were estimated. By making use of the estimated parameters, the IDF curve is constructed. And these local IDF curves are used to observe the impacts of climate change on design municipal water management infrastructure such as sewers, storm water management ponds or detention basins, street curbs and gutters, catch basins, culverts, etc. These curves are also used to design safe and economical flood control measures and to predict when an area will be flooded, or to pinpoint when a certain rainfall rate or a specific volume of flow will recur in the future based on the current global phenomena.

IDF equations were developed based on the mathematical expression suggested by Wenzel, (1982). Because of its simplicity, applicability for most locations and suitability for Miduss software, equation developed by Wenzel is used for estimation of IDF parameters for this study.

3.3.1 Statistical Down Scaling Methods (SDSM 4.2.2)

SDSM which is designed to downscale climate information from coarse resolution of GCMs to local or site level is applied here to downscale the precipitation, maximum and minimum temperatures for the study area. SDSM uses linear regression techniques between predictor and pridictand to produce multiple realizations (ensembles) of synthetic daily weather sequences. The predictor variables provide daily information about large scale atmosphere condition, while the pridictand described the condition at the site level.

It is appropriate to use this software when the impact assessments is require at small scale or regional level, provided that quality observational data and large scale daily GCMs climate variables are available. Additionally, the model can also produces a range of statistical parameters such as variances, frequencies of extremes and spell lengths for the downscaled climatic parameters (R.L. Wilby and C.W.Dawson, 2007).

SDSM software is published in different version at various times, among them the latest version is adopted for this particular study (i.e. version 4.2.2 SDSM software coded in Visual Basic 6.0). The main reasons to apply the SDSM model for the study are;

- It is widely applied in many regions of the world over a range of different climatic condition.
- It can be runs on PC based systems and has been tested on Windows 98/NT/2000/XP.
- The availability of the software (i.e. new users can register and download freely the software package at https://co-public.lboor.ac.uk/cocwd/SDSM/)
- Compared to other downscaling methods, the knowledge of atmospheric chemistry required by the SDSM is less.
- The required time for simulating the surface weather parameter is low.
- The ability of the model to permit risk/uncertainty analyses by using the generated ensembles.

Drawbacks related SDSM

The limitation related to SDSM model can be summarized as follows;

- ✓ The relationship between the predictor and predictand is achieved by only considering the data statistical condition, i.e. the model does not take in to consideration the physical nature of the catchments (major drawback).
- ✓ It requires high quality data for model calibration;
- ✓ The model is highly sensitive to the choice of predictor variables and empirical transfer scheme.

Even if global climate models in the future are run at high resolution there will remain the need to ‘downscale’ the results from such models to individual sites or localities for impact studies (DOE, 1996; p34***)***

A decision support tool for assessing local climate change impacts using a robust statistical down scaling technique. SDSM 4.2 (**S**tatistical **D**own **S**caling **M**odel) facilitates the rapid development of multiple, low cost, single site scenarios of daily surface weather variables under present and future climate forcing. Additionally, the software performs ancillary tasks of data quality control and transformation, predictor variable pre screening, automatic model calibration, basic diagnostic testing, statistical analyses and graphing of climate data.

The SDSM software reduces the task of statistically downscaling daily weather series into seven discrete steps:

- ➢ quality control and data transformation
- ➢ screening of predictor variables;
- ➢ model calibration;
- ➢ weather generation (using observed predictors);
- ➢ statistical analyses;
- ➢ graphing model output;
- ➢ Scenario generation (using climate model predictors).

3.3.2 Issues for Statistical Downscaling

Performance criteria: assessment of climate change impact on the water resource and related infrastructures were evaluated by using different performance criteria in the previous studies or researches which are conducted in various place of the world.

Performance criteria provide a measure of just how well a plan or management policy performs. The performances criteria of the water resource system can be derived, once the hydrological inputs are simulated and produces what one believes could occur in the future (Loucks, 1997). These time series value themselves can be measured by the major and most commonly used statistical performance criteria; these are reliability, resilience and vulnerability. The relative sustainability of the system with respect to each of these criteria is higher when there is greater reliability and resilience, and smaller vulnerability.

Generally, reliability measures the probability that the system will remain in non failure state and resilience describes the ability of a system to return to non-failure state after a failure occurred while vulnerability measures the likely damages of failure events.

Choice of statistical method: The choice of statistical method is to some extent determined by the nature of the local predictand. A local variable that is reasonably normally distributed, such as mean temperature will require nothing more complicated than(multiple) regression, since large scale climate predictors tend to be normally distributed assuming linearity of the relationship. A local variable that is highly heterogeneous and discontinues in space and time such as daily precipitation will require a more complicated nonlinear approach or transformation of the raw data.

Choice of predictors: Identifying empirical relationships between gridded predictors (such as mean sea level pressure) and single site predictands (such as station precipitation) is central to all statistical downscaling methods.

The main purpose of the Screen Variables operation is to assist the user in the selection of appropriate downscaling predictor variables. This is one of the most challenging stages in the development of any statistical downscaling model since the choice of predictors largely determines the character of the downscaled climate scenario. The decision process is also complicated by the fact that the explanatory power of individual predictor variables varies both spatially and temporally. Screen Variables facilitates the examination of seasonal variations in predictor skill**.**

3.3.3 Calibration, Verification of the model and Generation of future data

Data Quality

Few meteorological stations have complete and/or fully accurate data sets. Handling of missing and imperfect data is necessary for most practical situations. Prior to model calibration it may also be necessary to check the quality of the data. SDSM enables data quality checking of an input file for missing data and/or suspect values. So the input data was checked using quality control button.

The quality control session of SDSM enables to see the minimum, maximum, mean, number of values in the file, missing data value and its code.

Station data

Testing for Outliers

An outlier is an observation that deviates significantly from the bulk of the data, which may be due to errors in data collection, or recording, or due to natural causes. The presence of outliers in the data causes difficulties when fitting a distribution to the data. Low and high outliers are both possible and have different effects on the analysis (Rao and Hamed, 2000).The retention or deletion of these outliers can significantly affect the magnitude of statistical parameters computed from the data, especially for small samples.

As it is cited in Rao and Hamed (2000) Grubbs and Beck (G-B) (1972) test is used to detect outliers. In this test the quantities X_H and X_L are calculated using the following equations.

$$X_H=\exp(x+k_n*s) \quad (3.1)$$

$$X_L=\exp(x-k_n*s) \quad (3.2)$$

Where : X and S are the mean and standard deviations of the natural logarithm of the annual rainfall peaks respectively and Kn , is the G-B statistic tabulated for various sample sizes and significant levels by Grubbs and Beck(1972). At 10% significant level, the following approximation proposed by Pilon et al. (1985) is used, where n is the sample size.

$$\mathbf{K_n=-3.62201+6.28446n^{1/4}-2.49835n^{1/2}+0.49146n^{3/4}-0.037911n}$$

Sample values greater than X_H are considered to be high outliers, while those less than X_L are considered to be low outliers. All stations are cheched for the downscaled and observed data.

Screening Downscaling Predictor Variables

The next step is to identify empirical relationships between gridded predictors (such as mean sea level Pressure, precipitation) and single site predictands (such as station precipitation) which is central to all statistical downscaling methods and is often the most time consuming step in the process. The purpose of the Screen Variables option is to assist the User in the choice of appropriate downscaling predictor variables for model calibration. To investigate potentially useful predictor predictand relationships the screening section plays an important role. Some stations (Nefase Mewcha) could not have relationship with the predictor around it that is way it was left out from analysis.The model never run for those stations like Nefase Mewcha or it runs for the wrong assumption.

This is one of the most challenging stages in the development of any statistical downscaling model since the choice of predictors largely determines the character of the downscaled climate scenario. The decision process is also complicated by the fact that the explanatory power of individual predictor variables varies both spatially and temporally. Screen Variables facilitates the examination of seasonal variations in predictor skill.

Structure and operations of SDSM

The structure and operations of SDSM can be best described with respect to seven tasks as indicated in ***bold box*** in the following figure (R.L. Wilby and C.W.Dawson, 2007).

Figure 3. 1 SDSM (version 4.2) Climate scenario generations

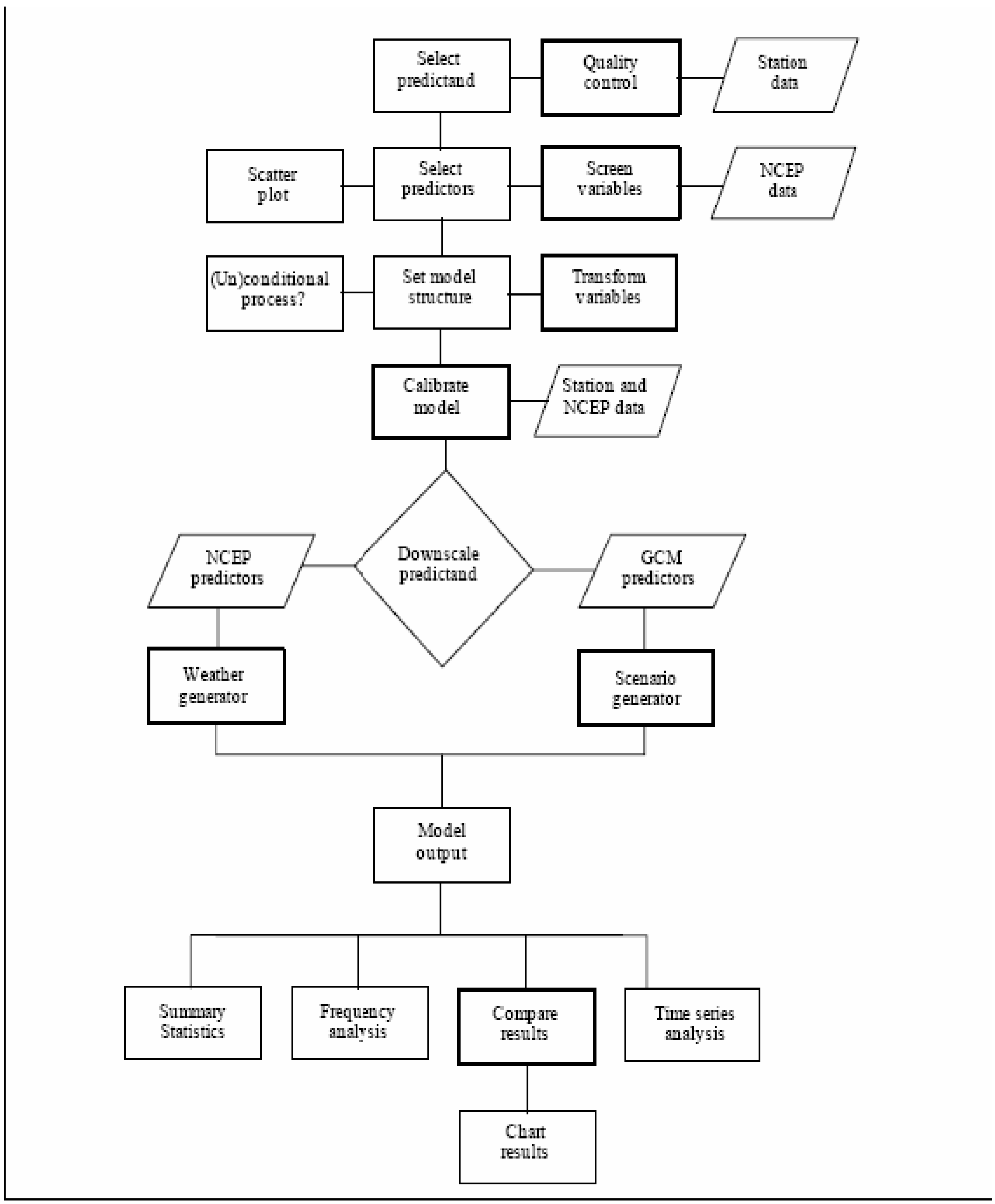

The **Calibrate Model** process constructs downscaling models based on multiple regression equations, given daily weather data (the predictand) and regional scale, atmospheric (predictor) variables. The parameters of the regression model are written to a standard format file with the extension *.PAR, along with meta data recording details of the calibration period, model type, predictors used. SDSM optimizes the model using either dual simplex or ordinary least squares optimization.

The User specifies the model structure: whether monthly, seasonal or annual sub–models are required; whether the process is unconditional or conditional. In unconditional models a direct link is assumed between the predictors and predictand (e.g., local wind speeds may be a function of regional airflow indices). In conditional models, there is an intermediate process between regional forcing and local weather (e.g., local precipitation amounts depend on wet /dry day occurrence, which in turn depend on regional–scale predictors such as humidity and atmospheric pressure.For the predictand and the predictor data taken for model calibration were from 1991-2000 calender year for all stations and selected grid data.

Main processes in calibrating of the Model

Variance Inflation: Controls the magnitude of variance inflation in downscaled daily weather variables. The default value produces approximately normal variance inflation (prior to any transformation). Larger values increase the variance of downscaled properties. Variance inflation is de–activated by setting the parameter to zero. This parameter also affects changes in the mean estimate. In calibrating the model the default variance inflation which is 12 was kept constant to compensate by the change in the bias correction.

Bias Correction: Compensates for any tendency to over or under estimate the mean of conditional processes by the downscaling model (e.g., mean daily rainfall totals). The default value is 1.0, indicating no bias correction. The model was calibrated by varying the bias correction from zero to two.The processes stops when the graph of the statistical parameters of the observed and the generated data have of the same pattern. As shown below for kombolcha station.This graphs are used for verifying of the nature of relationship between the predictor and predictand.

Graphical model out puts or graphical analysis:-Three options for graphical analysis are provided by SDSM 4.2 through the Frequency Analysis, Compare Results, and the Time Series Analysis screens.

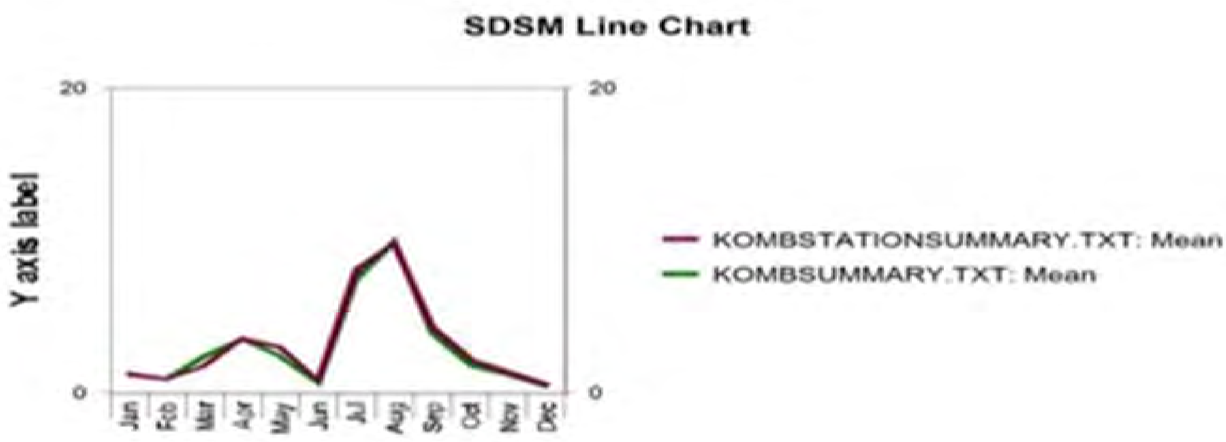

Figure 3.2 graph that shows the relation of the staticall parameter mean of the observed and scenario data of Kombolcha station.

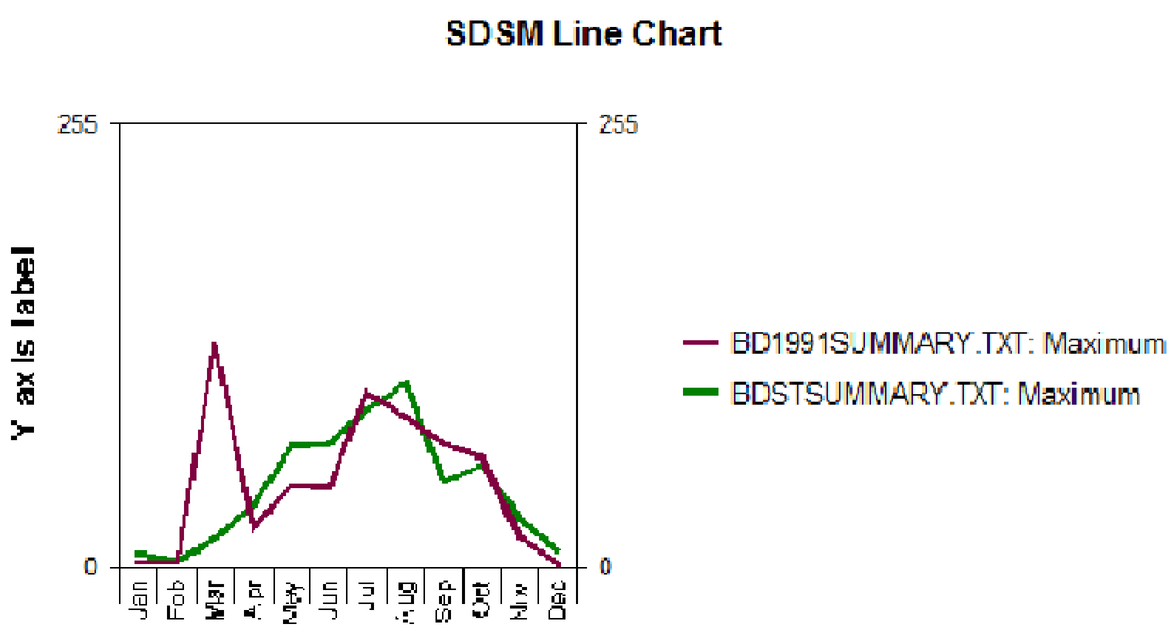

Figure 3.3 graph that shows the relation of the staticall parameter maximum of the observed and scenario data of Bahirdar station.

Weather generator: The Weather Generator operation produces ensembles of synthetic daily weather series given observed atmospheric predictor variables and regression model weights produced by the Calibrate Model operation.

The Weather Generator enables the verification of calibrated models (assuming the availability of independent data) as well as the synthesis of artificial time series representative of present climate conditions. The Weather Generator can also be used to reconstruct predictands or to infill missing data.

Analysis of Observed and Downscaled data: Statistical analyses of observed and downscaled weather data are handled in slightly different ways by SDSM but both are performed in the Summary Statistics screen. Common diagnostic tests are available for both observed and synthetic data. These statistics include the variable mean, sum maximum, minimum, variance, peaks above/below thresholds, percentiles, percent wet days, and wet/dry day spell lengths, computed on a calendar month, seasonal or annual basis.

After the preparation of the above statistical natures of a data whether observed or synthesized, the compare results screen displays what the relationship looks like for selected item (eg mean, sum).Then if it is ok as show in the above figure above, the scenario generation follows.

Scenario Generator operation: produces ensembles of synthetic daily weather series given daily atmospheric predictor variables supplied by a GCM (either under present or future greenhouse gas forcing). The GCM predictor variables must be normalised with respect to a reference period (or control run) and available for all variables used in model calibration. After observing the performance of the model calibration processes from the summary statistics and compare results screen,the scenario of 2031-2040 and 2091-2100 calendar year were generated for the stations considered.

Conditional Selection: Adjusts the way in which conditional processes (e.g., rainfall amounts) are sampled. The default (Stochastic) allows the outcome to be entirely based on chance. Fixed Threshold allows the User to increase the chance of a conditional event (by setting the threshold closer to zero), or reducing the chance (by setting closer to 1.0).

Optimisation Algorithm: SDSM 4.2 provides two means of optimising the model Dual Simplex (as in earlier versions of SDSM) and Ordinary Least Squares. Although both approaches give comparable results, Ordinary Least Squares is much faster. The User can also select a Stepwise

Regression model by ticking the appropriate box. Stepwise regression works by progressively including more variables and selecting the most parsimonious model of the predictand according to one of two metrics either Akaike's Information Criterion (AIC) or the Bayesian Information Criterion (BIC).

3.3.4 Disaggregation of daily rainfall

Rainfalls for shorter durations were not available for the selected eleven stations located in the study area under climate change scenario. Consequently, a convenient method of converting 24-Hr rainfalls depths into rainfalls depths of different durations was adopted to constitute 5-min, 10-min and other smaller durations' rainfall depths required in constructing IDF curves. The method, rainfall ratio method is briefly presented below.(Ethiopian road authority drainage design manual 2002).

The Rainfall Ratio Method (Transport and Road Research Laboratory, Department of Environment, TRRL Laboratory Report 623; The Prediction of Storm Rainfall in East Africa, B. Fiddes, G.A Forsgate & A.O. Grigg) was used to estimate the rainfall depth to be distributed at required duration based on a 24 hour rainfall. For this, the following the relationship can be applied.

$R_t / R = (t / 24) [(b + 24)^n / (b + t)^n]$……………………………………………(3.3)

where:

R_t/R: Rainfall ratio Rt: R24

Rt: Rainfall in a given duration't' (hr)

R24: Rainfall in 24 hours but for this study R_{24} refers daily maximum rainfall.

n: constant

b: constant

t: time (hr)

Based on studies of a large number of rainfall gauges in East Africa, the average values of b and n are found to be 0.3 and 0.9 respectively (range of n is 0.78 to 1.09). These values have been adopted for the study area.

Assuming that the durinal variation of these constants such as b and n is constant, the conversion of the daily maximum rainfall into smaller hours is made using the above rainfall ratio method. The following graphs show that there is good relationship between the daily maximum rainfall and the hourly rainfall with correlation coefficient of one and the above constants will also be used in the future.

The following graph and table shows the relationship between the observed rainfall and the disaggregated rainfall at Bahirdar station of 12 hr.

Table 3.2 Relationship of observed and disaggregated rainfall at Bahirdar station for 12 hr duration.

Year	Observed rainfall of 12hr	Disaggregated rainfall of 12hr
1991	60.1	62.01
1992	52.1	59.15
1993	31.3	34.60
1994	41.5	38.29
1995	46.6	54.81
1996	45	43.74
1997	63.8	59.42
1998	39.7	37.74
1999	45.7	44.20
2000	98.9	92.18

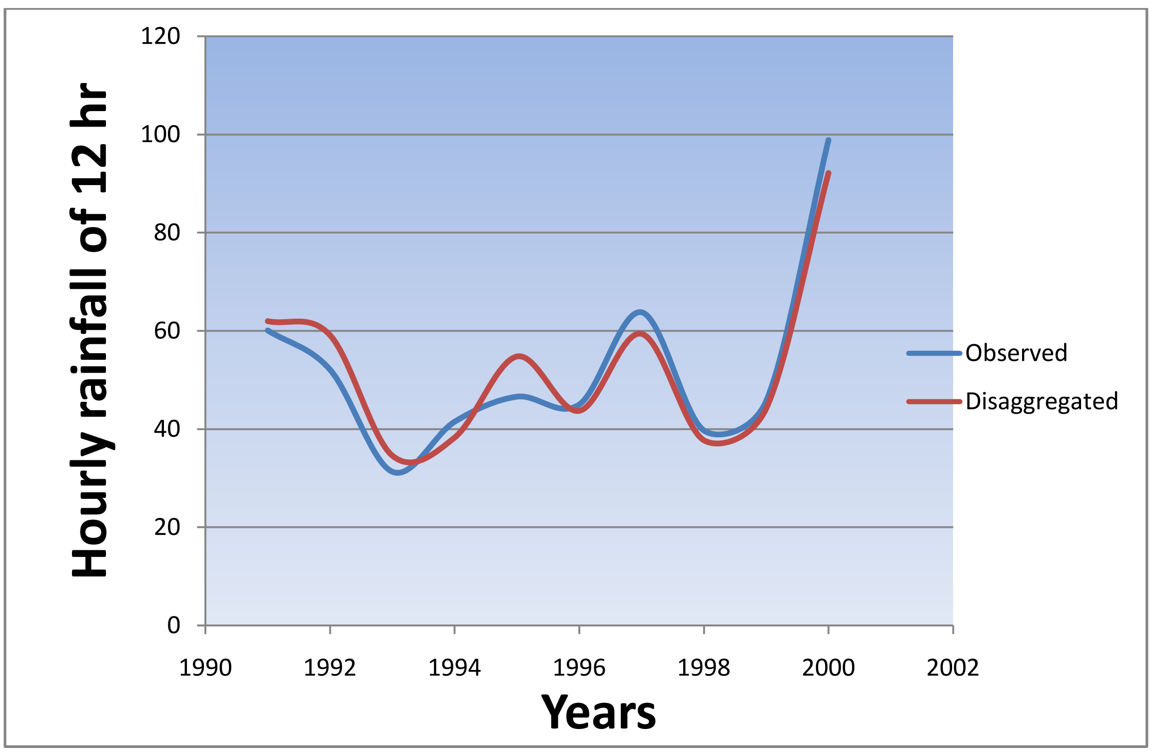

Figure 3.4 graph that shows the relationship between Observed hourly and disaggregated rainfall data at Bahirdar station.

The graph shows that there is good relationship between observed and disaggregated rainfall data.

3.3.5 Mathematical IDF Equation Development

The Intensity duration frequency (IDF) analysis starts by gathering time series records of different durations. After time series data is gathered, annual extremes are extracted from the record of each durations. The annual extreme data is then fit to a probability distribution which is necessary to standardize the character of rainfall across stations with same lengths of record.

Based on the estimated quantiles intensity of rainfall is determined. With the help of IDF curve fit tool (Miduss software version 2.25) and calculated intensity values, IDF parameters were estimated. By making use of the estimated parameters, the IDF curve is constructed. And these local IDF curves are used to design municipal water management infrastructure such as sewers, storm water management ponds or detention basins, street curbs and gutters, catch basins ,culverts, etc. These curves are also used to design safe and economical flood control measures and to predict when an area will be flooded, or to pinpoint when a certain rainfall rate or a specific volume of flow will recur in the future.

IDF equations were developed based on the mathematical expression suggested by Wenzel, (1982). Because of its simplicity, applicability for most locations and suitability for Miduss software (version 2.25), equation developed by Wenzel is used for estimation of IDF parameters for this study.

4 .0 DATA ANALYSIS, RESULTS AND DISCUSION

4.1 Selection and evaluation of parent distributions for the rainfall data

4.1.1The probability distributions: The distribution models which are recommended by WMO for annual maximum data series (Cunnane, 1989) are;

1. Normal distribution (N)
2. Two parameter Log-Normal distribution (LN2)
3. Three parameter Log Normal distribution (LN3)
4. Exponential distribution (EX)
5. Two parameter Gamma distribution (G2)
6. Pearson three distribution (PIII)
7. Log Pearson three distributions (LP3)
8. Generalized extreme value distribution (GEV)
9. Extreme value type one distribution (EVI)
10. Weibul distribution (W)
11. The five parameter Wakeby distribution (WAK5)
12. The four parameter Wakeby distribution (WAK4)
13. The generalized Pareto distribution (GP)
14. Log Logistic distribution (LLg)
15. Generalized Logistic distribution (GL)

4.1.2 Moment Ratio Diagrams

For each station, pairs of coefficient of skew ness (Cs) and coefficient of kurtosis (Ck) can be computed and plotted on the Cs - Ck diagram for each stations. The location of the sample estimate with respect to the distributions gives an indication of the suitability of the distribution to the data. However, if the sample size is small, the bias in the values of higher moments may be larger enough to give misleading results. The bias correction depends on the sample size, parent skewness and the form of the parent distributions (Cunnane, 1989, App.3)

4.1.3 L-Moment Ratio Diagrams

Analogous to the conventional MRDs, the L-moment ratio diagrams are based on the relations between the L-moment ratios. A diagram based on L-Cs (τ3) versus L-Ck (τ4) is used to identify appropriate distributions that best fits the rainfall data. For each station the sample L-moment ratios t3 and t4 are plotted on the L-moment ratio diagrams. A suitable parent distribution is that which the average value of (t3, t4) gets close to it (Rao et. al. 2000).

The L-moment ratio diagrams are based on unbiased sample quantities in contrast to Cs and Ck which have to be corrected for bias. It was shown by Hosking (1990) that Cs and Ck values from several samples drawn from three different distributions lay close to a single line on the graph and overlaps each other offering little hope of identifying the population distribution. In contrast, the sample L-moment ratios plot as fairly well separated groups and permit better discrimination between the distributions. Thus, the identification of a parent distribution can be achieved much more easily by using L-moment ratio diagrams than conventional moment ratio diagrams especially for skewed distributions.

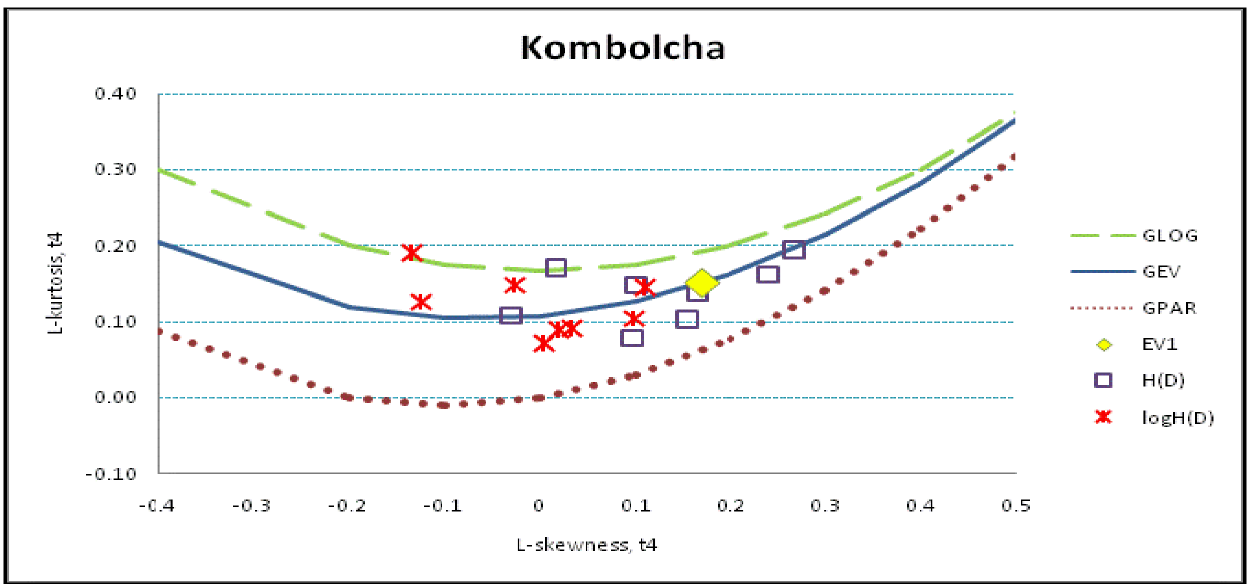

Fig 4.1 L-moment diagram

4.1.4 Selection of parent distribution

- ✓ Most of the stations in Amhara regional state are represented by gama family (two parameter gama distributions and pearson III) distributions.(Asres Geda 2008).
- ✓ A previous study of the regional frequency analysis identified general extreme value (GEV) is considered most likely parent distribution particularily for longer durations of more than 3hours.
- ✓ EV1(2) best fits the annual maximum rainfall of 24hour duration while pearson III best fits 3hour duration.(Asres Geda 2008)
- ✓ An extreme value type I distribution is selected as a parent distribution for the northern Ethiopia (cherkose Tefera 2002).
- ✓ Practically three different probability distributions; lognormal log pearson,and gumbel extreme value type I which are the most commonly candidates for extreme value distributions analysis have been considered in Ethiopia. The probability distribution which best fits the sample data among the three is selected using curve fitting method.(ERA manual 2002)
- ✓ For return period less 100 years, most probability distributions have almost similarity in quantile estimation results .

According to the thesis conducted by Asres Geda ,applying the common conventional approach, best fitted distributions for the indicated durations depending on the smallest Standard Error of estimate of 24 hour are:

Table 4.1 parent distributions for the selected stations and parameter estimation techniques

Station name	Selected parent distribution	Parameter estimation techniques
Gonder	GEV	MOM
Dangilla	G_2	MOM
Debre Markose	EV_1	ML
Haike	G_2	PWM
kombolcha	P_3	MOM
Bahirdar	G2	ML

Based on the easy fit software and goodness of fit measures, the above parent distribution in the table was checked using the easy fit software and the following improvements were made for the analysis period of 1991-2000.Table 4.2 Modified parent distributions for the selected stations and Gumbel distribution was selected for the remaining five stations.

Table 4.2 Modified parent distributions for the selected stations and parameter estimation techniques

Station	Selected parent distribution	Parameter estimation techniques
Gonder	GEV	MOM
Dangilla	EV1	MOM
Debre Markose	EV1	MOM
Haike	Logistic	ML
kombolcha	Logistic	ML
Bahirdar	EV1	MOM
Nekemte	EV1	MOM
Shambu	EV1	ML
Assossa	EV1	MOM
Fiche	EV1	ML
Alem ketema	EV1	ML

4.2 Probability Plots and Goodness-of-fit tests

Probability plots are used to visually evaluate the agreement between distribution and observed data and also extremely useful for visually revealing the character of a data set. If the fitted distribution is the exact parent distribution, this relationship should appear as a straight line through the origin with a 450 slope. Plots are an effective way to see what the data looks like and to determine if fitted distributions appear consistent with the data. Analytical goodness of fit criteria are useful for gaining an appreciation for whether the lack of fit is likely to be due to sample to sample variability, or whether a particular departure of the data from a model is statistically significant. In most cases several distributions will provide statistically acceptable fits to the available data so that goodness of fit tests is unable to identify the "true" or "best" distribution to use. Such tests are valuable when they can demonstrate that some distributions appear inconsistent with the data (Rao et. al., 2000).So in this thesis I use the above testes to evaluate some distributions.

The graphical evaluation of the adequacy of the fitted distribution is generally performed by plotting the observations so that they would fall approximately on a straight line if a postulated distribution were the true distribution from which the observations were drawn. This can be done with the use of special commercially available probability papers for some distributions.

4.3 Parameters and Quantiles Estimation

Parameters of the best fitted distributions are estimated based on the methods described in table after which, quantile estimates (X_T) corresponding to different return periods may be computed. The relation between return period and the probability of non-expedience (F) is given by:

$$F = 1 - \frac{1}{T} \text{---------------------} \quad (4.1)$$

Where; F=F (XT) is the probability of having a flood of magnitude XT or smaller.

The problem thus reduces to evaluating XT for a given value of F. Chow (1964)

proposed a general for calculating XT as follows.

$$X_T = U_1' K_T \sqrt{\mu_2} \text{----------------} \quad (4.2)$$

Where; K_T is the frequency factor which is a function of the return period and of the parameters of the distribution u_1' *and* μ_2 are the moments of the distribution

Based on the selected distributions the estimated quantiles for different rainfall

durations at Bahir Dar station for historic data of 1991-2000 years and scenario data of 2031-2040 and 2091-2100 is shown in table 4.3 below at different times.

Table 4.3.1

Time in minutes	Quantiles of rainfall (mm) using historical data of 1991-2000 for different return period at Bahirdar station					
	2	5	10	25	50	100
1440	64.6	72.2	77.3	83.7	88.4	93.1
720	59.6	66.7	71.3	77.2	81.6	85.9
360	54.4	60.9	65.1	70.5	74.5	78.4
300	53	59.3	63.4	68.6	72.5	76.4
180	48.7	54.5	58.3	63.1	66.6	70.2
120	44.9	50.2	53.8	58.2	61.5	64.8
60	37.5	42	44.9	48.6	51.4	54.1
30	29.1	32.5	34.8	37.6	39.8	41.9

Table 4.3.2

Time in minutes	Quantiles of rainfall (mm) using scenario data of 2031-2040 for different return period at Bahirdar station					
	2	5	10	25	50	100
1440	87.4	105	116.9	131.8	142.9	154
720	80.7	97	107.9	121.6	131.76	142
360	73.6	88.6	98.5	111	120.3	130
300	71.7	86.3	95.9	108.1	117.12	126
180	65.9	79.3	88.14	99.33	107.64	116
120	60.8	73.1	81.32	91.65	99.309	107
60	50.8	61.1	67.94	76.57	82.978	89.3
30	39.3	47.3	52.59	59.27	64.225	69.1

Table 4.3.3

Time in minutes	Quantiles of rainfall (mm) using scenario data of 2091-2100 for different return period at Bahirdar station					
	2	5	10	25	50	100
1440	73.3	82.3	88.2	95.7	101	107
720	67.6	75.9	81.4	88.3	93.4	98.5
360	61.8	69.3	74.3	80.6	85.3	90
300	60.1	67.5	72.3	78.5	83.1	87.6
180	55.3	62	66.5	72.1	76.3	80.5
120	51	57.2	61.3	66.6	70.4	74.3
60	42.6	47.8	51.3	55.6	58.8	62.1
30	33	37	39.7	43	45.5	48

Table 4.3 Estimated Quantiles for Bahirdar station at different time inteerval

The estimated quantiles for the rest of stations are tabulated in appendix B.

4.4. Intensity of Rainfall

The intensity is the time rate of precipitation, that is, depth per unit time (mm/hr or in/hr).Intensity of rainfall, i can be determined by using the following relation.

$$i = \frac{X_T}{D_i} = \frac{\text{rainfall depth (mm)}}{\text{duration of rainfall (minutes)}} \text{-----------------------------} (4.3)$$

Table 4.4 intensities of Bahirdar station at different times

Table 4.4.1 intensities of Bahirdar station at different times

Time in minutes	intensities of rainfall (mm/hr) using historical data of 1991-2000 for different return period at Bahirdar station					
	2	5	10	25	50	100
1440	2.69	3.01	3.22	3.49	3.68	3.88
720	4.97	5.55	5.94	6.43	6.8	7.16
360	9.07	10.1	10.9	11.7	12.4	13.1
300	10.6	11.9	12.7	13.7	14.5	15.3
180	16.2	18.2	19.4	21	22.2	23.4
120	22.5	25.1	26.9	29.1	30.7	32.4
60	37.5	42	44.9	48.6	51.4	54.1
30	58.1	65	69.5	75.3	79.5	83.8

Table 4.4.2 intensities of Bahirdar station at different times

Time in minutes	intensities of rainfall (mm/hr) using scenario data of 2031-2040 for different return period at Bahirdar station					
	2	5	10	25	50	100
1440	3.64	4.38	4.871	5.492	5.9542	6.41
720	6.72	8.09	8.99	10.13	10.98	11.8
360	12.3	14.8	16.42	18.5	20.05	21.6
300	14.3	17.3	19.18	21.62	23.424	25.2
180	22	26.4	29.38	33.11	35.88	38.6
120	30.4	36.6	40.66	45.82	49.655	53.5
60	50.8	61.1	67.94	76.57	82.978	89.3
30	78.6	94.6	105.2	118.5	128.45	138

Table 4.4.3 intensities of Bahirdar station at different times

Time in minutes	intensities of rainfall (mm/hr) using scenario data of 2091-2100 for different return period at Bahirdar station					
	2	5	10	25	50	100
1440	3.05	3.43	3.68	3.99	4.22	4.45
720	5.64	6.33	6.78	7.36	7.79	8.21
360	10.3	11.6	12.4	13.4	14.2	15
300	12	13.5	14.5	15.7	16.6	17.5
180	18.4	20.7	22.2	24	25.4	26.8
120	25.5	28.6	30.7	33.3	35.2	37.1
60	42.6	47.8	51.3	55.6	58.8	62.1
30	65.9	74	79.3	86.1	91.1	96.1

Table 4.4 shows the intensity for different durations and frequencies for Bahirdar station. The intensity for the rest of stations is tabulated in appendix D.

4.5 Estimation of the IDF Parameters

The IDF Curve Fit Tool (version 2.25) is used for this analysis which is a window version of the DOS program that estimate the parameter values from observed records of either depth or intensity within a range of time intervals and for a specified return interval based on the equation

$$I = \frac{A}{(D+B)^C} \text{--} (4.4)$$

Where; I= rainfall intensity (mm/hr)

D= duration of rainfall (minutes)

A= coefficient with units of mm/hr

B= time constant in minutes

C= an exponent usually less than one

The IDF Curve Fit tool manipulates data describing an Intensity Duration Frequency relates for a particular geographical locality and can be used in two modes:

(1) To compute the ‘A’, ‘B’ and ‘C’ parameters that most closely approximates a set of observed rainfall and scenario data.

(2) To compute the IDF curve for user supplied values of the three coefficients and compare this with observed and scenario data.

For any time interval the rainfall can be defined either as a total depth of rainfall or as an average intensity over the time interval (Gerbi, 2002).

4.5.1 The 'A' coefficient

The value of the 'A' coefficient depends on (i) the return interval in years of the storm and (ii) the system of units being used.

4.5.2 The B-constant

This constant in minutes is used to make the log-log correlation as linear as possible. Typical values range from 2 to 12 minutes. A value of zero for this parameter represents a special case of the IDF equation where

$$I = \frac{A}{D^{C}} \qquad (4.5)$$

In general, these results in poor agreement between observed values of intensity and duration and those represented by the IDF equation.

4.5.3 The C-exponent

This parameter is usually less than 1.0 and is obtained in the process of fitting the data to the power expression. Values are usually in the range of 0.75 to 1.0

Table 4.5 shows the computed parameters A, B, C of the IDF of various frequencies for all the stations considered as follows.

Table 4.5 the computed parameters A, B, C of the IDF equation of various frequencies

Table 4.5.1

station	Range of years	parameters	Values of each parameters for each return period					
			2	5	10	25	50	100
Bahirdar	1991-2000	A	1891.27	2113.43	2303.59	2444.04	2587.41	2766.95
		B	17.91	17.91	18.326	17.91	17.91	18.326
		C	0.8998	0.8997	0.9025	0.8994	0.8997	0.9020
	2031-2040	A	2593.03	3127.00	3414.98	3847.65	4167.84	4474.06
		B	18.326	18.326	17.910	17.910	17.910	17.910
		C	0.9017	0.9022	0.8994	0.8994	0.8993	0.8986
	2091-2100	A	2143.23	2442.92	2578.53	2796.82	2959.68	3110.74
		B	17.91	18.326	17.910	17.910	17.910	17.910
		C	0.8996	0.9019	0.8996	0.8995	0.8997	0.8989
Debre Markose	1991-2000	A	1334.17	1517.72	1708.64	1846.82	2009.17	2098.33
		B	17.91	16.945	18.326	17.910	18.326	17.910
		C	0.8995	0.8962	0.9019	0.8993	0.9020	0.8994
	2031-2040	A	1605.17	2008.	2265.68	1853.24	2307.64	2438.56
		B	17.910	18.326	19.305	18.269	17.910	17.910
		C	0.8997	0.9018	0.9065	0.9015	0.8997	0.8992
	2091-2100	A	1456.83	1594.61	1638.57	1723.90	1804.66	2103.13
		B	17.910	18.326	17.910	17.910	18.326	20.562
		C	0.8993	0.9011	0.8994	0.8989	0.8993	0.9160
Haike	1991-2000	A	1714.81	1788.72	1876.71	1920.35	1974.23	2028.44
		B	18.326	17.910	18.326	17.944	17.910	17.966
		C	0.9024	0.8998	0.9019	0.8996	0.8996	0.8998
	2031-2040	A	2253.84	2413.33	2504.33	2611.65	2708.95	2788.79
		B	17.910	17.910	17.910	18.331	17.910	17.910
		C	0.8996	0.8994	0.8993	0.8983	0.8997	0.8996
	2091-2100	A	1907.52	2074.93	2129.85	2245.93	2379.17	2397.99
		B	18.265	18.326	17.910	17.944	18.326	17.910
		C	0.9011	0.9017	0.8993	0.8998	0.9037	0.8994
kombolcha	1991-2000	A	1506.26	1615.20	1656.94	1722.96	1802.73	1847.74
		B	17.910	18.326	17.910	17.910	18.326	18.326
		C	0.8994	0.9004	0.8996	0.8994	0.9021	0.9017
	2031-2040	A	1783.13	1938.98	2064.24	2147.00	2274.21	2316.39
		B	17.910	17.910	18.326	17.910	18.326	17.910
		C	0.900	0.8993	0.9012	0.8991	0.902	0.8993
	2091-2100	A	2172.20	2405.75	2500.57	2707.97	2782.89	2952.08
		B	18.326	18.326	17.910	18.326	17.910	18.326
		C	0.9020	0.9020	0.8995	0.9020	0.8997	0.9022

Table 4.5.2

station	Range of years	Parameters	Values of each parameters for each return period					
			2	5	10	25	50	100
Danglla	1991-2000	A	1379.51	1565.24	1642.09	1803.39	1872.29	2001.22
		B	17.910	18.326	17.910	18.326	17.910	18.326
		C	0.8990	0.9020	0.8994	0.9020	0.8996	0.9021
	2031-2040	A	1641.85	1746.43	1848.13	1942.20	1983.72	2045.46
		B	17.910	17.910	18.326	18.326	17.910	17.910
		C	0.900	0.8994	0.9017	0.9019	0.8998	0.8993
	2091-2100	A	1894.60	2049.11	2199.05	2346.46	2417.14	2531.13
		B	18.326	17.910	18.326	18.292	17.910	17.910
		C	0.9018	0.8997	0.9020	0.9016	0.8990	0.8993
Gonder	1991-2000	A	1601.02	1870.33	1956.79	2088.09	2197.35	2222.27
		B	17.910	18.326	18.326	17.910	18.326	17.910
		C	0.8996	0.9023	0.8992	0.8998	0.9021	0.8995
	2031-2040	A	1909.51	2748.75	3573.52	5234.75	6973.45	9463.18
		B	17.910	18.103	17.910	18.103	17.910	17.910
		C	0.8994	0.9006	0.8994	0.9006	0.8994	0.8995
	2091-2100	A	1471.05	1440.59	1492.74	1554.69	1558.09	1586.20
		B	19.303	16.851	17.910	18.326	17.910	17.910
		C	0.9037	0.8976	0.8994	0.9017	0.8996	0.8998
Alem ketema	1991-2000	A	1877.40	2244.70	2528.15	2797.46	3025.77	3253.98
		B	17.910	17.910	18.27	17.910	17.910	17.910
		C	0.8994	0.8995	0.9017	0.8994	0.8994	0.8995
	2031-2040	A	2543.64	3178.88	3598.74	4128.97	4493.86	4913.23
		B	18.326	18.326	18.326	18.326	18.180	18.326
		C	0.9021	0.9021	0.9021	0.9021	0.9011	0.9021
	2091-2100	A	2354.26	3363.88	4059.91	4936.78	5591.40	6239.16
		B	18.326	17.910	17.910	17.910	17.910	17.910
		C	0.9021	0.8994	0.8994	0.8993	0.8994	0.8994

Table 4.5.3

station	Range of years	Parameters	Values of each parameters for each return period					
			2	5	10	25	50	100
Fiche	1991-2000	A	1721.44	1934.16	2055.23	2168.86	2321.86	2390.28
		B	17.910	18.326	18.326	17.910	18.326	17.910
		C	0.8994	0.9021	0.9021	0.8994	0.922	0.8994
	2031-2040	A	1791.54	2066.53	2226.83	2388.94	2536.17	2730.78
		B	17.910	18.326	18.326	17.910	17.910	18.326
		C	0.8994	0.9021	0.9020	0.8995	0.8994	0.9021
	2091-2100	A	1720.88	1918.17	2049.26	2175.32	2295.92	2415.59
		B	18.326	18.326	18.326	17.910	17.910	17.910
		C	0.9021	0.9021	0.9021	0.8994	0.8994	0.8994
Shambu	1991-2000	A	1898.36	2092.56	2193.75	2342.20	2634.53	2561.44
		B	17.910	18.103	17.910	17.910	20.56	17.910
		C	0.8995	0.9007	0.8994	0.8994	0.9097	0.8994
	2031-2040	A	1946.60	2155.87	2253.29	2425.21	2552.37	2679.19
		B	18.326	18.326	17.910	17.910	17.910	17.910
		C	0.9021	0.9021	0.8994	0.8994	0.8994	0.8994
	2091-2100	A	2286.78	2532.44	2675.64	2801.82	2929.17	3109.80
		B	17.910	18.279	18.326	17.910	17.910	18.326
		C	0.8994	0.9018	0.9021	0.8994	0.8995	0.9021
Nekemte	1991-2000	A	2712.56	3065.73	3209.05	3520.18	3644.90	3896.91
		B	17.910	18.326	17.910	18.326	17.910	18.326
		C	0.8994	0.9021	0.8994	0.9021	0.8994	0.9021
	2031-2040	A	2854.83	2989.95	3214.52	3369.22	3490.10	3747.07
		B	17.910	17.910	18.326	17.910	18.326	18.326
		C	0.8994	0.8994	0.9021	0.8994	0.8947	0.9021
	2091-2100	A	2357.18	2466.43	2584.22	2677.97	2746.86	2766.82
		B	17.910	17.910	18.326	18.326	18.326	17.910
		C	0.8994	0.8994	0.9021	0.9021	0.9021	0.8994
Assossa	1991-2000	A	1574.02	1903.59	2160.67	2397.81	2649.03	2857.21
		B	17.910	17.910	18.326	17.910	18.326	18.326
		C	0.8994	0.8994	0.9021	0.8994	0.9021	0.9021
	2031-2040	A	1563.79	1727.17	1824.83	1908.44	2029.41	2115.36
		B	17.910	18.326	18.326	17.910	18.326	18.326
		C	0.8993	0.9016	0.9020	0.8994	0.9021	0.9020
	2091-2100	A	1747.85	1925.56	2080.13	2193.30	2344.67	2412.76
		B	17.910	17.902	18.326	17.910	18.326	17.90
		C	0.8994	0.8994	0.9021	0.8995	0.9021	0.8994

From the above table a general trend of the following was observed. The “A” coefficient increases with an increase in return period and also in time for most of the stations considered generally. The “B” constant and the “C” exponent generally increase or decrease with increase or decrease of the “A” coefficient. For some exceptional stations a decrease of “B” and “C” for an increase in A was observed and also there is no significant increase or decrease of “B”and“C” in the three ranges of years such as 1991-2000,2031-2040 and 2091-2100.Besides, “B”and“C” slightly varies with an increase or decrease of return period and are not affected by climate change significantly.

Rainfall intensity of each station for all durations can easily be calculated based on the estimated IDF parameters with the general equation of the form

$i = \exp[(\ln(A) - C\ \ln(B + D))]$ ----------- (4.10)

Each station has different equation for different return period. The resulting six equations for each station can be used for intensity calculations in the area represented by that station. Listed below are the six equations for the IDF relationships at Bahirdar station by using the observed data (1991-2000) .

2 Year return period, i = exp [7.54 - 0.8998*ln (17.910+D)]

5 Year return period, i = exp [7.66 - 0.8997*ln (17.910+D)]

10 Year return period, i = exp [7.74 -0.9025*ln (18.326+D)]

25 Year return period, i = exp [7.80 - 0.8994*ln (17.910+D)]

50 Year return period, i = exp [7.86 - 0.8997*ln (17.910+D)]

100 Year return period, i = exp [7.93 - 0.9020*ln (18.326+D)]

Intensity Values generated from the above equations at Bahirdar station for different return periods are listed in table 4.7 below

Table 4.6 Calculated Intensity values for Bahirdar station at differ times

Table 4.6.1 Calculated Intensity values for Bahirdar station at differ times

duration (minute)	Intensity of rainfall(mm/hr) at Bahirdar station using the data observed in between 1991-2000					
	Intensity of rainfall(mm/hr) for the indicated frequency(years)					
	2	5	10	25	50	100
1440	2.68	3.02	3.21	3.48	3.69	3.63
720	4.94	5.58	5.93	6.43	6.81	6.7
360	9.02	10.2	10.8	11.7	12.4	12.3
300	10.5	11.9	12.7	13.7	14.5	14.3
180	16.2	18.2	19.4	21	22.3	21.9
120	22.4	25.2	26.9	29	30.8	30.4
60	37.4	42.2	44.9	48.6	51.5	50.7
30	57.9	65.3	69.4	75.2	79.7	78.4

Table 4.6.2 Calculated Intensity values for Bahirdar station at differ times

Intensity of rainfall(mm/hr) at Bahirdar in 2030s						
duration (minute)	Intensity of rainfall(mm/hr) for the indicated frequency(years)					
	2	5	10	25	50	100
1440	3.64	4.38	4.871	5.492	5.9542	6.41
720	6.72	8.09	8.99	10.13	10.98	11.8
360	12.3	14.8	16.42	18.5	20.05	21.6
300	14.3	17.3	19.18	21.62	23.424	25.2
180	22	26.4	29.38	33.11	35.88	38.6
120	30.4	36.6	40.66	45.82	49.655	53.5
60	50.8	61.1	67.94	76.57	82.978	89.3
30	78.6	94.6	105.2	118.5	128.45	138

Table 4.6.3 Calculated Intensity values for Bahirdar station at different times

Intensity of rainfall(mm/hr) at Bahirdar in 2090s						
duration (minute)	Intensity of rainfall(mm/hr) for the indicated frequency(years)					
	2	5	10	25	50	100
1440	3.05	3.43	3.68	3.99	4.22	4.45
720	5.64	6.33	6.78	7.36	7.79	8.21
360	10.3	11.6	12.4	13.4	14.2	15
300	12	13.5	14.5	15.7	16.6	17.5
180	18.4	20.7	22.2	24	25.4	26.8
120	25.5	28.6	30.7	33.3	35.2	37.1
60	42.6	47.8	51.3	55.6	58.8	62.1
30	65.9	74	79.3	86.1	91.1	96.1

4.6 Sensitivity of the IDF parameters

With an increase of the three IDF parameters by 10% and computation of rainfall Intensities using increased parameters, the sensitivity of IDF parameters were evaluated. Intensity obtained from the optimized IDF parameters and increased IDF parameters was compared. From the comparison it is observed that the “C” exponent is the most sensitive parameter. An increase in “C” exponent by 10% resulted in a difference of 26%-48% between the two values of rainfall optimimized and the increased one. This is a good indication that care has to be taken in determining the “C” exponent. Increasing the “A” coefficient by 10% resulted in a slight increase on the intensity by approximately 10% which indicate that the rate of increase or decrease in “A” coefficient causes a slight increase or decrease of the intensity of rainfall but the most sensitive parameter towards climate change is “A” as it is seen in table 4.7 below. An increase in the “B” constant has no significant change on the intensity of rainfall but there is slight change by 5% to 10% the optimized value.

The Table 4.7 shown below graphical comparison of the intensity of rainfall obtained from the optimized parameters and the increased parameters.

Results of the sensitivity test on the IDF parameters at on a return period 2 years at Bahirdar station using the following equation .

2 Year return period, i = exp [7.54 - 0.8998*ln (17.910+D)]

i-intensity of the given duration

D-Duration in minute

The Table 4.7 Tabular comparison of the intensity of rainfall obtained from the optimized parameters and the increased parameters.

Duration(min)	Intensity(0ptimize) A ,B and C	Intensity of 10% increase of" C"	Intensity of 10% increase of" A"	Intensity of 10% increase of"B"
30	57.88	40.86	63.96	61.89
60	37.37	25.25	41.30	40.46
120	22.35	14.34	24.70	24.42
180	16.15	10.03	17.85	17.70
300	10.54	6.27	11.65	11.59
360	9.02	5.29	9.97	9.93
720	4.94	2.72	5.46	5.45
1440	2.67	1.39	2.95	2.95

4.7 Evaluation of the method of parameter estimation

Graphical/Visual verification

Observed and computed intensities are plotted on the same graph and goodness of fit is evaluated. The result of the graph indicated that, the plot fall approximately on a straight line and the efficiency (R2) is approaching to 100% for all frequency.

Figure 4.2 shows the graphical comparisons of the computed and observed intensities and in addition observed and computed rainfall depths are compared graphically.

From the graph given below, it can be concluded that the estimated values using parameters describe the observed values.

Figure 4.2 Comparison of observed versus computed intensities values at Bahir Dar station for 100 year return period.

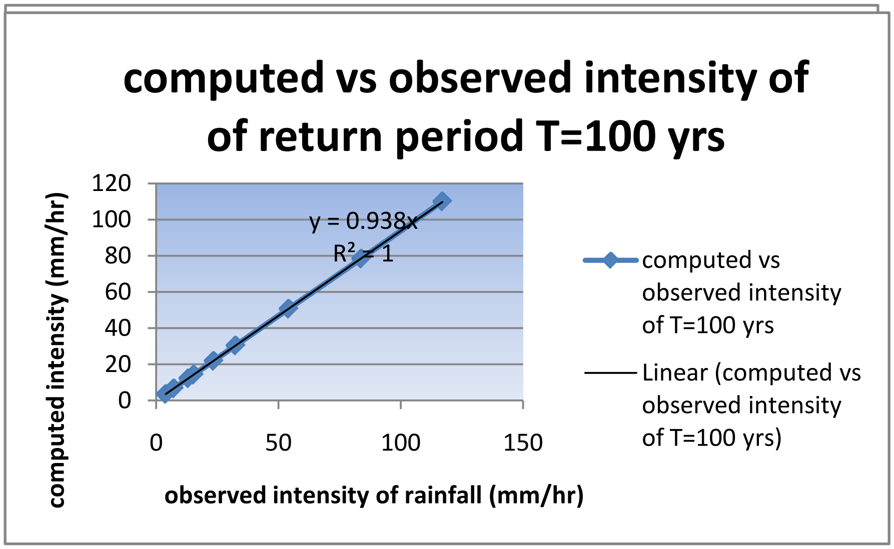

4.8 Construction of the IDF curve

The IDF curves were plotted on a double logarithmic scale, the duration D as abscissa and the intensity I as ordinate with the help of IDF curve fit tool. Figure 4.3 shows the IDF curves plotted on double logarithmic scale and for Bahir Dar station. The rest of the IDF curves for all the stations are compiled in appendix C.

Figure 4.3.1 IDF curves plotted on double logarithmic scale for Bahir Dar Station for different time periods.

Figure 4.3.1 IDF curves plotted on double logarithmic scale for Bahir Dar Station

Bahirdar from 1991-2000

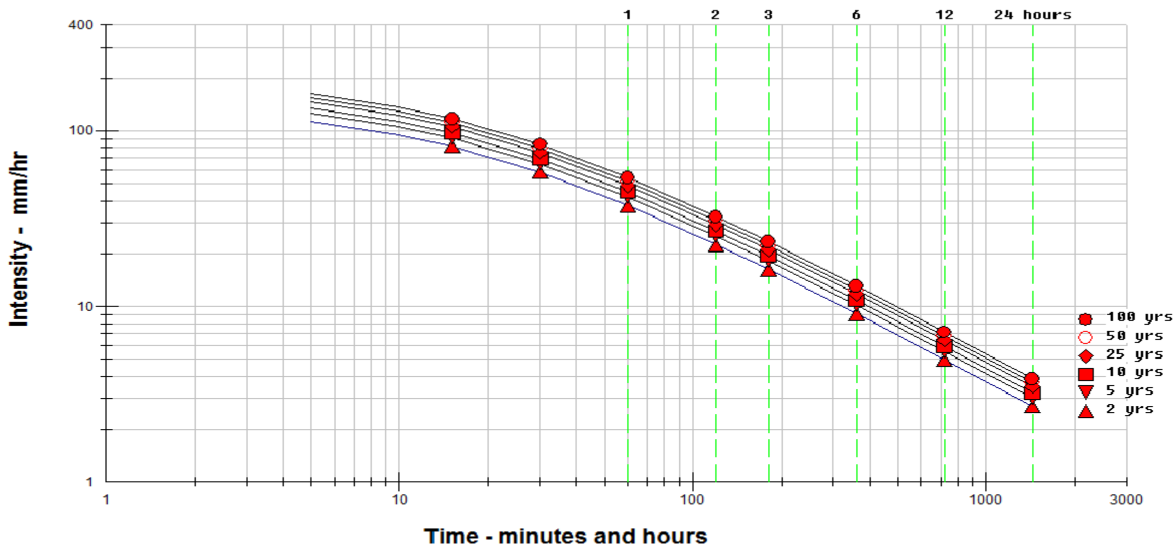

Figure 4.3.2 IDF curves plotted on double logarithmic scale for Bahir Dar Station
Bahirdar from 2031-2040

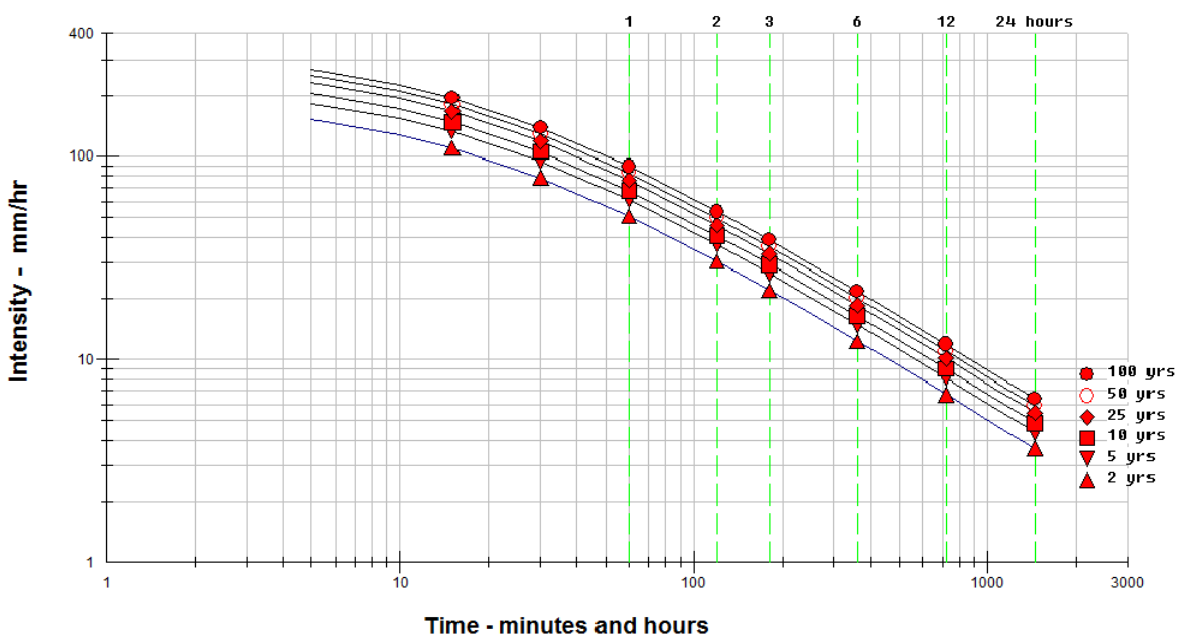

Fig 4.3.3 IDF curves plotted on double logarithmic scale for Bahir Dar Station

Bahirdar from 2091-2100

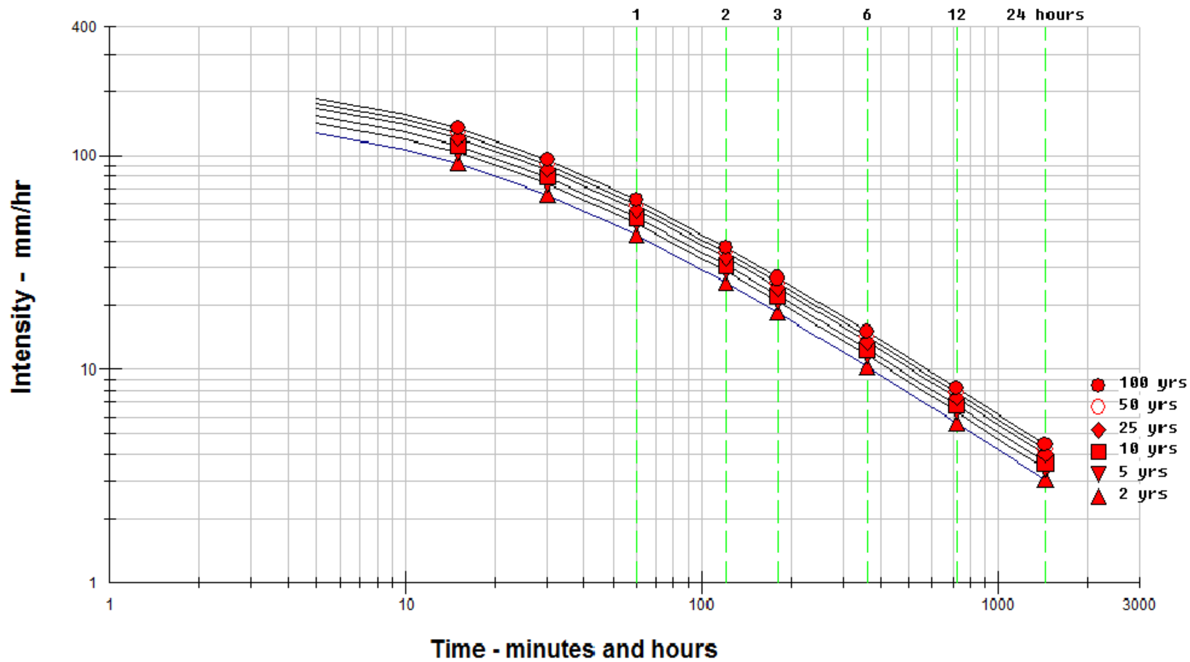

4.9 spatial variations in the development of IDF curve and equations

For a single station I used the same parent distribution and parameter estimation for frequency analysis for the three time segments to make easy the comparisons and to observe the changes that could be happened in the three time segments such as 1991-2000,2031-2040 and 2091-2100.But,the change in different stations are not of similar in nature .For example at Gonder station the parent distribution GEV and the parameter estimation MOM was used to analyze the rainfall data observed in between 1991-2000 and the computed rainfall data in 2031-2040 and 2091-2100 ranges of years. The quantile estimated using the observed data was near to the actual value but for the computed data of 2031-2040 ,the quantile data calculated was over estimated. To the contrary, the same parent distribution and parameter estimation technique ,the quantiles computed using the scenario data of 2091-2100 range of years was under estimated.From this it could be understood that the parent distribution and parameter estimation techniques will no longer be the same for a station under the changing climatic condition. For clarification the IDF curve for the three time intervals are shown below in fig 4.4.

Fig 4.4.1 intensities with time and return period Gonder in 1991-2000

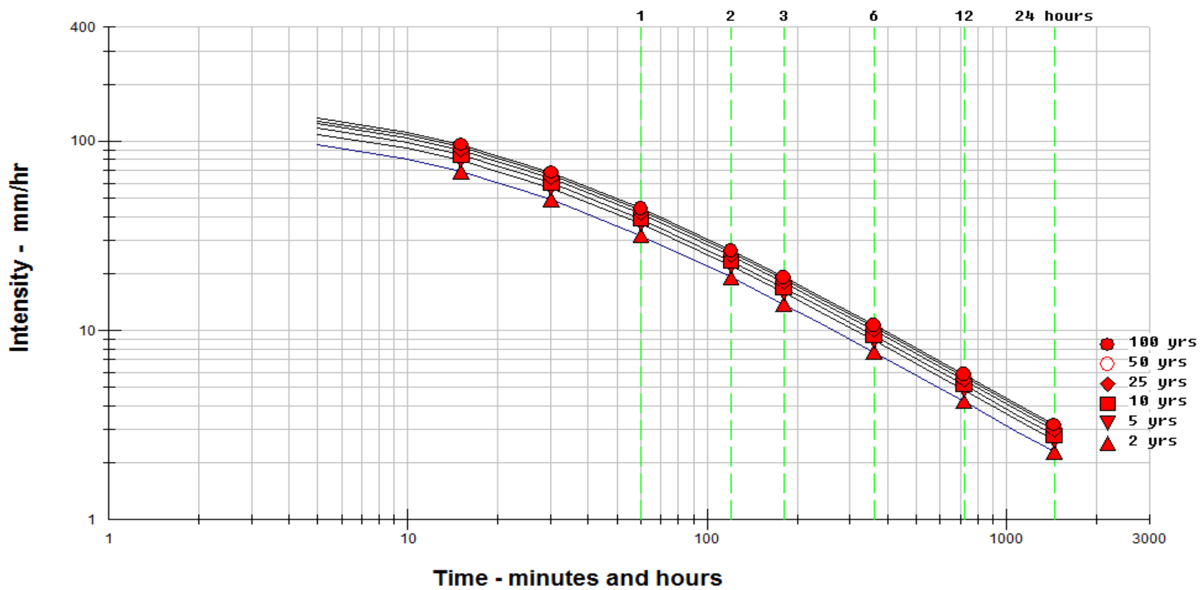

Fig 4.4. 2 Over estimated IDF curve using the scenario data of 2031-2040

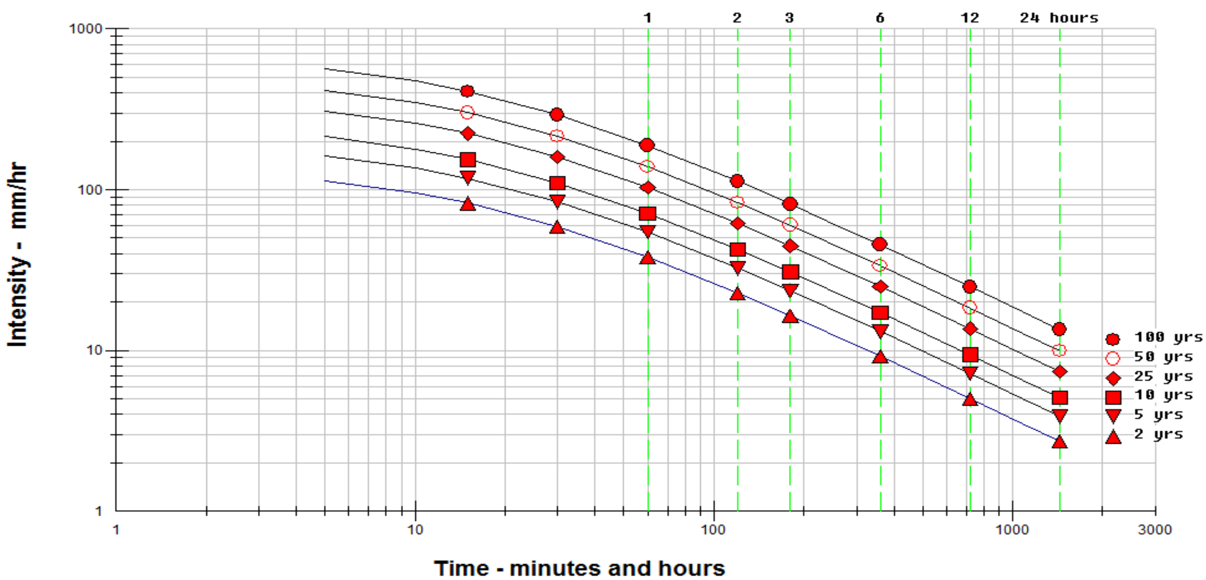

Fig 4.4.3 under estimated IDF curve of Gonder from 2091-2100

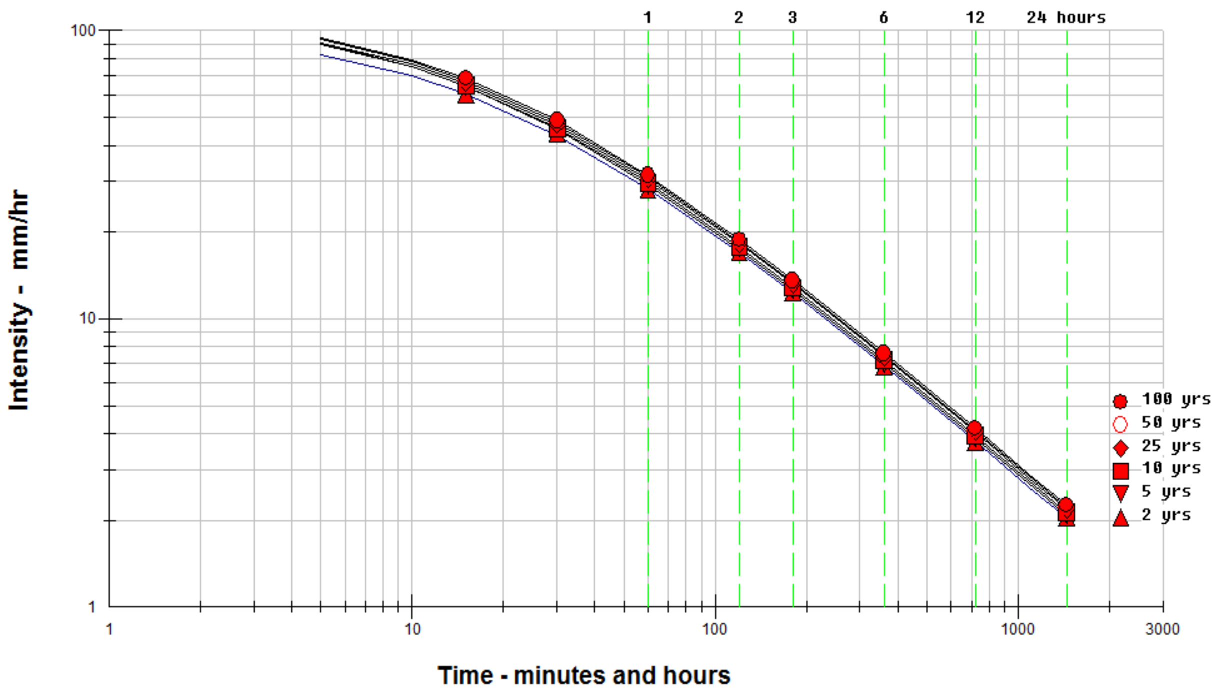

4.10 Different comparison between historically observed and generated data of different stations in the study area

4.10 .1 Comparison of collected and computed annual maximum rainfall data

Here the rainfall data collected from the NMSA and the rainfall computed for the period of 2031-2040 and 2091-2100 under the emerging scenario is compared and the change that would be happen in the future could be observed. The following table shows the changes at Bahirdar station in different ranges of years.

4.10.2 Comparison of estimated quantiles

It is clear that estimation of quantiles greatly depend on the parent distribution and the type of the parameter estimation for that specific distribution. Whenever different distributions and parameters estimation techniques are used to estimate quantiles of same station then there will be a possibility to obtain different values of quantiles for that station and also for different time periods due to climate change a single distribution proposed once may not be used for the other time it either over estimate or under estimate the quantile estimate deviating from the value nearest to the actual .This happened probably from the assumed scenario of the world activities.This could be observed from the following charts and tables.

Quantile estimate of daily rainfall (mm) at Bahirdar station for the three ranges of years are as follos in table 4.8 below

Table 4.8 Quantile estimate of daily rainfall (mm) at Bahirdar station with time and return period

return period	From observed Rainfall	From computed rainfall	From computed rainfall
	1991-2000	2031-2040	2091-2100
2	64.6	87.4	73.3
5	72	105	82.3
10	77.3	117	88.2
25	83.7	131.8	95.7
50	88.4	142.9	101
100	93.1	154	107

Figure 4.5 Charts showing the quantile daily rainfall variation of of the above data of Bahirdar station using the same parent distribution for the three time segments.

Fig 4.5 variation of quantiles daily rainfall of the above data of Bahirdar station

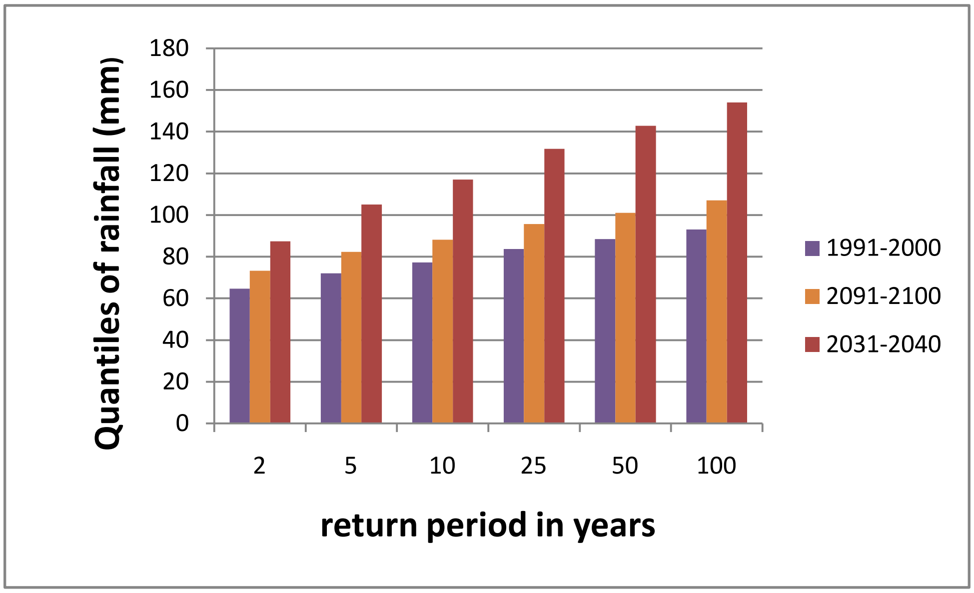

Table 4. 9 comparisons of daily rainfall in time and return period at Bahirdar Stations

Table 4.9.1 Variations of daily rainfall in time and return period at Bahirdar Stations

Quantiles of daily rainfall (mm) in different return period and in different range of years at bahirdar station.					
	Return period in years				
Range of years	2.	5	10	50	100
1991-2000	64.6	72	77.3	88.4	93.1
2031-2040	87.4	105	117	142.9	154
difference	22.8	33	39.7	54.5	60.9
Percentage of increase	35%	46%	51.4%	62%	65.4%

Table 4.9.2 Variations of daily rainfall in time and return period at Bahirdar Stations

Quantiles of daily rainfall(mm) in different return period and in different range of years at bahirdar station					
	Return period in years				
Range of years	2	5	10	50	100
1991-2000	64.6	72	77.3	88.4	93.1
2091-2100	73.3	82.3	88.2	101	107
difference	8.7	10.3	10.9	12.6	13.9
Percentage of increase	13.5%	14.3%	14.1%	14.3%	14.9%

Table 4.9.3 Variations of daily rainfall in time and return period at Bahirdar Stations

Quantiles of Rainfall (mm) in different return period and in different range of years of 24hr at bahirdar station					
	Return period in years				
Range of years	2	5	10	50	100
2031-2040	87.4	105	117	142.9	154
2091-2100	73.3	82.3	88.2	101	107
difference	14.1	22.7	28.8	41	47
Percentage of decrease	-16%	-21.62%	-24.6%	-28.7%	-30.5%

4.10.3 Comparison of estimated IDF parameters (using Miduss software)

IDF parameters were determined using Wenzel mathematical equation in combination with Miduss software version 2.25. Because different values of quantiles are observed in both time ranges of the study , the estimated IDF parameters computed are generally different in the time intervals of 1991-2000,2031-2040 and 2091-2100.This implies that the IDF parameters for a station will no longer be fixed in magnitude .Depending on the data length ,the global phenomena on climate change , the timely parent distribution and parameter estimation techniques, the IDF parameters shall be updated at some intervals of time to end up with preferable and reliable results of IDF relationships.

Table 4.10 Comparison of estimated IDF parameters for Kombolcha station in the three time frames of 1991-2000,2031-2040 and 2091-2100.

Ranges years	parameters	Estimated Parameters for the indicated frequency					
		2	5	10	25	50	100
1991-2000	A	1506.26	1615.20	1656.94	1722.96	1802.73	1847.74
2031-2040	A	1783.13	1938.98	2064.24	2147.00	2274.21	2316.39
2091-2100	A	2172.20	2405.75	2500.57	2707.97	2782.89	2952.08
Trend of A with time		increase	increase	increase	increase	increase	increase
1991-2000	B	17.910	18.326	17.910	17.910	18.326	18.326
2031-2040	B	17.910	17.910	18.326	17.910	18.326	17.910
2091-2100	B	18.326	18.326	17.910	18.326	17.910	18.326
Trend of B with time		Nearly constant	Nearly constant	Nearly constant	Nearly constant	Nearly constant	Nearly constant
1991-2000	C	0.8994	0.9004	0.8996	0.8994	0.9021	0.9017
2031-2040	C	0.9000	0.8993	0.9012	0.8991	0.9020	0.8993
2091-2100	C	0.9020	0.9020	0.8995	0.9020	0.8997	0.9022
Trend of C with time		Nearly constant	Nearly constant	Nearly constant	Nearly constant	Nearly constant	Nearly constant

From the above table it is seen that the parameter “A” increases not only with the increase of return period but also with climate change that could happen but “B” and “C” will be nearly constant.

5 .0 SUMMARY CONCLUSION AND RECOMMENDATION

5.1 Summary

This paper presents indicative study on IDF relationships which are developed for Upper Blue Nile region under the emerging climate scenario. For the analysis work, maximum annual rainfall depths of 24 hour were collected for eleven selected stations in the study area from available data of NMSA and scenario data from the international water management institute, Ethiopia.

The study briefly presents the relationship between extreme rainfall characteristics with other climate variables (temperature, humidity, wind) in order to develop rainfall IDF models that could be used for evaluating the impact of climate change and variability on the magnitude and frequency of occurrence of extreme precipitation events.

The quality of all the collected data was checked in order to make it ready for analysis work. Different methods like conventional moment ratio diagrams, L-moment ratio diagrams, and easy fit software were used in order to select parent distribution and to estimate quantiles.

Using IDF Curve fit tool, estimation of IDF parameters was done and based on the estimated parameters IDF Curves were drawn for the selected eleven stations of the three time segments .And based on the given scenario, the impacts of climate change was observed by increasing the magnitude and variability of the rainfall specially in the 2050s and would decline afterwards.

Graphical evaluation between observed and computed intensities was done and satisfactory result was obtained.

With the help of Arc GIS 9.3 software, maps were developed for the study area and location of the eleven stations was fixed.

For the establishment of IDF relationship, disaggregation of the daily rainfall for all stations considered within the study area and neighboring stations using rainfall ratio method.

5.2 Conclusion

IDF relationships or IDF curves established for stations with long record length has good accuracy and good representation of the reality than those stations with short record length, but this thesis used short length of record that is ten years of data since there were no scenario data better than this data length even if it fulfills the minimum requirement.

In the general mathematical form of IDF [$I= A/ (B+D)^C$],the “A” coefficient increases with an increase in return period and with climate change based on the assumed scenario for most of the stations and with the changes that could happen. The “B” constant and the “C” exponent generally slightly increase or decrease with an increase or decrease of the “A” coefficient or it seems that “B” constant and the “C” will not change with time depending the emerging scenario.

Any of the IDF relationships developed for the study area can be used to estimate the magnitude and direction of the impact of climate change and obtain intensity or depth of rainfall of specific duration and frequency for water resource projects within the study area

It can be concluded that the projected precipitation reveals an annual increase for the two time horizons (i.e.2000s and 2050s) and annual decreasing trend is observed during in 2090s. This shows that the A1B emission scenario which assumes a future world of very rapid economic growth, global population that peaks in mid-century and declines thereafter is the approximate position.

Water resource professionals, designers and concerned institutions in the study area can effectively utilize one or all of the procedures of this study to derive the IDF value in any part of the region under the climate change. And in addition the network of automatic recording stations of this area must be improved in number so that the IDF relationships of the study area can be revised and updated time to time for further improvement of the research area on IDF.

5.3 Recommendation

Depending on the data length, the global phenomena on climate change, the timely parent distribution and parameter estimation techniques, the IDF parameters shall be updated at some intervals of time to end up with preferable and reliable results of IDF relationships.

Since more recent data is available from now onwards, together with information presented in this report, it is recommended that use of the current standard be reviewed, and updated considering the facts about the world climate phenomena.

The rainfall patterns in the region will most certainly change with the climate change. This report quantifies these changes and their impact on design, operation and maintenance of water management infrastructure (such as roads, bridges, culverts, drains, sewer and conveyance systems, etc). The results are presented in terms of rainfall intensity duration frequency data for the study area.

The analysis performed in this paper indicates that:

- The rainfall magnitude (as well as intensity) will be different in the future.
- The wet climate scenario (recommended for use in storm water management design standards) reveals significant increase in rainfall magnitude (an Intensity) for a . range of durations and return periods
- The increase in rainfall intensity and magnitude has major implications on ways in which current (and future) water management infrastructure is designed, maintained .
- The design standards and guidelines currently employed by the study area should be reviewed and/or revised in the lights of the results of this research to reflect the impacts of climatic change.
- In order to assure the development of water resource and agricultural efficiency of poor countries like Ethiopia as well as the region of Africa, further studies which incorporate the impact of climate change with land use and land cover change on run off and on the

Other hand on IDF should be undertaken by using more than one and more finer resolution of Global Circulation Models (GCMs). These studies should also investigate the adaptation options for the impact of climate change consequences

Reference

Asres G, (2008) on development and Regionalization of Intensity Duration Frequency (IDF) Relationships for Amhara and Tigray Regions.

Coulibaly, P. and Dibike, Y. B. (2004). Downscaling of Global Climate Model Outputs for Flood Frequency Analysis in the Saguenay River System. Final Project Report prepared for the Canadian Climate Change Action Fund, Environment Canada, Hamilton, Ontario, Canada

Chow, V.T, Maidment, D.R., and Mays, L.W. (1988). Applied Hydrology McGraw-Hill Book Company, Singapore.

Chow, V.T. (1964). Hand Book of Applied Hydrology. McGraw Hill.

Cunnane, C. (1989). Statistical Distributions for Flood Frequency Analysis.

Dingmans, L.S. (2002). Physical Hydrology, 2ndedition. Prentice Hall. Inc. New Jersey

DuPont, B.S & Allen, D.L. (2000). Revision of the Rainfall Intensity Curves for the Common Wealth of Kentucky. Research Report. Kentucky.

Edessa, C. (2007). Establishment of Intensity-Duration-Frequency Relationships for Oromia Regional National State. Msc Thesis. Arbaminch University,Arbaminch, Ethiopia.

Gebeyehu, A.(1989). Regional Flood Frequency Analysis, PHD thesis report.

Gerbi, F. (2002). Development of Intensity-Duration-Frequency Relationships for the SNNPR. MSc. Thesis .Arba Minch University, Arbaminch, Ethiopia.

Guide to Hydrological Practices.Data acquisition and Processing, Analysis, Forecasting and Other Applications.WMO-No. 168. 5th Edition. Geneva, Switzerland.

Hirschfield, D.M. (1961). Rainfall Frequency Atlas of the United States,US Weather Bureau Technical Paper 40. Washington, DC.

Hosking, J.R.M. and Wallis, J.R. (1993). Some Statistics Useful in Regional frequency Analysis. Water Resource Research, Volume 29, No.2. New York.

IPCC-TGICA,(2007): General Guidelines on the Use of Scenario Data for Climate Impact and Adaptation Assessment. Version 2. Prepared by T.R. Carter on behalf of the Intergovernmental Panel on Climate Change, Task Group on Data and Scenario Support for Impact and Climate Assessment, 66 pp.

IPCC (2001). Climate Change (2001): Scientific Basis. Contribution of the Working Group I to the Third Assessment Report of the Intergovernmental Panel on Climate Change Cambridge University Press, Cambridge, United Kingdom.

Kolbert, E. (2006). Field notes from a catastrophe: man, nature, and climate change. Bloomsbury Publishing, New York.

Lall, U. and Sharma, A. (1996). "A nearest neighbor bootstrap for time series resampling." Water Resources Research, 32(3), 679-693.

MacLaren, J. F. (1962). Technical Discussion on Sewage and Drainage Works for Areas Annexed in 1961 by the City of London. MacLaren Associates, Toronto, Ontario, Canada.

Markus, M., Angel, J. R., Yang, L., and Hejazi, M. I. (2007). "Changing estimates of design precipitation in northeastern illinois: Comparison between different sources and sensitivity analysis." Journal of Hydrology, accepted for publication.

Mehdi, B., Mrena, C., and Douglas, A. (2006). Adapting to climate change: An introduction for Canadian Municipalities. Canadian Climate Impacts and Adaptation Research Network (C-CIARN), http://www.c-ciarn.ca/.

MTO (1997). Ministry of Transportation of Ontario Drainage Management Manual.Drainage and Hydrology Section,Transportation Engineering Branch,and Quality Standards Division, Ministry of Transportation of Ontario, Ottawa, Ontario, Canada.

Maidment, D.R., 1993. Hand Book of Hydrology, McGRAW-Hill. Inc. USA Rao, K.H, & Hamed, A.R. (2000). Flood Frequency Analysis. CRC press LLC, Florida.

Nakicenovic, N. and Swart, R. (2000). IPCC Special Report on Emissions Scenarios, Intergovernmental Panel on Climate Change. Cambridge University Press, Cambridge, United Kingdom.

Sine, A. (2004). Regional Flood Frequency Analysis for Blue Nile River Basin, Ethiopia, Msc Thesis. Arba Minch University, Arbaminch, Ethiopia.

Tefera, C. (2002). Intensity-Duration-Frequency Relationships for Northern Ethiopia. MSc. Thesis. Addis Ababa University, Addis Ababa, Ethiopia.

Tsegaye.E.,(2006) Regionalization of potential Evapotranspiration prediction for Blue Nile (Abbay) river basin, Ethiopia, Msc Thesis, Arba-Minch University, Ethiopia.

Wenzel, H.G.(1982).Rainfall for Urban Storm Design. American Geological Union.Washington DC.World Meteorological Organization. 1994.

ANNEXES

Appendix A: Annual maximum rainfall of the stations considered

Year	Observed annual maximum Daily rainfall(mm) for the indicated station				
	Shambu	Alem ketema	Fiche	Nekemte	Assossa
1991	50.2	51.2	49	55.9	26.15
1992	85.1	42.8	49	63.9	27.97
1993	51.5	65.9	49	80	25.77
1994	57.8	74.5	49	78.4	56.8
1995	45.7	22.16	60	67.3	65.9
1996	66.2	18.2	82.5	105.4	41.2
1997	58.7	103.4	40.9	72.3	28.38
1998	70	43.9	37	126.5	26.15
1999	55.1	54.8	56.4	86.4	27.97
2000	45	32.6	51.7	84.2	93

Year	Scenario data of the period from 2031-2040				
	Daily annual maximum rainfall(mm) for the indicated station Under climate change scenario				
	Shambu	Alem ketema	Fiche	Nekemte	Assossa
2031	71.6	29.54	29.54	75.21	39.88
2032	77.5	33.25	55.48	75.9	50.27
2033	60.82	50.31	58.55	89.25	46.13
2034	56.69	76.43	51.21	84.17	40.35
2035	34.05	29.61	58.52	60.14	49.08
2036	46.73	59.32	60.05	84.41	44.6
2037	70.38	36.77	65.17	95.54	54.07
2038	40.8	41.28	32.29	88.13	37.74
2039	67.67	109.88	33.74	124.63	52.9
2040	54.09	163.36	82.34	68.64	70.73

YEAR	Scenario data of the period from 2091-2100 Daily annual maximum rainfall(mm) for the indicated station Under climate change scenario				
	Shambu	Alem ketema	Fiche	Nekemte	Assossa
2091	76.55	41.26	36.82	75.54	52.57
2092	62.96	40.86	70.4	75.9	50.8
2093	56.59	50.82	58.5	89.34	63.63
2094	55.72	77.09	33.8	78.09	40.73
2095	71.45	54.84	47.62	80.52	44.67
2096	91.5	33.5	45.22	72.34	44.16
2097	91.5	40.99	61.38	74.37	44.66
2098	61.88	52.71	32.29	79.37	70.42
2099	83.93	41.06	62.54	82.01	46.11
2100	56.39	276.12	59.78	59.82	76.3

year	Observed annual maximum Daily rainfall(mm) for the indicated station					
	Bahirdar	Gonder	Dangilla	Debre Markose	Kombolcha	haike
1991	90.5	50.27	21.93	49.2	42.2	56.5
1992	53.8	36.8	40	41.1	52.4	76
1993	71.3	39.29	43.2	49.189	50.7	62.7
1994	38.8	40.1	58.8	58.4	58.5	61.6
1995	58.6	39.59	38.2	34.6	38.7	52.6
1996	51.1	39.29	47.2	44.8	38.8	48.4
1997	69.2	72.3	48.5	86.9	54.3	47
1998	51.5	64.6	46.7	34.5	68.4	71.6
1999	64.6	58.1	68	35.9	61.2	43.2
2000	105.3	85.2	67	57.3	50.6	56.7

Scenario data of the period from 2031-2040						
year	Daily annual maximum rainfall(mm) for the indicated station Under climate change scenario					
	Bahirdar	Gonder	Dangilla	Debre Markose	Kombolcha	Haike
2031	81.27	48.67	46.46	35.75	68.45	92.62
2032	74.70	53.53	66.57	216.52	68.70	77.25
2033	70.87	63.85	50.49	75.07	98.64	86.97
2034	48.64	57.89	60.42	47.12	62.14	39.44
2035	48.04	60.56	60.19	38.13	41.67	76.57
2036	117.14	46.30	75.51	97.67	63.11	67.73
2037	54.07	44.64	57.04	46.42	39.19	72.13
2038	159.22	46.82	51.88	66.48	51.97	85.92
2039	63.18	55.32	53.97	44.37	62.58	100
2040	177.05	31.92	42.12	46.01	51.97	72.21

Scenario data of the period from 2091-2100						
year	Daily annual maximum rainfall(mm) for the indicated station under climate change scenario					
	Bahirdar	Gonder	Dangilla	D/markose	Kombolcha	haike
2091	75.95	49.08	60.37	45.70	84.94	52.79
2092	111.91	70.92	50.65	61.52	67.41	42.55
2093	52.50	47.48	103.63	40.58	49.57	63.31
2094	103.19	35.94	63.69	36.80	50.53	54.13
2095	90.90	66.10	76.27	63.31	80.89	96.75
2096	68.79	45.95	57.81	46.16	84.33	51.74
2097	52.44	82.68	56.20	57.36	53.63	51.56
2098	41.67	43.98	185.27	41.83	122.42	388.34
2099	60.06	38.89	65.11	49.40	48.60	74.17
2100	85.77	67.13	47.21	60.70	88.61	235.08

AppendixB: Estimated quantiles for the indicated durations a frequencies

Estimated Quantiles(mm) at Kombolcha station using observed data of 1991-2000						
Duration (minutes)	Estimated quantiles(mm) for the indicated frequency(years)					
	2	5	10	25	50	100
1440	51.58	54.8	56.7	59	60.6	62.3
720	47.6	50.6	52.3	54.4	56	57.5
360	43.46	46.2	47.8	49.7	51.1	52.5
300	42.31	45	46.5	48.4	49.7	51.1
180	38.88	41.3	42.7	44.5	45.7	46.9
120	35.87	38.1	39.4	41	42.2	43.3
60	29.98	31.9	32.9	34.3	35.2	36.2
30	23.2	24.7	25.5	26.5	27.3	28

Estimated Quantiles(mm) at Kombolcha station using computed scenario data of 2031-2040						
Duration (minutes)	Estimated quantiles(mm) for the indicated frequency(years)					
	2	5	10	25	50	100
1440	60.8	66.4	70	73.7	76.5	79.4
720	56.1	61.3	64	68	70.6	73.2
360	51.3	56	59	62.1	64.5	66.9
300	49.9	54.5	57	60.4	62.8	65.1
180	45.9	50.1	53	55.5	57.7	59.8
120	42.3	46.2	48	51.2	53.2	55.2
60	35.4	38.6	41	42.8	44.5	46.1
30	27.4	29.9	31	33.1	34.4	35.7

Estimated Quantiles(mm) at Kombolcha station using computed scenario data of 2091-2100						
Duration (minutes)	Estimated quantiles(mm) for the indicated frequency(years)					
	2	5	10	25	50	100
1440	73.1	81	85.6	91.2	95.2	99.2
720	67.4	74.7	79	84.1	87.9	91.6
360	61.6	68.2	72.1	76.8	80.2	83.6
300	60	66.4	70.2	74.8	78.1	81.4
180	55.1	61	64.5	68.7	71.8	74.8
120	50.8	56.3	59.5	63.4	66.2	69
60	42.5	47.1	49.7	53	55.3	57.7
30	32.9	36.4	38.5	41	42.8	44.6

Estimated Quantiles(mm) at Debre Markose station using observed data of 1991-2000						
Duration (min)	Estimated quantiles(mm) for the indicated frequency(years)					
	2	5	10	25	50	100
1440	46	53	57.5	63.3	67.6	71.86
720	42.4	48.8	53.1	58.41	62.4	66.32
360	38.8	44.6	48.5	53.33	57	60.55
300	37.7	43.4	47.2	51.92	55.4	58.95
180	34.7	39.9	43.4	47.72	51	54.18
120	32	36.8	40	44.03	47	49.98
60	26.7	30.8	33.4	36.79	39.3	41.76
30	20.7	23.8	25.9	28.47	30.4	32.32

Estimated Quantiles(mm) at Debre Markose station using computed scenario data of 2031-2040						
	Estimated quantiles(mm) for the indicated frequency(years)					
Duration(min)	2	5	10	25	50	100
1440	54.9	62.6	67.7	74.1	78.9	83.6
720	50.6	57.7	62.4	68.4	72.8	77.2
360	46.2	52.7	57	62.4	66.4	70.4
300	45	51.3	55.5	60.8	64.7	68.6
180	41.4	47.2	51	55.9	59.5	63
120	38.2	43.5	47.1	51.5	54.9	58.2
60	31.9	36.4	39.3	43.1	45.8	48.6
30	24.7	28.1	30.4	33.3	35.5	37.6

Estimated Quantiles(mm) at Debre Markose station using computed scenario data of 2091-2100						
	Estimated quantiles(mm) for the indicated frequency(years)					
Duration(min)	2	5	10	25	50	100
1440	49.9	53.6	56.1	59.2	62	63.8
720	46.1	49.5	51.8	54.6	57	58.8
360	42.1	45.2	47.2	49.9	52	53.7
300	40.9	44	46	48.5	50	52.3
180	37.6	40.4	42.3	44.6	46	48.1
120	34.7	37.3	39	41.2	43	44.4
60	29	31.2	32.6	34.4	36	37.1
30	22.5	24.1	25.2	26.6	28	28.7

Estimated Quantiles(mm) at Dangila station using observed data of 1991-2000						
Duration (min)	Estimated quantiles(mm) for the indicated frequency(years)					
	2	5	10	25	50	100
1440	47.4	52.7	56.2	60.7	64	67.3
720	43.7	48.6	51.9	56	59.1	62.1
360	39.9	44.4	47.4	51.1	53.9	56.7
300	38.8	43.2	46.1	49.8	52.5	55.2
180	35.7	39.7	42.4	45.8	48.3	50.7
120	32.9	36.6	39.1	42.2	44.5	46.8
60	27.5	30.6	32.7	35.3	37.2	39.1
30	21.3	23.7	25.3	27.3	28.8	30.3

Estimated Quantiles(mm) at Danglla station using computed scenario data of 2031-2040						
Duration (min)	Estimated quantiles(mm) for the indicated frequency(years)					
	2	5	10	25	50	100
1440	56	59.8	62.3	65.4	67.8	70.1
720	51.7	55.18	57.5	60.4	62.5	64.7
360	47.2	50.38	52.5	55.1	57.1	59
300	46	49.05	51.1	53.7	55.6	57.5
180	42.2	45.08	47	49.3	51.1	52.8
120	39	41.59	43.3	45.5	47.1	48.7
60	32.6	34.75	36.2	38	39.4	40.7
30	25.2	26.9	28	29.4	30.5	31.5

Estimated Quantiles(mm) at Danglla station using computed scenario data of 2091-2100						
Duration (min)	Estimated quantiles(mm) for the indicated frequency(years)					
	2	*5*	10	25	50	100
1440	63.9	*70*	74	79.2	83	86.7
720	58.9	64.6	68.3	73	76.6	80
360	53.8	59	62.4	66.7	69.9	73.1
300	52.4	57.4	60.7	64.9	68	71.1
180	48.1	52.8	55.8	59.7	62.5	65.4
120	44.4	48.7	51.5	55.1	57.7	60.3
60	37.1	40.7	43	46	48.2	50.4
30	28.7	31.5	33.3	35.6	37.3	39

Estimated Quantiles(mm) at Haike station using observed data of 1991-2000						
Duration (min)	Estimated quantiles(mm) for the indicated frequency(years)					
	2	5	10	25	50	100
1440	57.6	61.1	63.2	65.7	67.5	69.3
720	53.2	56.4	58.3	60.6	62.3	63.9
360	48.6	51.5	53.2	55.3	56.9	58.4
300	47.3	50.2	51.8	53.9	55.4	56.8
180	43.4	46.1	47.6	49.5	50.9	52.2
120	40.1	42.5	44	45.7	46.9	48.2
60	33.5	35.5	36.7	38.2	39.2	40.3
30	25.9	27.5	28.4	29.5	30.4	31.2

Estimated Quantiles(mm) at Haike station using computed scenario data of 2031-2040						
Duration (min)	Estimated quantiles(mm) for the indicated frequency(years)					
	2	5	10	25	50	100
1440	77.1	82.6	85.8	89.8	92.6	95.4
720	71.1	76.2	79.2	82.8	85.45	88
360	64.9	69.6	72.3	75.6	78.02	80.4
300	63.2	67.8	70.4	73.6	75.96	78.3
180	58.1	62.3	64.7	67.7	69.81	71.9
120	53.6	57.5	59.7	62.4	64.4	66.4
60	44.8	48	49.9	52.2	53.81	55.4
30	34.7	37.2	38.6	40.4	41.65	42.9

Estimated Quantiles(mm) at Haike station using computed scenario data of 2091-2100						
Duration(min)	Estimated quantiles(mm) for the indicated frequency(years)					
	2	5	10	25	50	100
1440	64.6	69.9	73	76.7	79.4	82.1
720	59.6	64.5	67.3	70.8	73.3	75.8
360	54.4	58.8	61.5	64.6	66.9	69.2
300	52.9	57.3	59.8	62.9	65.1	67.4
180	48.7	52.7	55	57.8	59.9	61.9
120	44.9	48.6	50.7	53.3	55.2	57.1
60	37.5	40.6	42.4	44.6	46.2	47.7
30	29	31.4	32.8	34.5	35.7	36.9

Estimated Quantiles(mm) at Gonder station using observed data of 1991-2000						
Duration (min)	Estimated quantiles(mm) for the indicated frequency(years)					
	2	5	10	25	50	100
1440	54.8	62.8	67.1	71.3	73.9	76.1
720	50.5	58	61.9	65.8	68.2	70.2
360	46.1	52.9	56.5	60.1	62.3	64.1
300	44.9	51.5	55	58.5	60.6	62.4
180	41.3	47.4	50.5	53.8	55.7	57.3
120	38.1	43.7	46.6	49.6	51.4	52.9
60	31.8	36.5	39	41.5	43	44.2
30	24.6	28.3	30.2	32.1	33.2	34.2

Estimated Quantiles(mm) at Gonder station using computed scenario data of 2031-2040						
Duration(min)	Estimated quantiles(mm) for the indicated frequency(years)					
	2	5	10	25	50	100
1440	65.4	93.4	122.4	177.8	238.9	323.9
720	60.3	86.1	112.9	164.1	220.4	298.9
360	55.1	78.7	103.1	149.8	201.2	272.9
300	53.6	76.6	100.4	145.8	195.9	265.7
180	49.3	70.4	92.24	134	180.1	244.2
120	45.5	64.9	85.1	123.7	166.1	225.3
60	38	54.3	71.11	103.3	138.8	188.2
30	29.4	42	55.04	79.97	107.4	145.7

Estimated Quantiles(mm) at Gonder station using computed scenario data of 2091-2100						
	Estimated quantiles(mm) for the indicated frequency(years)					
Duration(min)	2	5	10	25	50	100
1440	48.7	50.2	51.1	52.4	53.3	54.2
720	44.9	46.3	47.2	48.3	49.2	50
360	41	42.3	43.1	44.1	44.9	45.6
300	39.9	41.1	41.9	42.9	43.7	44.4
180	36.7	37.8	38.5	39.5	40.2	40.8
120	33.9	34.9	35.6	36.4	37	37.7
60	28.3	29.1	29.7	30.4	31	31.5
30	21.9	22.6	23	23.6	24	24.4

Estimated Quantiles(mm) at Shambu station using observed data of 1991-2000						
	Estimated quantiles(mm) for the indicated frequency(years)					
Duration (min)	2	5	10	25	50	100
1440	64.98	71.06	75.09	80.18	83.95	87.7
720	59.963	65.573	69.292	73.989	77.468	80.928
360	54.75	59.87	63.26	67.55	70.73	73.89
300	53.3	58.29	61.59	65.77	68.86	71.94
180	48.986	53.57	56.608	60.445	63.287	66.114
120	45.195	49.424	52.227	55.767	58.389	60.997
60	37.763	41.296	43.638	46.596	48.787	50.967
30	29.228	31.963	33.776	36.065	37.761	39.448

Estimated Quantiles(mm) at Shambu station using computed scenario data of 2031-2040						
Duration (min)	Estimated quantiles(mm) for the indicated frequency(years)					
	2	5	10	25	50	100
1440	65.47	72.5	77.15	83.03	87.39	91.72
720	60.415	66.902	71.193	76.619	80.642	84.638
360	55.16	61.08	65	69.95	73.63	77.28
300	53.7	59.47	63.28	68.11	71.68	75.24
180	49.355	54.655	58.161	62.593	65.88	69.144
120	45.536	50.425	53.659	57.749	60.781	63.793
60	38.048	42.133	44.835	48.253	50.786	53.303
30	29.449	32.611	34.702	37.347	39.308	41.256

Estimated Quantiles(mm) at Shambu station using computed scenario data of 2091-2100						
Duration (min)	Estimated quantiles(mm) for the indicated frequency(years)					
	2	5	10	25	50	100
1440	78.3	85.34	90	95.89	100.26	104.59
720	72.254	78.751	83.051	88.486	92.519	96.514
360	65.97	71.9	75.83	80.79	84.47	88.12
300	64.23	70	73.82	78.66	82.24	85.79
180	59.028	64.335	67.848	72.288	75.582	78.847
120	54.459	59.356	62.597	66.693	69.733	72.744
60	45.504	49.595	52.303	55.726	58.266	60.782
30	35.22	38.386	40.482	43.132	45.097	47.045

Estimated Quantiles(mm) at Nekemte station using observed data of 1991-2000						
Duration (min)	Estimated quantiles(mm) for the indicated frequency(years)					
	2	5	10	25	50	100
1440	92.87	103.1	109.87	118.43	124.78	131.082
720	85.699	95.139	101.39	109.29	115.15	120.96
360	78.245	86.864	92.567	99.779	105.13	110.44
300	76.18	84.57	90.12	97.14	102.4	107.5
180	70.011	77.723	82.827	89.28	94.067	98.818
120	64.593	71.708	76.417	82.37	86.787	91.17
60	53.971	59.9162	63.8505	68.8251	72.5154	76.1778
30	41.77	46.37	49.42	53.27	56.13	58.96

Estimated Quantiles(mm) at Nekemte station using computed scenario data of 2031-2040						
Duration (min)	Estimated quantiles(mm) for the indicated frequency(years)					
	2	5	10	25	50	100
1440	97.754	102.394	108.115	115.343	120.705	126.028
720	90.206	94.488	99.767	106.44	111.38	116.3
360	82.36	86.269	91.089	97.179	101.7	106.18
300	80.18	83.99	88.68	94.61	99.01	103.4
180	73.693	77.191	81.504	86.953	90.995	95.008
120	67.99	71.217	75.196	80.223	83.953	87.655
60	56.8093	59.5059	62.8306	67.0311	70.1472	73.2407
30	43.97	46.06	48.63	51.88	54.29	56.69

Estimated Quantiles(mm) at Nekemte station using computed scenario data of 2091-2100						
Duration (min)	Estimated quantiles(mm) for the indicated frequency(years)					
	2	5	10	25	50	100
1440	80.705	84.46	86.94	90.08	92.41	94.72
720	74.473	77.939	80.227	83.125	85.275	87.406
360	67.995	71.159	73.249	75.894	77.857	79.803
300	66.2	69.28	71.31	73.89	75.8	77.7
180	60.841	63.671	65.541	67.908	69.665	71.406
120	56.132	58.744	60.469	62.652	64.273	65.88
60	46.90	49.08	50.52	52.34	53.70	55.04
30	36.3	37.99	39.11	40.52	41.57	42.61

Estimated Quantiles(mm) at Assossa station using observed data of 1991-2000						
Duration (min)	Estimated quantiles(mm) for the indicated frequency(years)					
	2	5	10	25	50	100
1440	53.89	65.19	72.66	82.11	89.12	96.08
720	49.729	60.156	67.05	75.77	82.239	88.661
360	45.403	54.924	61.217	69.179	75.085	80.949
300	44.204	53.473	59.601	67.352	73.102	78.811
180	40.626	49.144	54.776	61.9	67.184	72.431
120	37.482	45.341	50.536	57.109	61.985	66.826
60	31.318	37.8849	42.2261	47.7179	51.7917	55.8365
30	24.24	29.323	32.683	36.933	40.087	43.217

Estimated Quantiles(mm) at Assossa station using computed scenario data of 2031-2040						
Duration (min)	Estimated quantiles(mm) for the indicated frequency(years)					
	2	5	10	25	50	100
1440	53.57	58.28	61.4	65.35	68.27	71.17
720	49.434	53.78	56.659	60.304	62.999	65.675
360	45.134	49.102	51.731	55.059	57.519	59.962
300	43.942	47.805	50.365	53.605	56	58.379
180	40.384	43.935	46.287	49.265	51.466	53.653
120	37.259	40.535	42.705	45.452	47.483	49.5
60	31.132	33.8692	35.6824	37.9779	39.6748	41.3602
30	24.096	26.215	27.618	29.395	30.708	32.013

Estimated Quantiles(mm) at Assossa station using computed scenario data of 2091-2100						
Duration (min)	Estimated quantiles(mm) for the indicated frequency(years)					
	2	5	10	25	50	100
1440	59.86	65.95	69.98	75.07	78.85	82.61
720	55.238	60.858	64.577	69.274	72.762	76.231
360	50.433	55.564	58.959	63.248	66.433	69.6
300	49.101	54.097	57.402	61.578	64.678	67.762
180	45.126	49.717	52.755	56.593	59.442	62.277
120	41.634	45.87	48.672	52.213	54.842	57.457
60	34.78	38.33	40.67	43.63	45.82	48.01
30	26.925	29.665	31.48	33.767	35.467	37.16

Estimated Quantiles(mm) at Fiche station using observed data of 1991-2000						
Duration (min)	Estimated quantiles(mm) for the indicated frequency(years)					
	2	5	10	25	50	100
1440	58.94	65.07	69.13	74.25	78.06	81.83
720	54.389	60.046	63.792	68.517	72.033	75.512
360	49.658	54.823	58.243	62.557	65.767	68.943
300	48.35	53.37	56.71	60.9	64.03	67.12
180	44.43	49.05	52.11	55.97	58.85	61.69
120	41.00	45.26	48.08	51.64	54.29	56.91
60	34.25	37.82	40.17	43.15	45.36	47.56
30	26.511	29.269	31.095	33.398	35.112	36.807

Estimated Quantiles(mm) at Fiche station using computed scenario data of 2031-2040						
	Estimated quantiles(mm) for the indicated frequency(years)					
	2	5	10	25	50	100
1440	61.34	69.51	74.92	81.75	86.82	91.85
720	56.604	64.143	69.135	75.438	80.116	84.758
360	51.68	58.563	63.121	68.876	73.147	77.385
300	50.32	57.02	61.45	67.06	71.22	75.34
180	46.24	52.4	56.48	61.63	65.45	69.24
120	42.66	48.34	52.10836	56.86	60.39	63.88
60	35.65	40.4	43.54	47.51	50.46	53.38
30	27.591	31.266	33.699	36.771	39.052	41.314

Estimated Quantiles(mm) at Fiche station using computed scenario data of 2091-2100						
Duration (min)	Estimated quantiles(mm) for the indicated frequency(years)					
	2	5	10	25	50	100
1440	57.88	64.52	68.92	74.48	78.61	82.7
720	53.411	59.538	63.598	68.729	72.54	76.314
360	48.765	54.359	58.066	62.751	66.23	69.676
300	47.48	52.92	56.53	61.09	64.48	67.84
180	43.63	48.64	51.96	56.15	59.26	62.34
120	40.27	44.87	47.94	51.80	54.67	57.52
60	33.64	37.5	40.05	43.28	45.68	48.06
30	26.035	29.021	31	33.501	35.359	37.199

Estimated Quantiles(mm) at Alem ketema station using observed data of 1991-2000						
Duration (min)	Estimated quantiles(mm) for the indicated frequency(years)					
	2	5	10	25	50	100
1440	64.29	76.89	85.24	95.78	103.6	111.363
720	59.326	70.953	78.658	88.384	95.601	102.76
360	54.165	64.781	71.816	80.696	87.285	93.825
300	52.74	63.07	69.92	78.57	84.98	91.35
180	48.466	57.965	64.259	72.205	78.1	83.953
120	44.71	53.48	59.29	66.62	72.06	77.46
60	37.362	44.684	49.537	55.662	60.207	64.718
30	28.92	34.59	38.34	43.08	46.6	50.09

Estimated Quantiles(mm) at Alem ketema station using computed scenario data of 2031-2040						
Duration (min)	Estimated quantiles(mm) for the indicated frequency(years)					
	2	5	10	25	50	100
1440	85.57	106.90	121.029	138.88	152.11	165.26
720	78.963	98.65	111.68	128.16	140.36	152.5
360	72.094	90.069	101.97	117.01	128.16	139.23
300	70.19	87.69	99.28	113.9	124.8	135.6
180	64.508	80.591	91.239	104.7	114.67	124.58
120	59.52	74.35	84.18	96.59	105.8	114.9
60	49.729	62.127	70.336	80.71	88.398	96.04
30	38.49	48.09	54.44	62.47	68.42	74.33

Estimated Quantiles(mm) at Alem ketema station using computed scenario data of 2091-2100						
Duration (min)	Estimated quantiles(mm) for the indicated frequency(years)					
	2	5	10	25	50	100
1440	79.18	115.17	138.99	169.1053	191.44	213.61
720	73.066	106.28	128.26	156.05	176.66	197.12
360	66.711	97.033	117.1	142.47	161.29	179.97
300	64.95	94.47	114	138.7	157	175.2
180	59.691	86.823	104.78	127.48	144.32	161.03
120	55.07	80.1	96.67	117.6	133.2	148.6
60	46.015	66.931	80.773	98.275	111.25	124.14
30	35.62	51.8	62.52	76.06	86.11	96.08

Appendix C: IDF curves on double logarithmic scale for stations considered

Debre markose 1991-2000

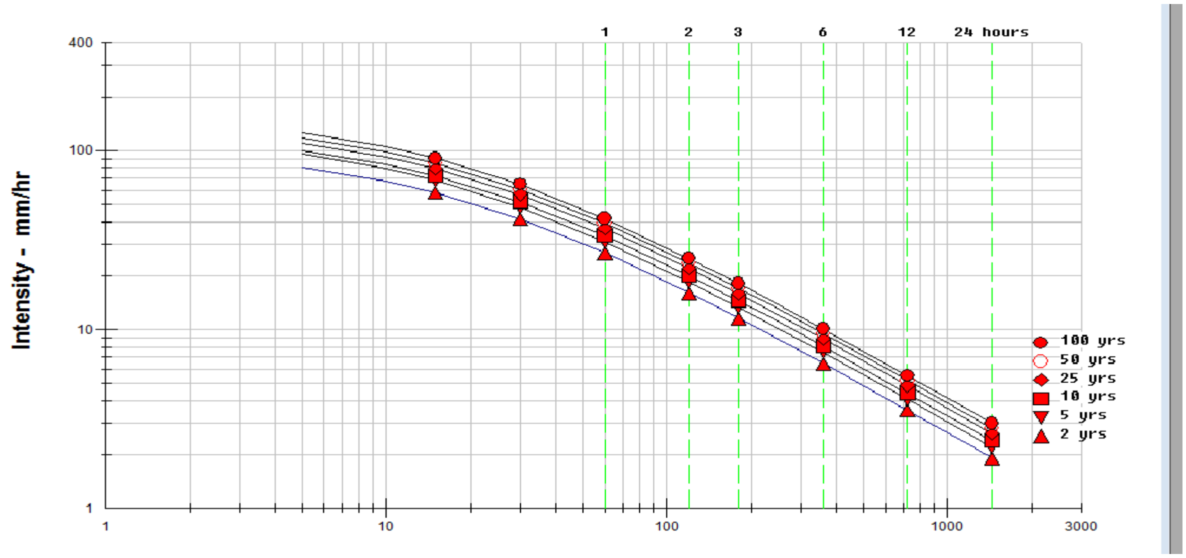

Debre markose from 2031-2040

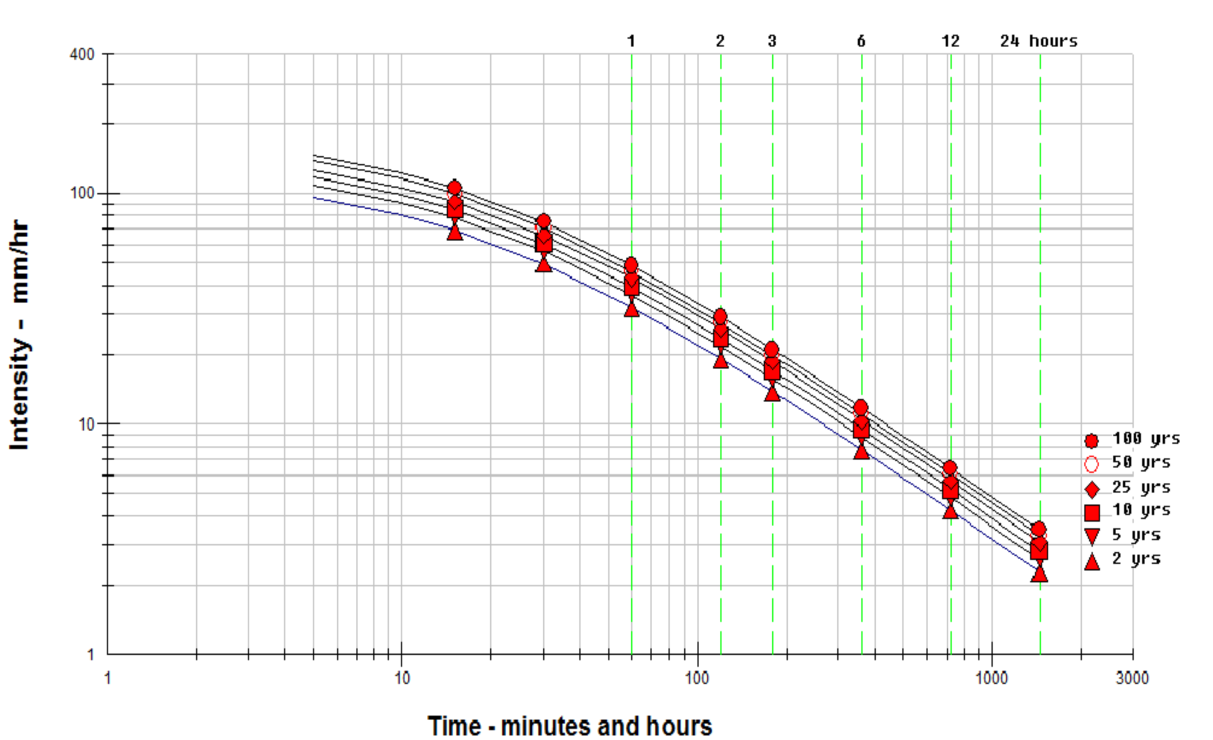

Debre Markose from 2091-2100

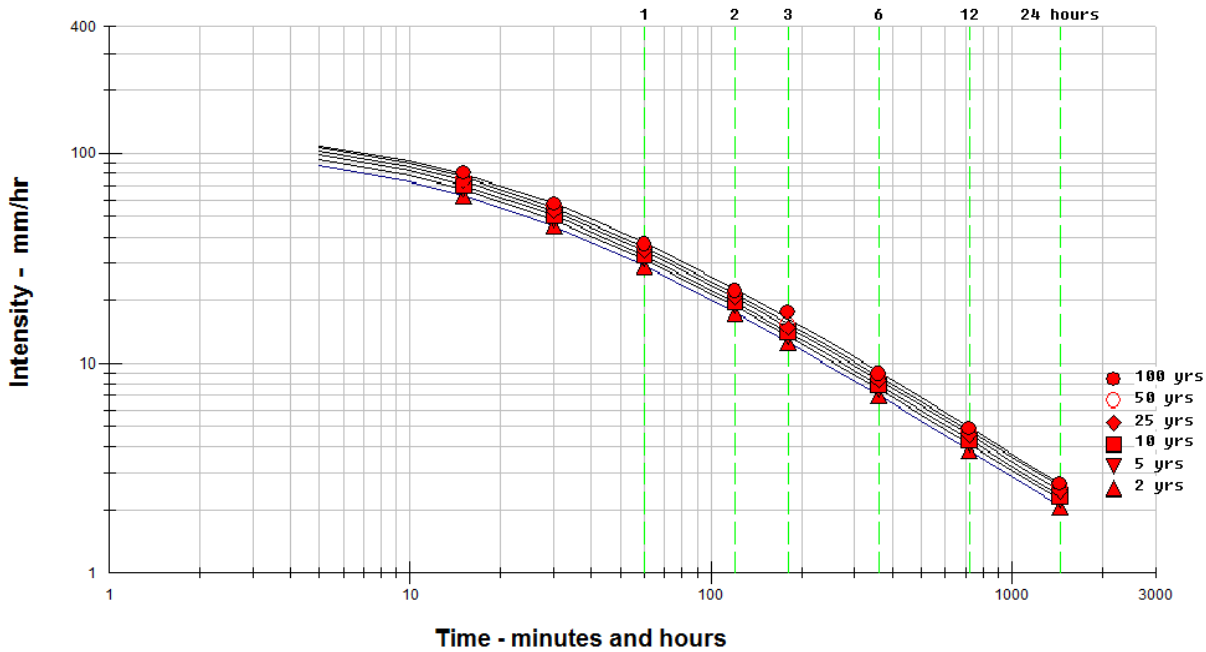

Danglla from 1991-2000

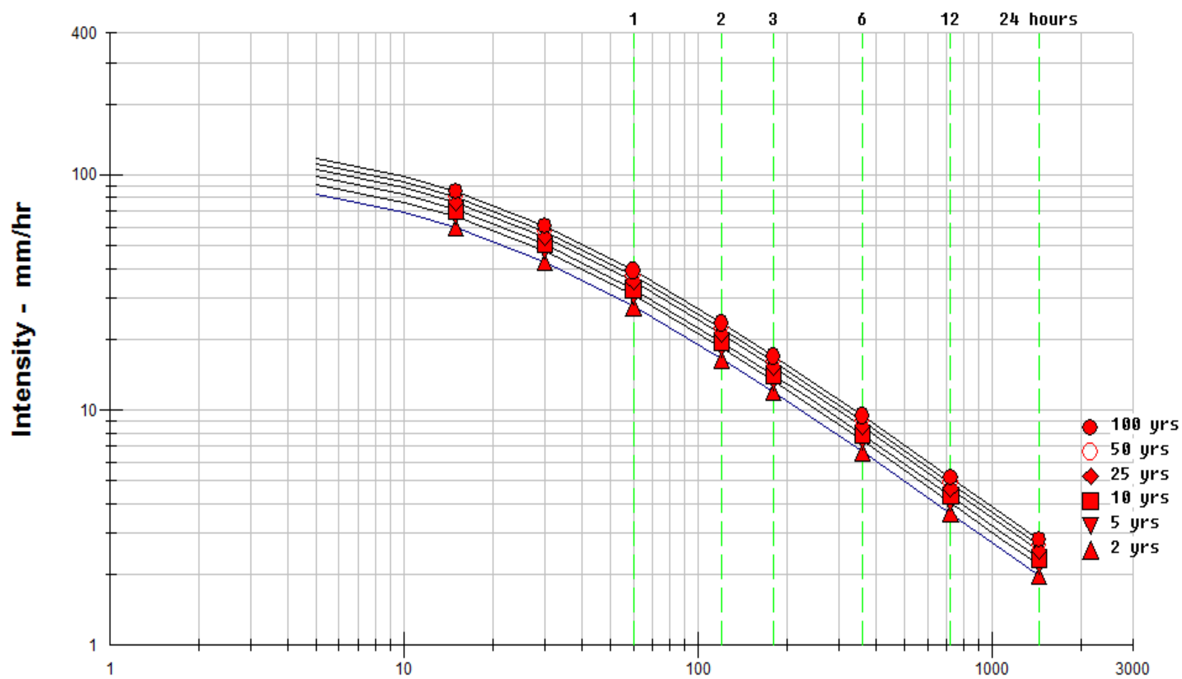

Danglla from 2031-2040

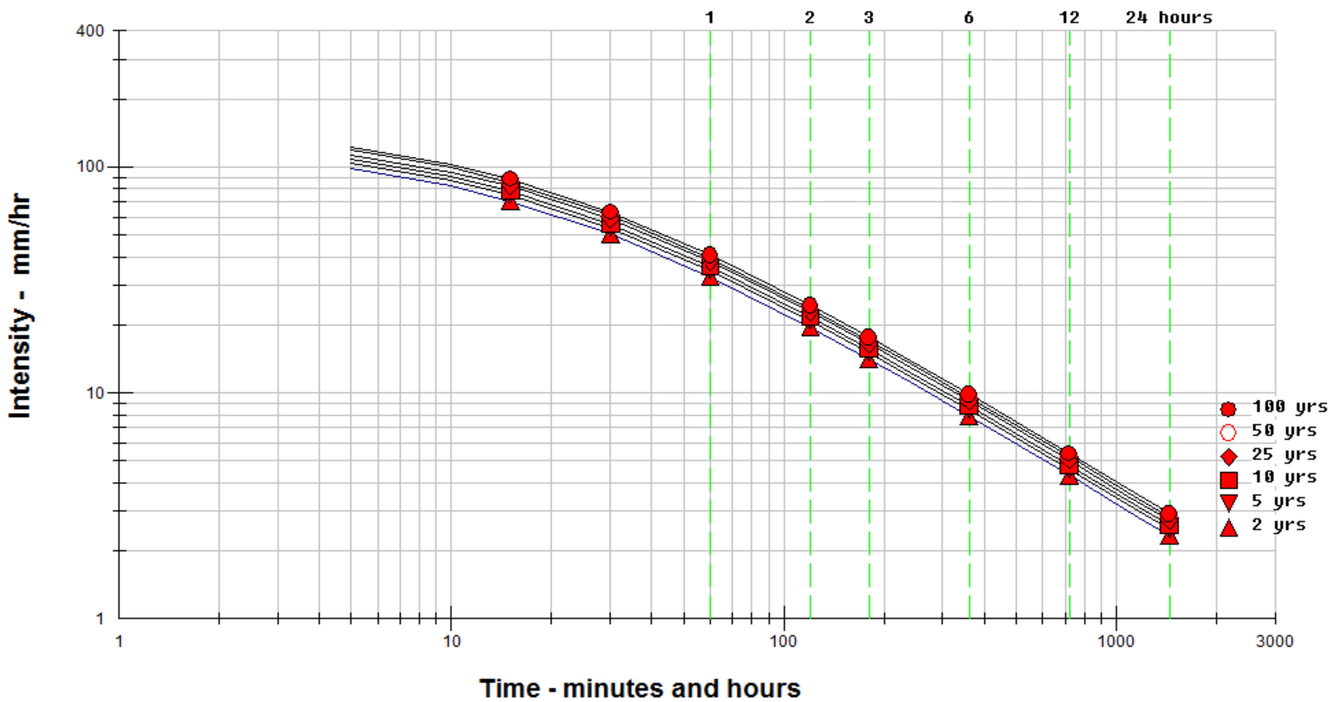

Danglla from 2091-2100

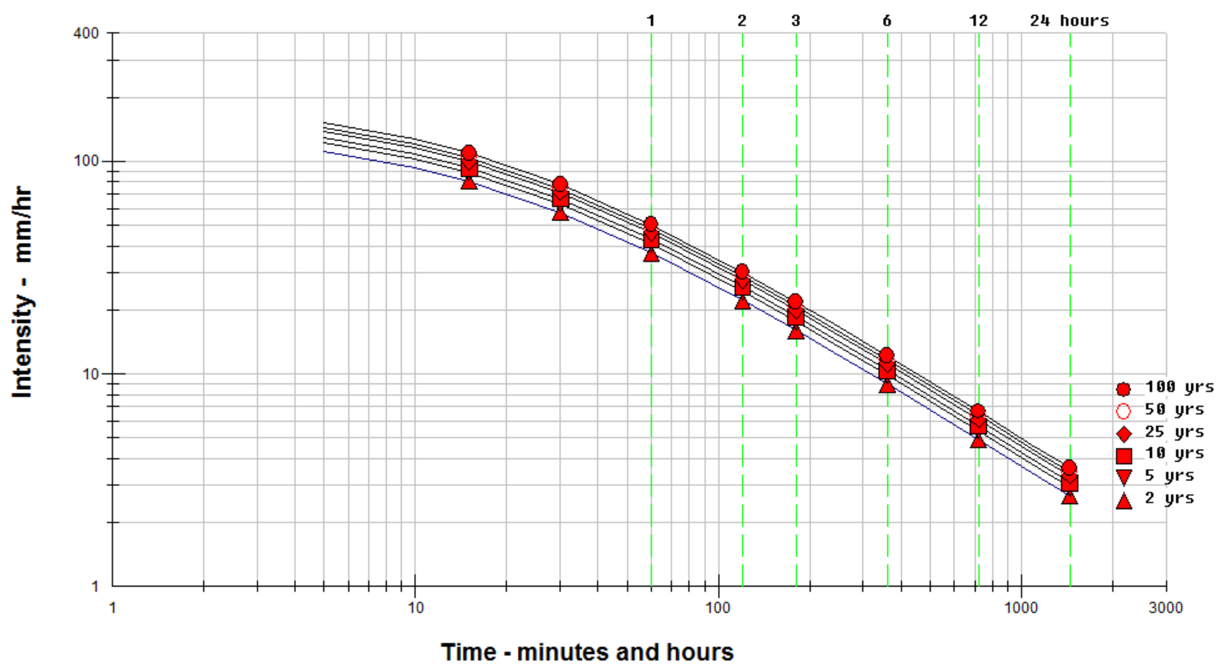

Kombolcha from 1991-2000

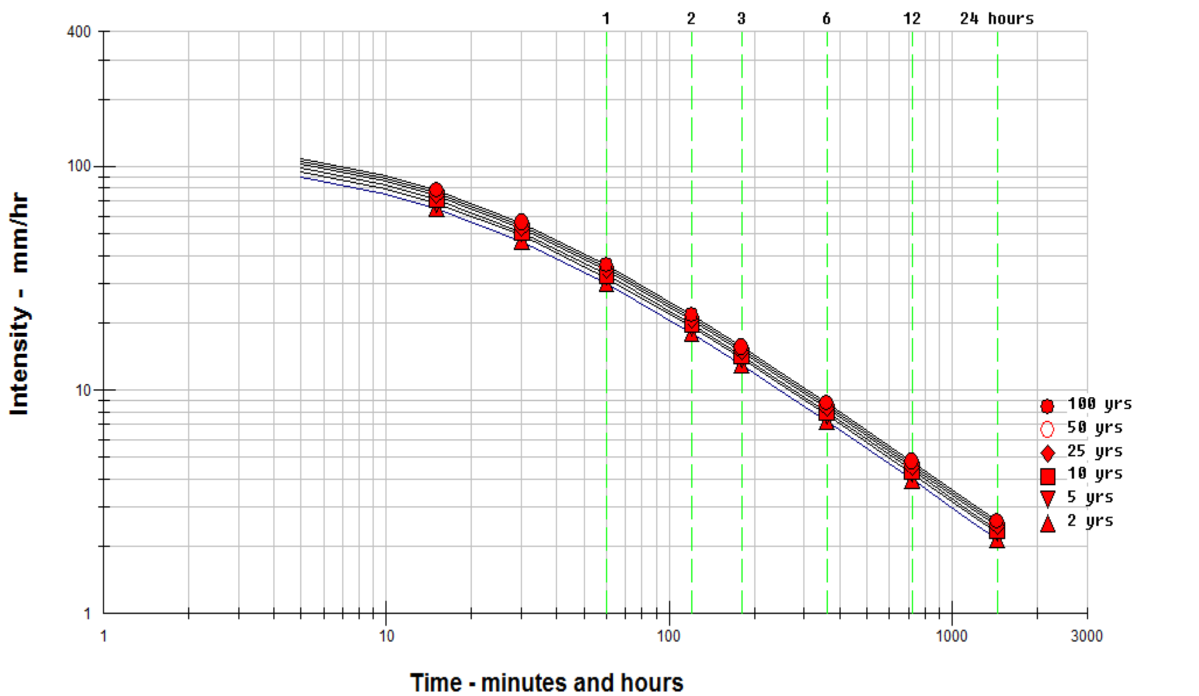

Kombolcha from 2031-2040

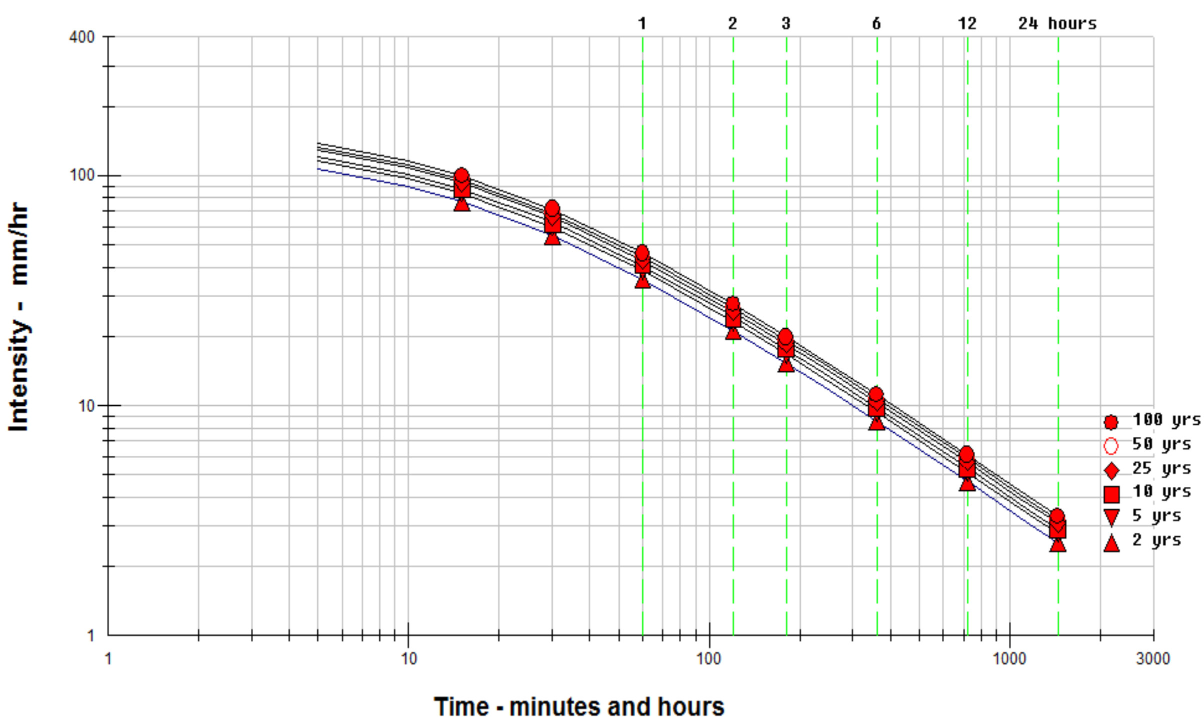

Kombolcha from 2091-2100

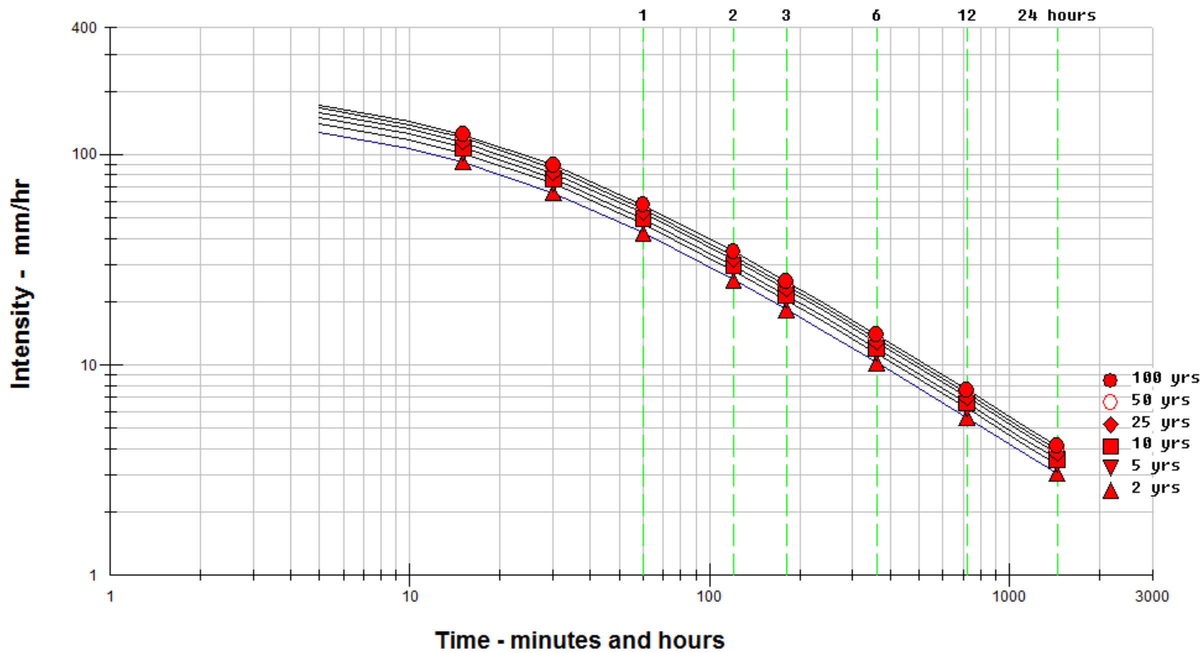

Haike from 1991-2000

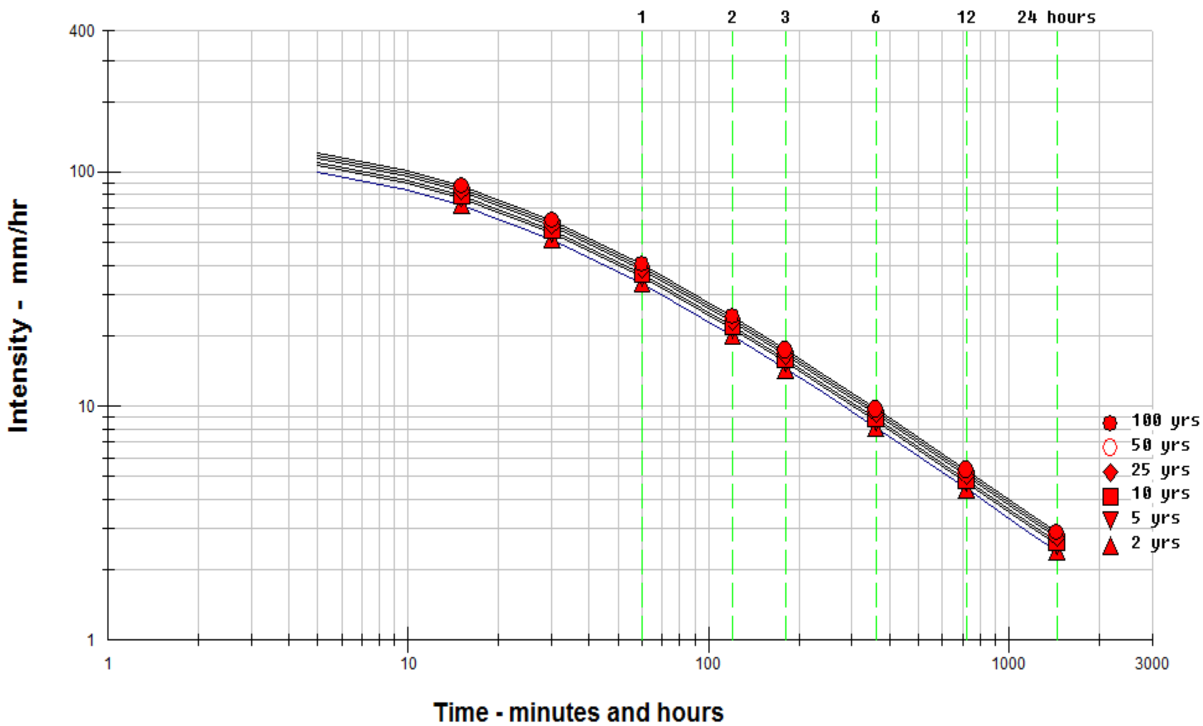

Haike from 2031-2040

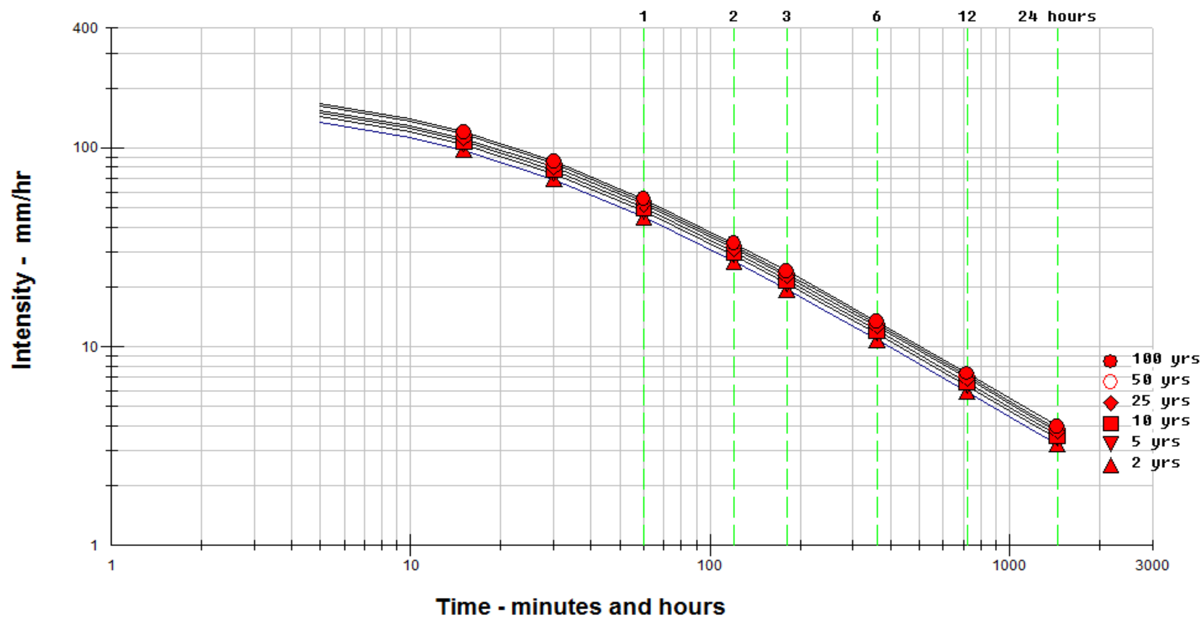

Haike from 2091-2100

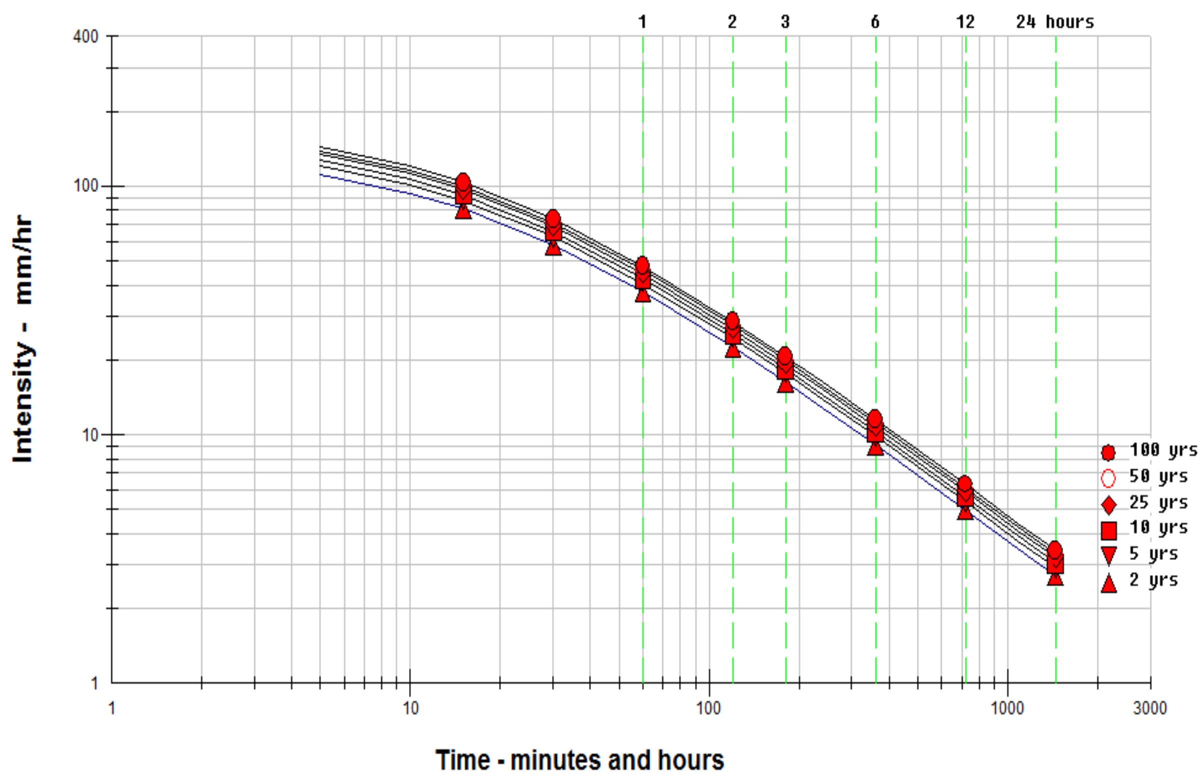

Alem ketema from 1991-2000

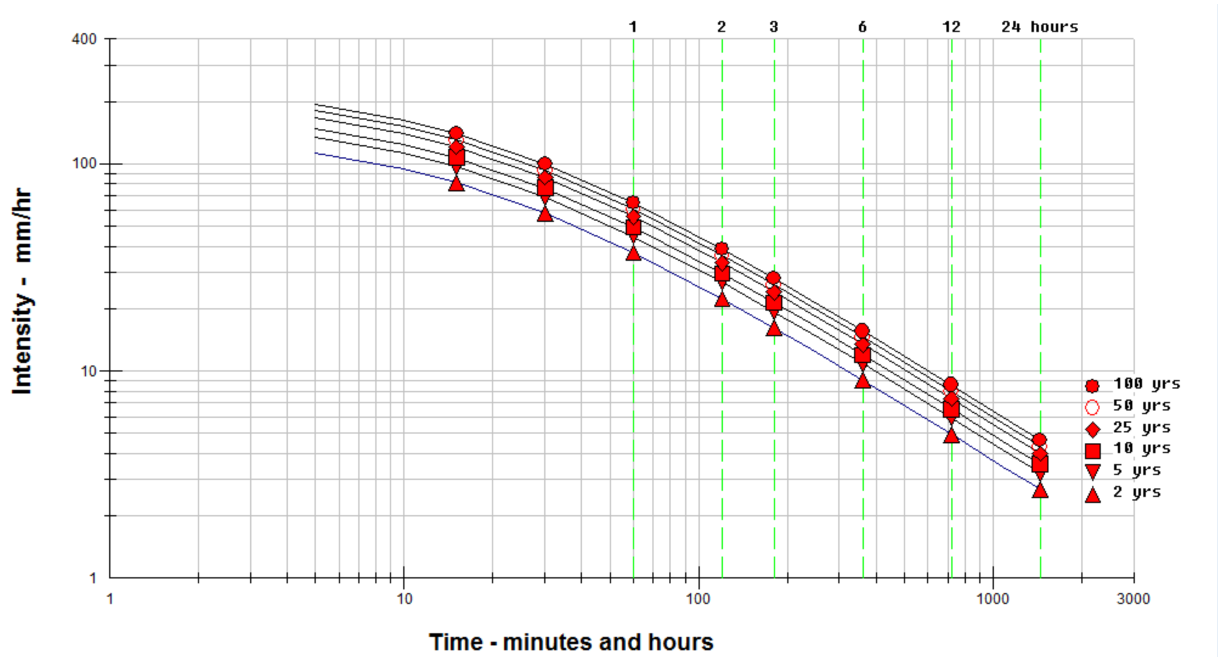

Alem ketema from 2031-2040

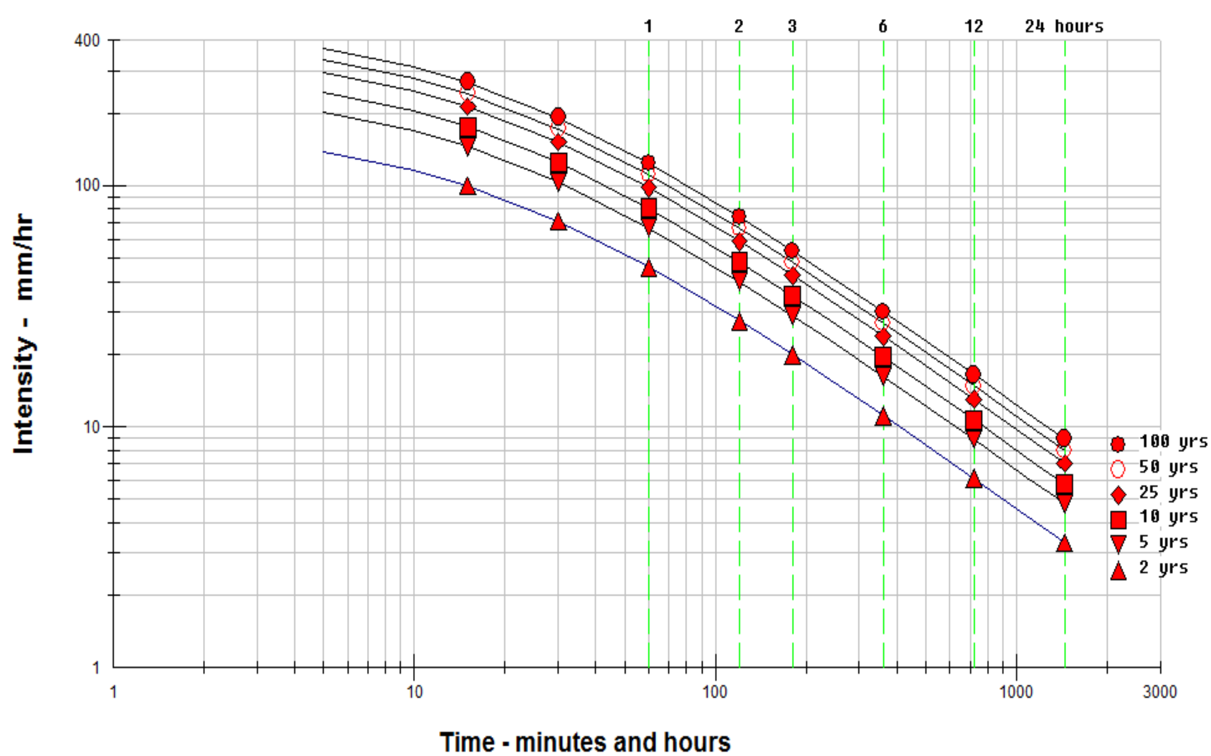

Alem ketema from 2091-2100

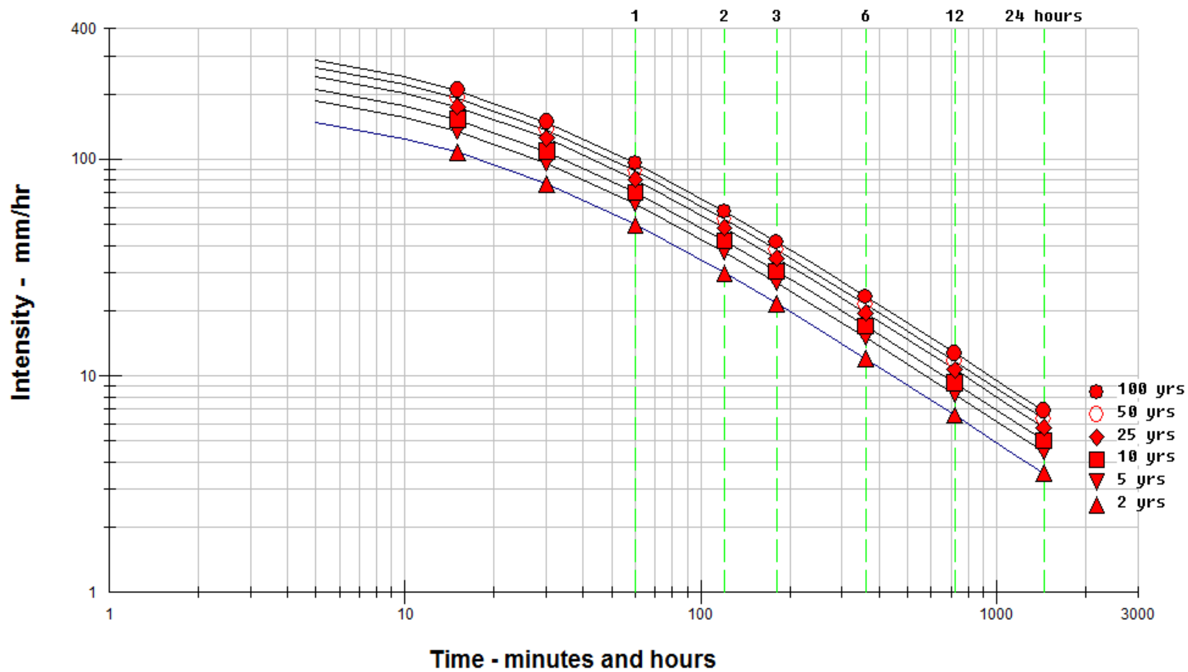

Fiche from 1991-2000

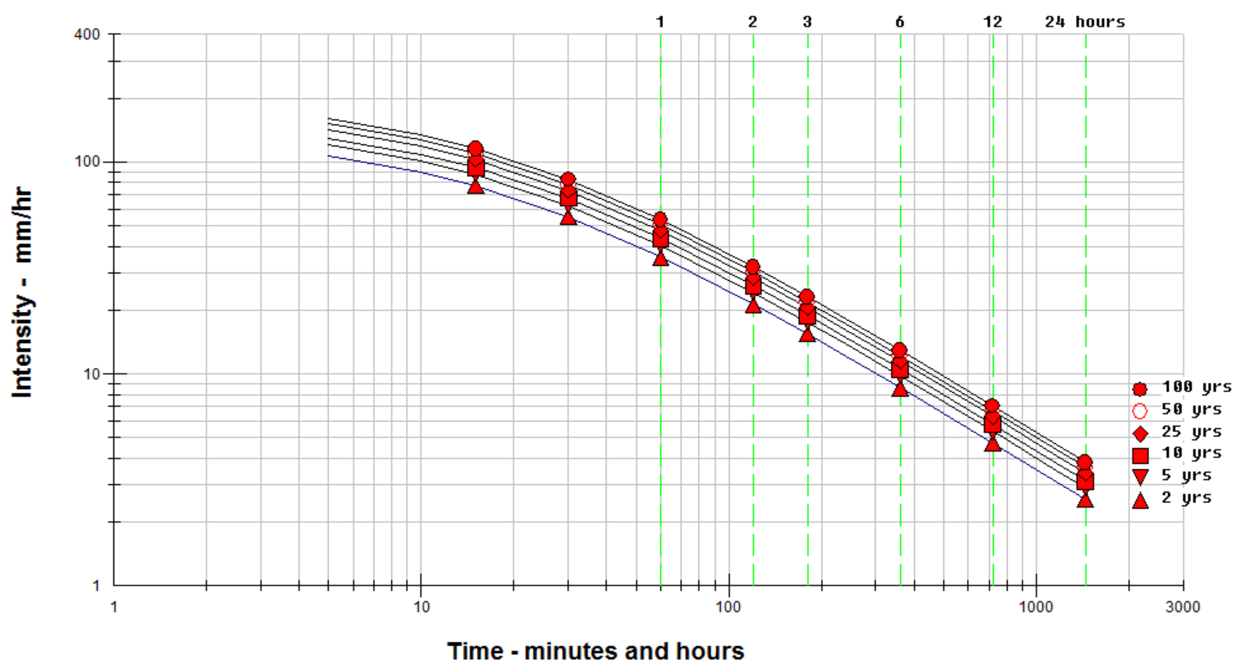

Fiche from 2031-2040

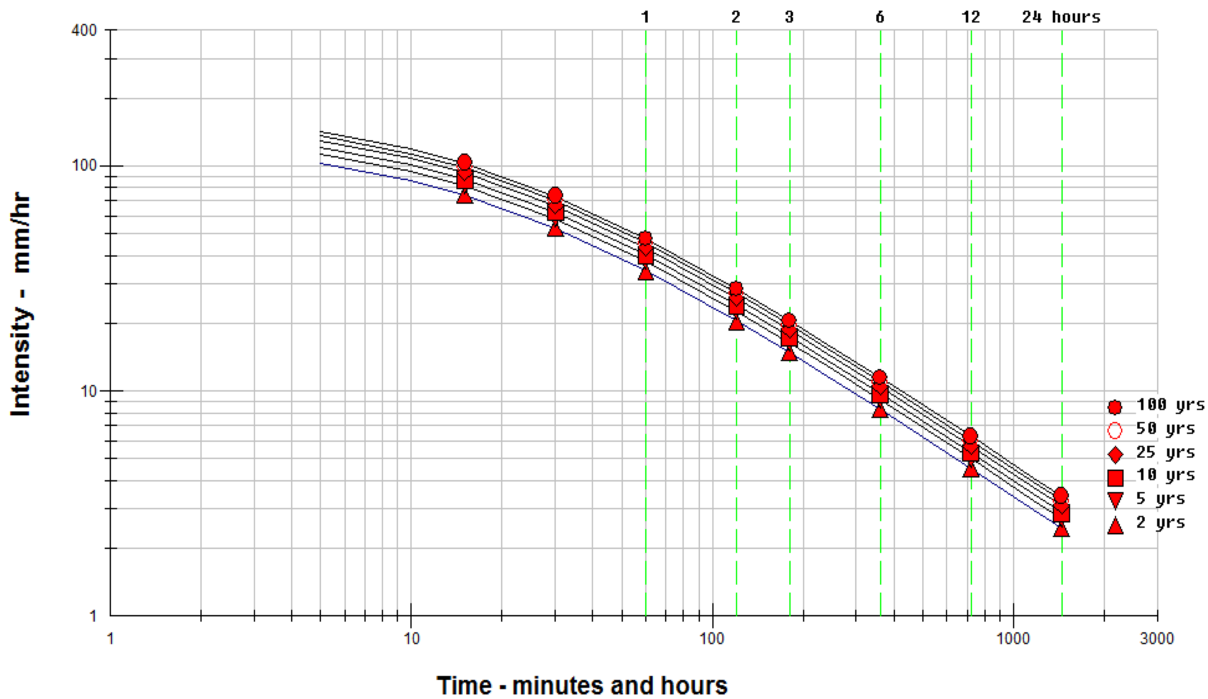

Fiche from 2091-2100

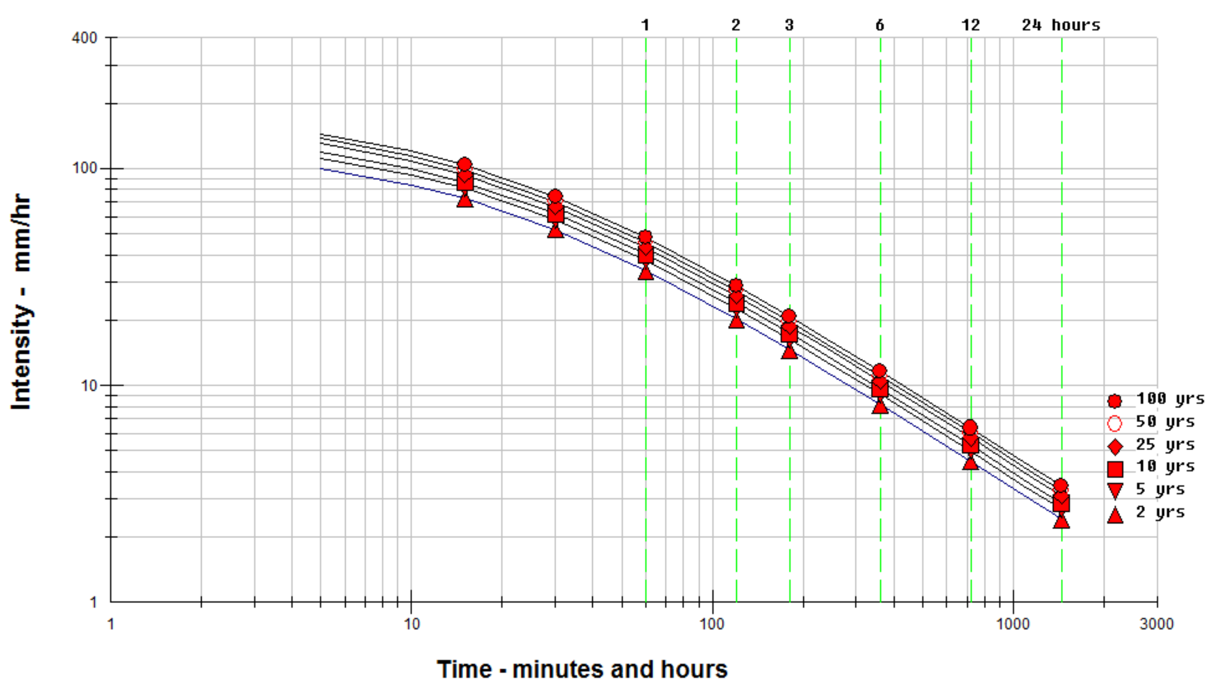

Shambu from 1991-2000

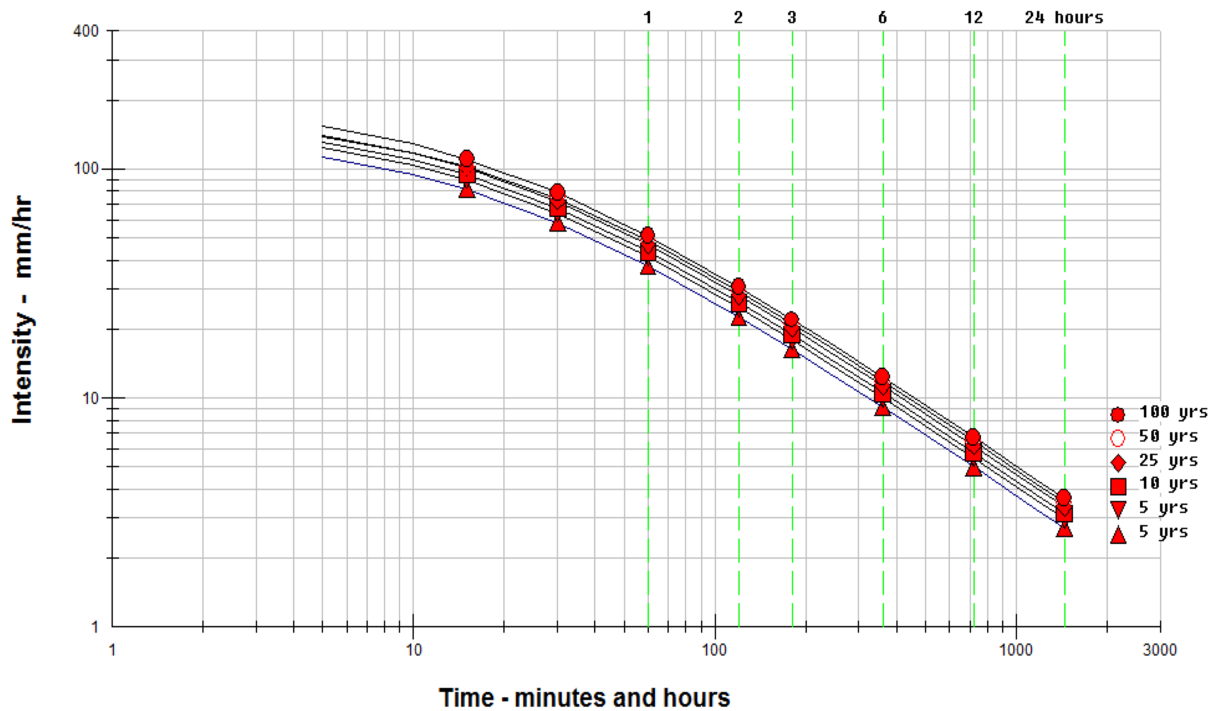

Shambu from 2031-2040

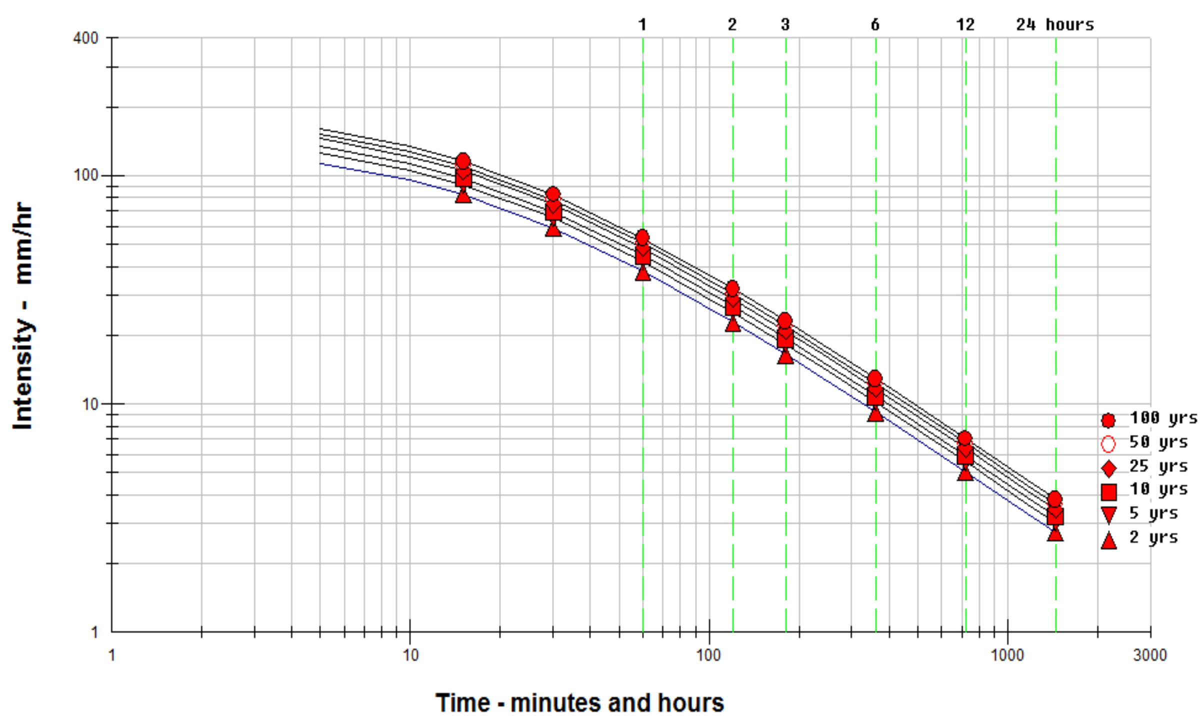

Shambu from 2091-2100

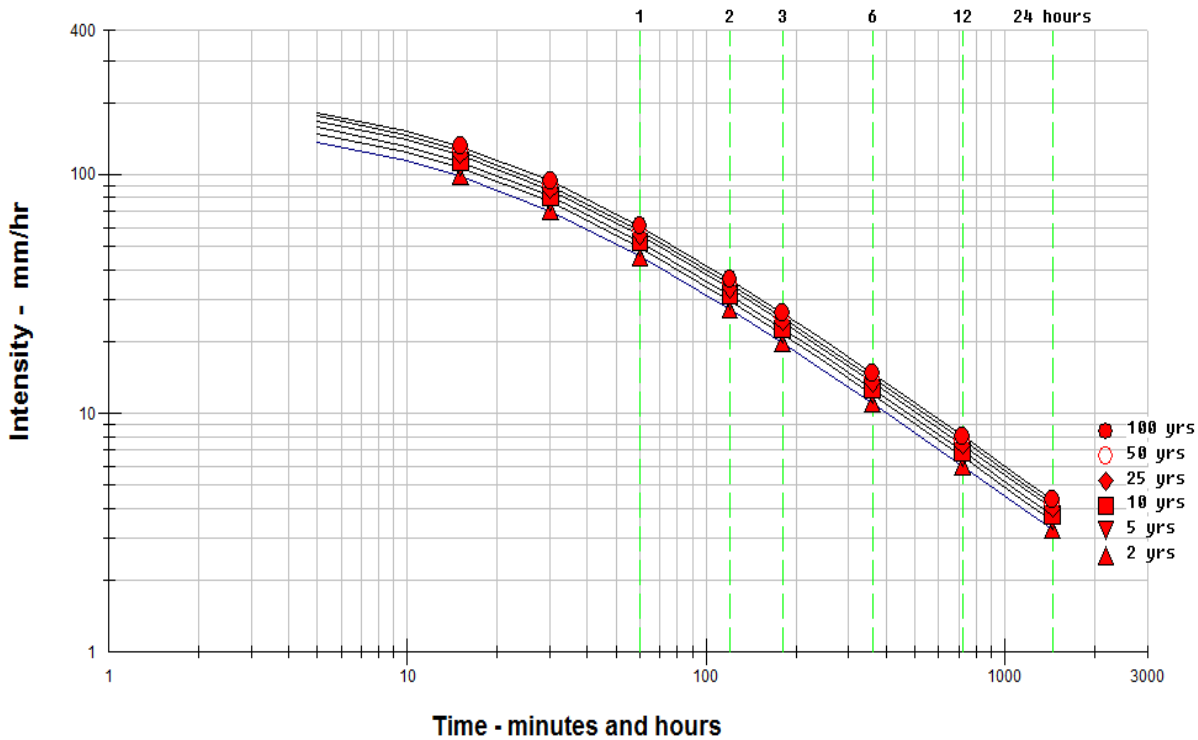

Nekemte from 1991-2000

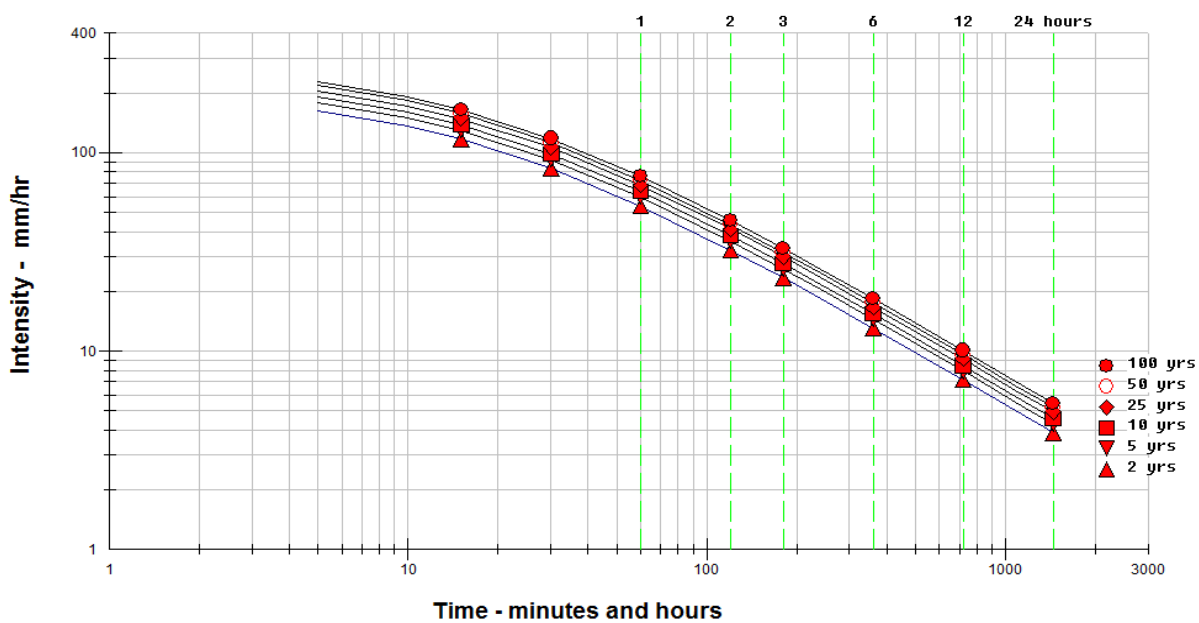

Nekemte from 2031-2040

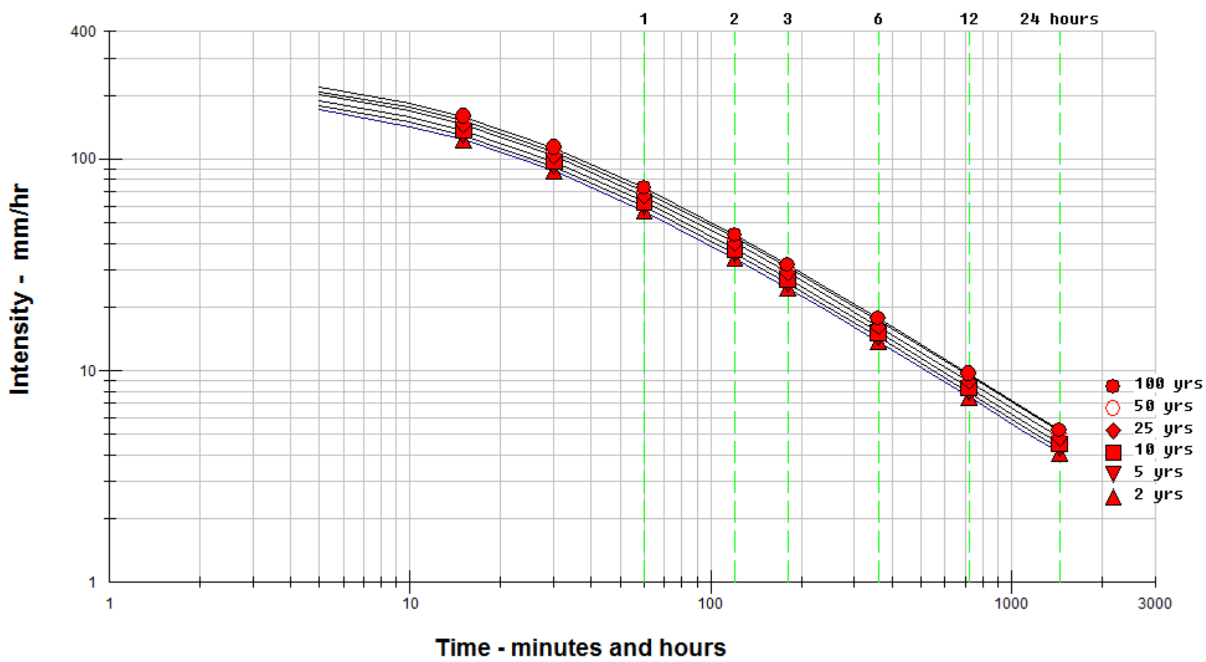

Nekemte from 2091-2100

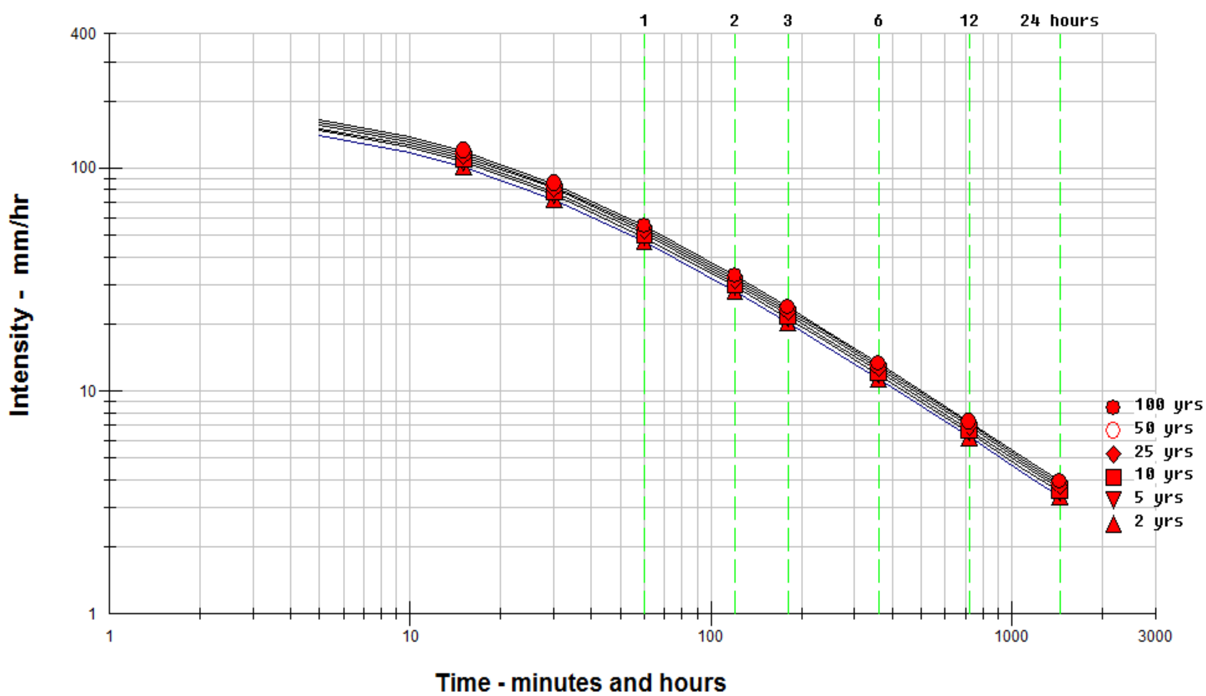

Assossa from 1991-2000

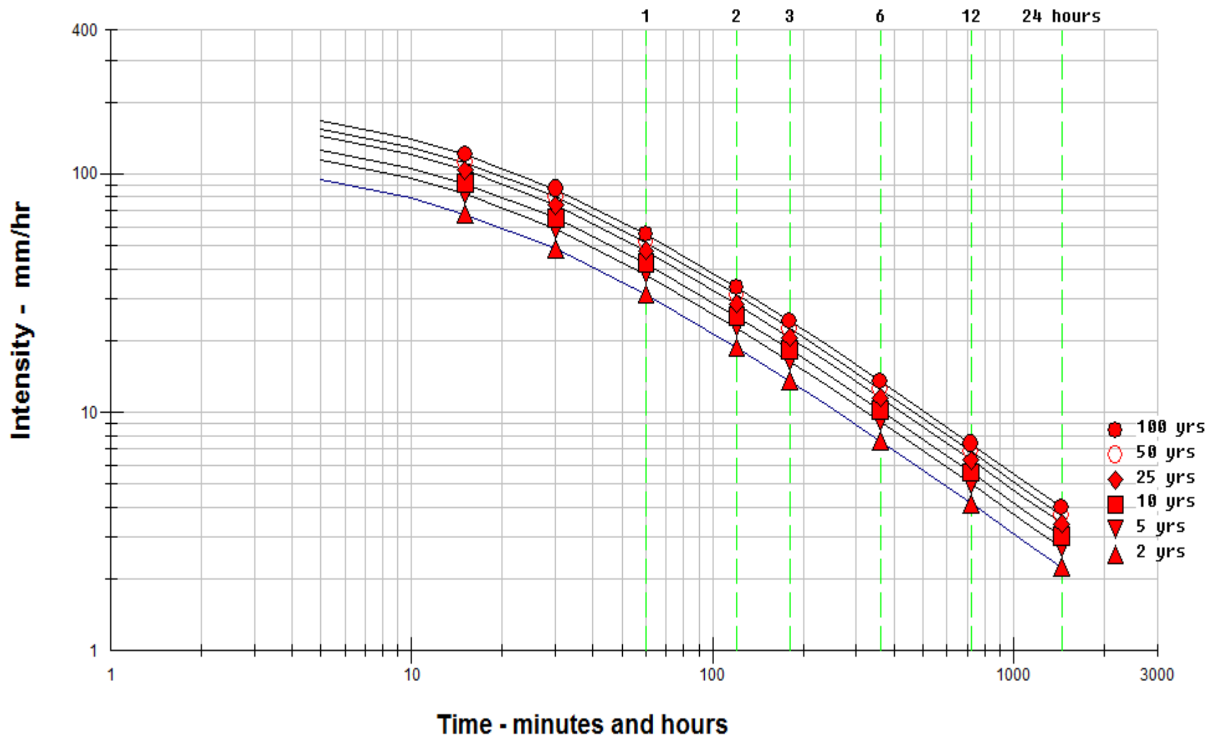

Assossa from 2031-2040

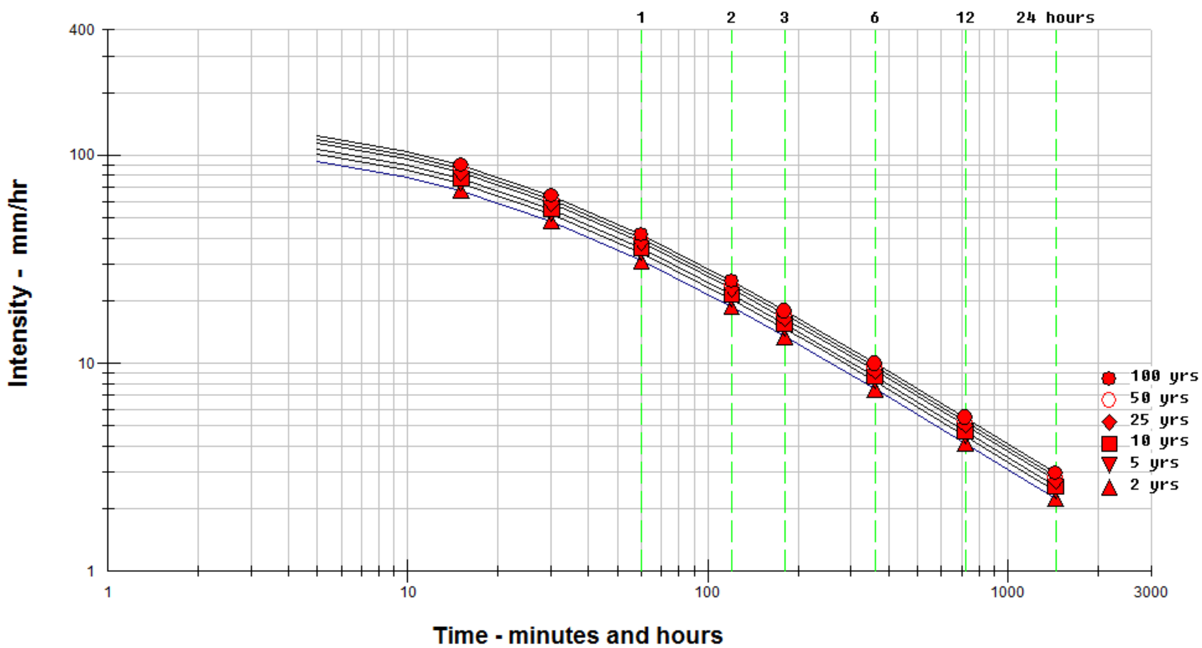

Assossa from 2091-2100

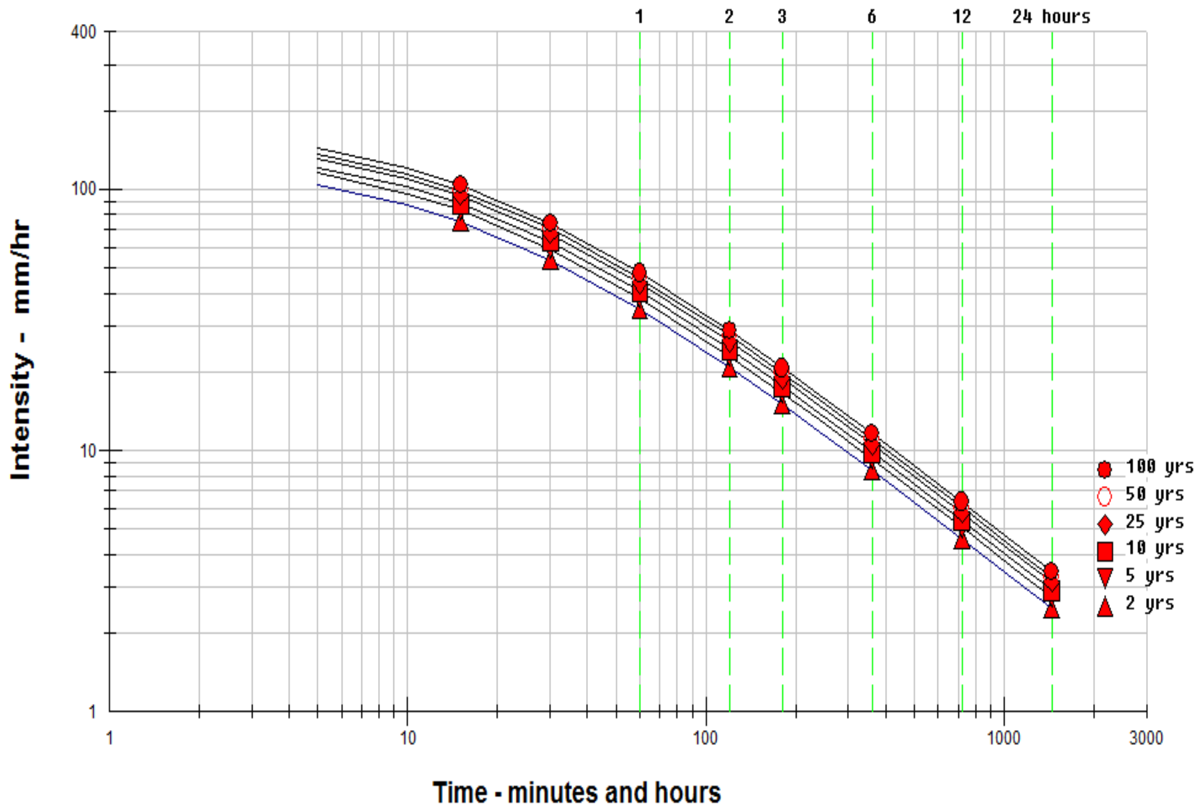

Appendix D: Estimated intensities of the considered stations for the indicated durations and frequencies

Intensity of rainfall(mm/hr) at Gondar in 1990s						
Duration (min)	Intensity of rainfall(mm/hr) for the indicated frequency(years)					
	2	5	10	25	50	100
1440	2.28	2.62	2.79	2.97	3.08	3.17
720	4.21	4.83	5.16	5.49	5.68	5.85
360	7.69	8.82	9.41	10	10.4	10.7
300	8.98	10.3	11	11.7	12.1	12.5
180	13.8	15.8	16.8	17.9	18.6	19.1
120	19	21.9	23.3	24.8	25.7	26.4
60	31.8	36.5	39	41.5	43	44.2
30	49.3	56.5	60.3	64.2	66.5	68.4

Intensity of rainfall(mm/hr) at Gondar in 2030s						
Duration (min)	Intensity of rainfall(mm/hr) for the indicated frequency(years)					
	2	5	10	25	50	100
1440	2.72	3.89	5.098	7.408	9.952	13.5
720	5.03	7.18	9.409	13.67	18.37	24.91
360	9.18	13.1	17.18	24.96	33.54	45.48
300	10.7	15.3	20.07	29.17	39.18	53.13
180	16.4	23.5	30.75	44.68	60.02	81.39
120	22.7	32.5	42.55	61.83	83.06	112.6
60	38	54.3	71.11	103.3	138.8	188.2
30	58.8	84	110.1	159.9	214.9	291.4

Intensity of rainfall(mm/hr) at Gonder in 2090s						
Duration (min)	Intensity of rainfall(mm/hr) for the indicated frequency(years)					
	2	5	10	25	50	100
1440	2.03	2.09	2.13	2.18	2.22	2.26
720	3.74	3.86	3.93	4.03	4.1	4.17
360	6.84	7.04	7.18	7.35	7.48	7.61
300	7.99	8.23	8.39	8.59	8.74	8.89
180	12.2	12.6	12.8	13.2	13.4	13.6
120	16.9	17.4	17.8	18.2	18.5	18.8
60	28.3	29.1	29.7	30.4	31	31.5
30	43.8	45.1	46	47.1	47.9	48.7

Intensity of rainfall(mm/hr) at Debre Markose in 1990s						
Duration (min)	Intensity of rainfall(mm/hr) for the indicated frequency(years)					
	2	5	10	25	50	100
1440	1.92	2.21	2.4	2.638	2.82	2.994
720	3.54	4.07	4.42	4.868	5.2	5.526
360	6.46	7.43	8.08	8.889	9.49	10.09
300	7.55	8.68	9.43	10.38	11.1	11.79
180	11.6	13.3	14.5	15.91	17	18.06
120	16	18.4	20	22.01	23.5	24.99
60	26.7	30.8	33.4	36.79	39.3	41.76
30	41.4	47.6	51.7	56.95	60.8	64.65

Intensity of rainfall(mm/hr) at Debre Markose in 2030s						
Duration (min)	Intensity of rainfall(mm/hr) for the indicated frequency(years)					
	2	5	10	25	50	100
1440	2.29	2.61	2.82	3.09	3.29	3.48
720	4.22	4.81	5.2	5.7	6.06	6.43
360	7.71	8.79	9.5	10.4	11.1	11.7
300	9	10.3	11.1	12.2	12.9	13.7
180	13.8	15.7	17	18.6	19.8	21
120	19.1	21.8	23.5	25.8	27.4	29.1
60	31.9	36.4	39.3	43.1	45.8	48.6
30	49.4	56.3	60.9	66.7	71	75.2

Intensity of rainfall(mm/hr) at Debre Markose in 2090s						
Duration (min)	Intensity of rainfall(mm/hr) for the indicated frequency(years)					
	2	5	10	25	50	100
1440	2.08	2.23	2.34	2.47	2.6	2.66
720	3.84	4.12	4.31	4.55	4.7	4.9
360	7.01	7.53	7.87	8.31	8.6	8.96
300	8.19	8.8	9.2	9.71	10	10.5
180	12.5	13.5	14.1	14.9	15	16
120	17.4	18.6	19.5	20.6	21	22.2
60	29	31.2	32.6	34.4	36	37.1
30	44.9	48.2	50.5	53.2	55	57.4

Intensity of rainfall(mm/hr) at Danglla in 1990s						
Duration (min)	Intensity of rainfall(mm/hr) for the indicated frequency(years)					
	2	5	10	25	50	100
1440	1.97	2.2	2.34	2.53	2.67	2.8
720	3.64	4.05	4.32	4.67	4.92	5.18
360	6.65	7.4	7.89	8.52	8.99	9.45
300	7.77	8.64	9.22	9.96	10.5	11
180	11.9	13.2	14.1	15.3	16.1	16.9
120	16.5	18.3	19.6	21.1	22.3	23.4
60	27.5	30.6	32.7	35.3	37.2	39.1
30	42.6	47.4	50.6	54.6	57.6	60.5

Intensity of rainfall(mm/hr) at Danglla in 2030s						
Duration (min)	Intensity of rainfall(mm/hr) for the indicated frequency(years)					
	2	5	10	25	50	100
1440	2.34	2.492	2.6	2.73	2.83	2.92
720	4.31	4.598	4.79	5.03	5.21	5.39
360	7.87	8.397	8.75	9.19	9.52	9.84
300	9.19	9.81	10.2	10.7	11.1	11.5
180	14.1	15.03	15.7	16.4	17	17.6
120	19.5	20.8	21.7	22.8	23.6	24.4
60	32.6	34.75	36.2	38	39.4	40.7
30	50.4	53.79	56	58.9	61	63

Intensity of rainfall(mm/hr) at Danglla in 2090s						
Duration (min)	Intensity of rainfall(mm/hr) for the indicated frequency(years)					
	2	5	10	25	50	100
1440	2.66	2.92	3.09	3.3	3.46	3.61
720	4.91	5.38	5.69	6.09	6.38	6.67
360	8.97	9.83	10.4	11.1	11.6	12.2
300	10.5	11.5	12.1	13	13.6	14.2
180	16	17.6	18.6	19.9	20.8	21.8
120	22.2	24.3	25.7	27.5	28.8	30.2
60	37.1	40.7	43	46	48.2	50.4
30	57.4	63	66.6	71.2	74.6	78

Intensity of rainfall(mm/hr) at kombolcha in 1990s						
Duration (min)	Intensity of rainfall(mm/hr) for the indicated frequency(years)					
	2	5	10	25	50	100
1440	2.149	2.28	2.36	2.46	2.53	2.6
720	3.966	4.21	4.36	4.54	4.66	4.79
360	7.243	7.7	7.96	8.28	8.51	8.74
300	8.462	8.99	9.3	9.68	9.95	10.2
180	12.96	13.8	14.2	14.8	15.2	15.6
120	17.94	19.1	19.7	20.5	21.1	21.7
60	29.98	31.9	32.9	34.3	35.2	36.2
30	46.4	49.3	51	53.1	54.6	56

Intensity of rainfall(mm/hr) at kombolcha in 2030s						
Duration (min)	Intensity of rainfall(mm/hr) for the indicated frequency(years)					
	2	5	10	25	50	100
1440	2.54	2.77	2.9	3.07	3.19	3.31
720	4.68	5.11	5.4	5.66	5.89	6.1
360	8.54	9.33	9.8	10.3	10.7	11.1
300	9.98	10.9	11	12.1	12.6	13
180	15.3	16.7	18	18.5	19.2	19.9
120	21.2	23.1	24	25.6	26.6	27.6
60	35.4	38.6	41	42.8	44.5	46.1
30	54.7	59.8	63	66.3	68.9	71.4

Intensity of rainfall(mm/hr) at kombolcha in 2090s						
Duration (min)	Intensity of rainfall(mm/hr) for the indicated frequency(years)					
	2	5	10	25	50	100
1440	3.05	3.37	3.57	3.8	3.97	4.13
720	5.62	6.23	6.58	7.01	7.32	7.63
360	10.3	11.4	12	12.8	13.4	13.9
300	12	13.3	14	15	15.6	16.3
180	18.4	20.3	21.5	22.9	23.9	24.9
120	25.4	28.2	29.8	31.7	33.1	34.5
60	42.5	47.1	49.7	53	55.3	57.7
30	65.8	72.8	77	82	85.7	89.3

Intensity of rainfall(mm/hr) at Haike in 1990s						
Duration (min)	Intensity of rainfall(mm/hr) for the indicated frequency(years)					
	2	5	10	25	50	100
1440	2.4	2.55	2.63	2.74	2.81	2.89
720	4.43	4.7	4.86	5.05	5.19	5.33
360	8.09	8.59	8.87	9.22	9.48	9.73
300	9.45	10	10.4	10.8	11.1	11.4
180	14.5	15.4	15.9	16.5	17	17.4
120	20	21.3	22	22.8	23.5	24.1
60	33.5	35.5	36.7	38.2	39.2	40.3
30	51.8	55	56.9	59.1	60.7	62.3

Intensity of rainfall(mm/hr) at Haike in 2030s						
Duration (min)	Intensity of rainfall(mm/hr) for the indicated frequency(years)					
	2	5	10	25	50	100
1440	3.21	3.44	3.58	3.74	3.858	3.98
720	5.93	6.35	6.6	6.9	7.121	7.34
360	10.8	11.6	12.1	12.6	13	13.4
300	12.6	13.6	14.1	14.7	15.19	15.7
180	19.4	20.8	21.6	22.6	23.27	24
120	26.8	28.7	29.9	31.2	32.2	33.2
60	44.8	48	49.9	52.2	53.81	55.4
30	69.3	74.3	77.2	80.7	83.3	85.8

Intensity of rainfall(mm/hr) at Haike in 2090s						
Duration (min)	Intensity of rainfall(mm/hr) for the indicated frequency(years)					
	2	5	10	25	50	100
1440	2.69	2.91	3.04	3.2	3.31	3.42
720	4.96	5.37	5.61	5.9	6.11	6.31
360	9.06	9.81	10.2	10.8	11.2	11.5
300	10.6	11.5	12	12.6	13	13.5
180	16.2	17.6	18.3	19.3	20	20.6
120	22.4	24.3	25.4	26.7	27.6	28.6
60	37.5	40.6	42.4	44.6	46.2	47.7
30	58.1	62.8	65.6	69	71.4	73.9

Intensity of rainfall(mm/hr) at Fiche in 1990s						
Duration (min)	Intensity of rainfall(mm/hr) for the indicated frequency(years)					
	2	5	10	25	50	100
1440	2.46	2.71	2.88	3.094	3.253	3.41
720	4.53	5	5.32	5.71	6.003	6.29
360	8.28	9.14	9.71	10.43	10.96	11.5
300	9.67	10.7	11.3	12.18	12.81	13.4
180	14.8	16.4	17.4	18.66	19.62	20.6
120	20.5	22.6	24	25.82	27.15	28.5
60	34.3	37.8	40.2	43.15	45.36	47.6
30	53	58.5	62.2	66.8	70.22	73.6

Intensity of rainfall(mm/hr) at Fiche in 2030s						
Duration (min)	Intensity of rainfall(mm/hr) for the indicated frequency(years)					
	2	5	10	25	50	100
1440	2.56	2.9	3.12	3.406	3.618	3.83
720	4.72	5.35	5.76	6.287	6.676	7.06
360	8.61	9.76	10.5	11.48	12.19	12.9
300	10.1	11.4	12.3	13.41	14.24	15.1
180	15.4	17.5	18.8	20.54	21.82	23.1
120	21.3	24.2	26.1	28.43	30.19	31.9
60	35.7	40.4	43.5	47.51	50.46	53.4
30	55.2	62.5	67.4	73.54	78.1	82.6

Intensity of rainfall(mm/hr) at Fiche in 2090s						
Duration (min)	Intensity of rainfall(mm/hr) for the indicated frequency(years)					
	2	5	10	25	50	100
1440	2.41	2.69	2.87	3.103	3.275	3.45
720	4.45	4.96	5.3	5.727	6.045	6.36
360	8.13	9.06	9.68	10.46	11.04	11.6
300	9.5	10.6	11.3	12.22	12.9	13.6
180	14.5	16.2	17.3	18.72	19.75	20.8
120	20.1	22.4	24	25.9	27.34	28.8
60	33.6	37.5	40.1	43.28	45.68	48.1
30	52.1	58	62	67	70.72	74.4

Intensity of rainfall(mm/hr) at Alem ketema in 1990s						
Duration (min)	Intensity of rainfall(mm/hr) for the indicated frequency(years)					
	2	5	10	25	50	100
1440	2.68	3.2	3.552	3.991	4.32	4.64
720	4.94	5.91	6.555	7.365	7.97	8.56
360	9.03	10.8	11.97	13.45	14.5	15.64
300	10.5	12.6	13.98	15.71	17	18.27
180	16.2	19.3	21.42	24.07	26	27.98
120	22.4	26.7	29.65	33.31	36	38.73
60	37.4	44.7	49.54	55.66	60.2	64.72
30	57.8	69.2	76.68	86.16	93.2	100.18

Intensity of rainfall(mm/hr) at Alem ketema in 2030s						
Duration (min)	Intensity of rainfall(mm/hr) for the indicated frequency(years)					
	2	5	10	25	50	100
1440	3.57	4.45	5.043	5.787	6.34	6.89
720	6.58	8.22	9.307	10.68	11.7	12.7
360	12	15	17	19.5	21.4	23.2
300	14	17.5	19.86	22.78	25	27.1
180	21.5	26.9	30.41	34.9	38.2	41.5
120	29.8	37.2	42.09	48.3	52.9	57.5
60	49.7	62.1	70.34	80.71	88.4	96
30	77	96.2	108.9	124.9	137	149

Intensity of rainfall(mm/hr) at Alem ketema in 2090s						
Duration (min)	Intensity of rainfall(mm/hr) for the indicated frequency(years)					
	2	5	10	25	50	100
1440	3.3	4.8	5.791	7.046	7.98	8.9
720	6.09	8.86	10.69	13	14.7	16.4
360	11.1	16.2	19.52	23.75	26.9	30
300	13	18.9	22.8	27.74	31.4	35
180	19.9	28.9	34.93	42.49	48.1	53.7
120	27.5	40.1	48.34	58.8	66.6	74.3
60	46	66.9	80.77	98.28	111	124
30	71.2	104	125	152.1	172	192

Intensity of rainfall(mm/hr) at Nekemte in 1990s						
Duration (min)	Intensity of rainfall(mm/hr) for the indicated frequency(years)					
	2	5	10	25	50	100
1440	3.87	4.3	4.58	4.93	5.2	5.462
720	7.14	7.93	8.45	9.11	9.6	10.08
360	13	14.5	15.4	16.6	17.5	18.41
300	15.2	16.9	18	19.4	20.5	21.5
180	23.3	25.9	27.6	29.8	31.4	32.94
120	32.3	35.9	38.2	41.2	43.4	45.59
60	54	59.9	63.9	68.8	72.5	76.18
30	83.5	92.7	98.8	107	112	117.9

Intensity of rainfall(mm/hr) at Nekemte in 2030s						
Duration (min)	Intensity of rainfall(mm/hr) for the indicated frequency(years)					
	2	5	10	25	50	100
1440	4.07	4.27	4.5	4.81	5.03	5.251
720	7.52	7.87	8.31	8.87	9.28	9.692
360	13.7	14.4	15.2	16.2	17	17.7
300	16	16.8	17.7	18.9	19.8	20.68
180	24.6	25.7	27.2	29	30.3	31.67
120	34	35.6	37.6	40.1	42	43.83
60	56.8	59.5	62.8	67	70.1	73.24
30	87.9	92.1	97.3	104	109	113.4

Intensity of rainfall(mm/hr) at Nekemte in 2090s						
Duration (min)	Intensity of rainfall(mm/hr) for the indicated frequency(years)					
	2	5	10	25	50	100
1440	3.36	3.52	3.62	3.75	3.85	3.947
720	6.21	6.49	6.69	6.93	7.11	7.284
360	11.3	11.9	12.2	12.6	13	13.3
300	13.2	13.9	14.3	14.8	15.2	15.54
180	20.3	21.2	21.8	22.6	23.2	23.8
120	28.1	29.4	30.2	31.3	32.1	32.94
60	46.9	49.1	50.5	52.3	53.7	55.05
30	72.6	76	78.2	81	83.1	85.22

Intensity of rainfall(mm/hr) at Assossa in 1990s						
Duration (min)	Intensity of rainfall(mm/hr) for the indicated frequency(years)					
	2	5	10	25	50	100
1440	2.25	2.72	3.03	3.42	3.71	4.003
720	4.14	5.01	5.59	6.31	6.85	7.388
360	7.57	9.15	10.2	11.5	12.5	13.49
300	8.84	10.7	11.9	13.5	14.6	15.76
180	13.5	16.4	18.3	20.6	22.4	24.14
120	18.7	22.7	25.3	28.6	31	33.41
60	31.3	37.9	42.2	47.7	51.8	55.84
30	48.5	58.6	65.4	73.9	80.2	86.43

Intensity of rainfall(mm/hr) at Assossa in 2030s						
Duration (min)	Intensity of rainfall(mm/hr) for the indicated frequency(years)					
	2	5	10	25	50	100
1440	2.23	2.43	2.56	2.72	2.84	2.965
720	4.12	4.48	4.72	5.03	5.25	5.473
360	7.52	8.18	8.62	9.18	9.59	9.994
300	8.79	9.56	10.1	10.7	11.2	11.68
180	13.5	14.6	15.4	16.4	17.2	17.88
120	18.6	20.3	21.4	22.7	23.7	24.75
60	31.1	33.9	35.7	38	39.7	41.36
30	48.2	52.4	55.2	58.8	61.4	64.03

Intensity of rainfall(mm/hr) at Assossa in 2090s						
Duration (min)	Intensity of rainfall(mm/hr) for the indicated frequency(years)					
	2	5	10	25	50	100
1440	2.49	2.75	2.92	3.13	3.29	3.442
720	4.6	5.07	5.38	5.77	6.06	6.353
360	8.41	9.26	9.83	10.5	11.1	11.6
300	9.82	10.8	11.5	12.3	12.9	13.55
180	15	16.6	17.6	18.9	19.8	20.76
120	20.8	22.9	24.3	26.1	27.4	28.73
60	34.8	38.3	40.7	43.6	45.8	48.01
30	53.9	59.3	63	67.5	70.9	74.32

Intensity of rainfall(mm/hr) at Shambu in 1990s						
Duration (min)	Intensity of rainfall(mm/hr) for the indicated frequency(years)					
	2	5	10	25	50	100
1440	2.71	3	3.129	3.34	3.5	3.65
720	5	5.5	5.774	6.17	6.46	6.74
360	9.13	10	10.54	11.3	11.8	12.3
300	10.7	12	12.32	13.2	13.8	14.4
180	16.3	18	18.87	20.1	21.1	22
120	22.6	25	26.11	27.9	29.2	30.5
60	37.8	41	43.64	46.6	48.8	51
30	58.5	64	67.55	72.1	75.5	78.9

Intensity of rainfall(mm/hr) at Shambu in 2030s						
Duration (min)	Intensity of rainfall(mm/hr) for the indicated frequency(years)					
	2	5	10	25	50	100
1440	2.73	3	3.215	3.46	3.64	3.82
720	5.03	5.6	5.933	6.38	6.72	7.05
360	9.19	10	10.83	11.7	12.3	12.9
300	10.7	12	12.66	13.6	14.3	15
180	16.5	18	19.39	20.9	22	23
120	22.8	25	26.83	28.9	30.4	31.9
60	38	42	44.84	48.3	50.8	53.3
30	58.9	65	69.4	74.7	78.6	82.5

Intensity of rainfall(mm/hr) at Shambu in 2090s						
Duration (min)	Intensity of rainfall(mm/hr) for the indicated frequency(years)					
	2	5	10	25	50	100
1440	3.26	3.6	3.75	4	4.18	4.36
720	6.02	6.6	6.921	7.37	7.71	8.04
360	11	12	12.64	13.5	14.1	14.7
300	12.8	14	14.76	15.7	16.4	17.2
180	19.7	21	22.62	24.1	25.2	26.3
120	27.2	30	31.3	33.3	34.9	36.4
60	45.5	50	52.3	55.7	58.3	60.8
30	70.4	77	80.96	86.3	90.2	94.1

Appendix E: List of Acronyms

BD1991SUMMARY.TXT.Maximum	statistical summary of maximum of data at Bahirdar station.
BDSTSUMMARY.TXT.maximum	statistical summary of maximum of generated data of station Bahirdar .
Kombstationsummary.txt.mean	statistical summary of mean of data at Kombolcha station
Kombsummary.txt.mean	statistical summary of mean of generated data of Station Kombolcha

PD	Partial duration of the series data
IDF	intensity duration frequency
DDF	depth duration frequency
AM	Annual maximum of the series
IWMI	international water management institute
GCM	Global circulation Model/s
MRD	Moment ratio diagram
WMO	world meteorology organization
IPCC	Inter Governmental Panel on Climate Change
ITCZ	Inter Tropical Convergent Zone
NMSA	Ethiopian National Metrological Service Agencr2 Correlation Coefficient
EV1	Gumbel probability distribution
GEV	General Extreme value probability distribution
MOM.	Method of moments
SDSM	statistical down scaling model
ML	Maximum likelihood
IPCC	Intergovernmental Panel on Climate Change